No. 14 / March 2014

Contributions to Gemology

Identification of a New Generation of Synthetic CVD-grown Blue, Pink and Yellow Diamonds

Classified Technical, New Discovery, Pink, Blue and Yellow, Fancy Colored CVD-grown Diamonds

Reading Level Expert Groups and Gemologists

GRS Investigates the Source of Ruby, Sapphire and Padparadscha from the Didy Mine in Madagascar

Classified Expedition, Source Analysis, Adventure-Details, World-Record Ruby, Sapphire and Padparadscha

Reading Level Gemstone Dealers, Gemologists and the Public

GRS GEMRESEARCH SWISSLAB

Editor / Publisher

Dr. A. Peretti, FGG, FGA, EurGeol
GRS Gemresearch Swisslab AG, P.O. Box 3628
6002 Lucerne, Switzerland, adolf@peretti.ch

Printed in March 2014 in Hong Kong, distributed and published by DR Peretti Co. LTD, Unit 501, Silom 19 Building, Soi 19, Silom, Bangrak, Bangkok 10500, Thailand

GRS welcomes our new Co-Editors Diana Jarrett & Matthias Alessandri

Diana Jarrett is an award winning veteran journalist for the gemstone and jewelry trade, earning multiple accolades from various trade journals for over 13 years. Jarrett is a Graduate Gemologist (GIA) a Registered Master Valuer (RMV) jewelry appraiser, and Contributing Member to New York Mineralogical Club (NYMC). While earning her graduate gemologist diploma in Los Angeles CA, she worked at Sotheby's Beverly Hills with Fine Jewelry auctions.

Her research colored diamond and gemstone reports have appeared in Rapaport Diamond Report, and Jewellery Business, and numerous regional US publications. Jarrett's column The Story Behind the Stone has delivered gemological updates to US jewelry retailers for over a decade in trade newspapers. She co-authored the reference guide Cameos Old & New, 4th edition, by Gemstone Press. She's a frequently invited speaker at US trade shows including the AGTA Tucson Gem Fair, in Tucson, AZ.

Jarrett joins her fellow colleagues at GemResearch Swisslab (GRS) in a supporting role for their published gemological research and leading-edge contributions to the gem trade.

Technical Co-Editor

Matthias Alessandri, FGA, GRS Lab (HK) Limited, Hong Kong

Review Board

Foreword

The diamond industry is undergoing one of the most dynamic changes of all time. Challenges confronting it today are in large part due to the massive influx of newer generations of synthetic diamonds and diamond treatments permeating every level of the market. Melees, colorless diamonds and perhaps most importantly fancy colored diamonds are experiencing upheaval in the marketplace.

As fancy diamond prices soar to world-record levels, the technology required to make imitations of their natural counterparts with synthetic colored diamonds is now available. This process includes various conventional techniques along with more recently perfected HPHT (high pressure, high temperature) methods. The technology performs all kinds of treatment and produces synthetics now that recreate most natural diamond colors including the blues.

The new stars on the horizon are the CVD (Carbon Vapor Deposition) diamonds. At first CVD was thought to be particularly important for diamond coating or for industrial application. That turned out to be a completely false assumption, however. Besides colorless diamonds, almost every color is now produced in facetable sizes including those over 1 carat which used to be their limit. To achieve all the different colors, additional treatments can be applied to CVD diamonds so that rare pink colors can be produced this way too. Until recently, what was missing were the CVD synthetic blue diamonds. Natural blue diamonds are one of the most expensive diamonds in the world next to natural pinks. It would therefore be just a matter of time before they too should appear on the market.

GRS and CGL-GRS laboratories determined that these challenges warranted a powerful pro-active response. Hence was found a network of 3 diamond research laboratories in Switzerland, Hong Kong and Canada who cooperated as a unified taskforce for the research and discovery of these new diamond synthetics and treatments in the highly competitive arena of major global laboratories. We accepted this daunting challenge.

With great pride, we reveal our enormous achievement in being the first laboratory to discover that new lab-grown CVD blue diamonds have actually entered the market. We also include our excursion into the world of natural and lab-grown pink diamonds in Part B and in Part C we perform experiments to create yellow colored synthetic diamonds from greyish CVD-grown diamonds performing multistep treatments.

The second part of this issue is also a first. We present the second instalment of our jungle expedition into Madagascar to the source of world-record setting rubies with significant progress into the mystery of the gemstone formation from Didy (Madagascar). We've also made considerable progress in our research presentation. Unlike previous gemological publications, we include QR codes that link to corresponding YouTube videos. Besides text and images, the reader can watch the videos to gain better insight into our research trips. GRS is the first to introduce this new type of interactive publishing in the world of gemology.

Let's celebrate together!

Dr. Adolf Peretti

New Generation of Synthetic Diamonds Reaches the Market

Part A: Identification of CVD-grown Blue Diamonds

Peretti A. [1]*, Herzog F. [2], Bieri W. [2], Alessandri M. [3], Günther D. [4], Frick D.A. [4], Cleveland, E. [5]
Zaitsev A.M. [6], Deljanin B. [7]

[1]DR Peretti Co LTD, Thailand and GRS Laboratories
[2]GRS Gemresearch Swisslab AG, Switzerland
[3]GRS Lab (Hong Kong) Ltd, Hong Kong, China
[4]Laboratory for Inorganic Chemistry, ETH Zurich, Switzerland
[5]Delaware, USA
[6]The City University of New York, USA
[7]CGL-GRS Swiss Canadian Gemlab Inc., Canada

*Corresponding author: adolf@peretti.ch

Abstract

A new type of synthetic blue diamonds appeared on the market. These diamonds were identified as CVD-grown. Optical spectroscopy revealed that they are of type IIa and their color is caused by strong absorption of very intense silicon-related SiV^- centre (negatively charged Silicon and Vacancy centre). A structural and chemical layering was identified by SEM-CC analyses. Enhanced concentration of Bi and Pb elements was found by LA-ICP-MS method. Reliable identification of silicon-doped blue CVD diamonds can be performed in different ways and these diamonds can be unambiguously distinguished from their blue natural and HPHT-grown synthetic counterparts. The most effective identification methods are absorption and photoluminescence spectroscopy in the visible spectral range, which reveal extremely intense SiV^- (737nm) centre. The silicon-doped blue CVD diamonds are not conductive. Thus the electrical conductance test is a method contributing to the recognition of these diamonds.

Keywords: Synthetic, CVD-grown, blue diamond, type IIa, SiV^- color centres

Introduction

On October 18, 2013 Rapaport Diamond Report issued a trade alert warning "Buyers beware; Persistent reports indicate that large amounts of synthetic lab-grown diamonds are being mixed with natural diamonds in parcels of melee and pointers. Know your supplier and insist the phrase 'natural, untreated diamonds' to be included on all invoices". More than 600 undisclosed CVD-grown diamonds of less than 0.70 carats came through major laboratories in both Antwerp and Hong Kong for certification in 2012 [1]. As prices for natural diamonds in India rise, synthetic diamonds are also gaining attraction [2]. 'The synthetic diamond market in India has captured around 1% of the overall diamond jewellery market,' said Vipul Shah, chairman of the Gems and Jewellery Export Promotion Council (GJEPC). Therefore, disclosure of these new synthetic diamonds is also a matter of concern.

Orion PDC Diamonds, a company producing CVD diamonds, asserts in their marketing brochure entitled PDC Company that both genuine earth-mined and synthetic diamonds are 'real diamonds'. Although theoretically correct in that they both share the same physical and chemical properties, this statement, when used within the gem-diamond market, is very misleading. It implies that these lab grown diamonds are 'natural', which is certainly not the case.

Synthetic diamonds are indeed an important part of today's commercial gemstone industry [3] and are being created by a variety of companies, like AOTC [4], Chatham, Scio Diamond, Gemesis, Washington Diamonds, and Orion PDC, all using various production methods (Fig. 1). To create different colors, a variety of treatments are applied to either natural or synthetic diamonds. Diamonds of practically any color including colorless, yellow, blue, green, orange, and pink and their countless variations may result from the controlled application of different combinations of irradiation, heat and high pressure. Commercial production of blue diamonds relies upon one of three methods;

- Electron irradiation with energy of a few MeV at moderate doses applied to practically any diamond (common treatment)
- High-pressure high-temperature (HPHT) annealing of initially natural grey-color (very rare) type IIb diamonds
- HPHT growth of synthetic boron-doped diamonds

Fig. 1: Scio Diamond Inc. facility in North Carolina, USA with many CVD-growers

No other technique, including that of Chemical Vapour Deposition (CVD) growth, has reportedly been used for commercial production of gem-grade diamonds with blue body color. Of late, synthetic gem diamonds produced by CVD method could appear as brown, pink (post grown irradiated), yellow or colorless. But quite recently, CVD-grown diamonds of a greyish-blue color have entered the marketplace (Fig. 2). The first characterisation and identification of these diamonds is the aim of this present publication.

Although published research does exist on CVD technique producing boron-doped blue color diamond coatings, blue diamonds created by this method have not previously been seen as faceted stones in the marketplace. Synthetic blue diamonds appearing closest to their natural counterparts are usually produced by HPHT growth [5].

In September 2013, one of the authors (AP) conducted a survey at the Bangkok Gems & Jewelry Fair and discovered that synthetic blue diamonds over 1 carat in size (See Fig. 2b) appeared in the market along with a variety of other colors (See Fig. 2a). Later on, in Hong Kong, we were able to acquire a few reference samples of the blue diamonds from the producer, along with other samples for this study (see Tab.1).

In this effort, we express our discovery of a new type of synthetic blue diamond which had not been previously identified in scientific literature. This is a key finding for the gem trade especially in light of recent developments in CVD technology which turns out higher quality, greater color range, and larger carat size synthetic diamonds.

Materials & Methods

The test group from the GRS and CGL-GRS collection totalled 151 samples including those listed in Tab.1. They underwent testing in the same run by FTIR, PL-LNT (405nm and 532nm) and UV-VIS-NIR-LNT, ED-XRF, Fluorescence Microscopy and SEM-charge contrast (SEM-CC) methods. The reference sample collection included natural, synthetic and treated diamonds of both natural and synthetic origin and of different colors, namely colorless, yellow, pink and blue from various producers:

- 15 Synthetic CVD diamonds from Scio Diamond, USA
- 12 Synthetic CVD diamonds from Orion PDC, Hong Kong
- 4 Synthetic CVD diamonds from Apollo, USA
- 3 Synthetic CVD diamonds from unknown producer
- 30 HPHT processed natural diamonds, mostly Suncrest, USA
- 10 HPHT synthetic diamonds of AOTC, Canada
- 4 HPHT synthetic diamonds from Chatham, USA
- 4 HPHT synthetic diamonds from Tairus, Russia
- 9 Synthetic diamonds from Gemesis, USA (some of which were irradiated + heated)
- 15 Natural diamonds of various fancy colors
- 5 Irradiated natural diamond
- 40 Natural brown to pink diamonds from Rio Tinto, Argyle diamond mine, WA, Australia

These reference samples are now permanently located at GRS or CGL-GRS laboratories, having been catalogued to cover most colors being produced to date with every known method. A database on these diamonds comprises 1200 spectra. From this database, we have selected both natural blue and synthetic blue diamonds produced by HPHT and CVD growth for direct comparison (Part A). In Part B we charactarize the CVD-grown pink diamonds.

Standard gemmological analyses included the study of internal growth features and inclusions with a gemmological binocular microscope set at 60x magnification including dark-field and fiber-optic illumination. Reaction to UV excitation was examined in a dark room with a long-wave (365nm) and short-wave (254nm) illumination from a UV lamp. A set of crossed polarizers mounted on a microscope were used to observe the birefringence patterns. An electrical conductivity tester was employed to measure the electrical conductance of the samples (see Fig. 4).

Fig. 2a: These CVD-grown diamonds produced by Orion PDC exhibit various tones of pink and blue color. CVD diamonds produced by Scio Diamond Technology USA, are yellowish brown.

Fig. 2b: This set of Fancy deep blue synthetic CVD diamonds from Orion PCD was offered in Hong Kong. The average weight of the stones is over 1.20ct each. Sets of same carat weight and color, calibrated diamonds are rare occurrences within natural colored diamonds.

Fig. 2c: An intense blue CVD diamond produced by Orion PDC weighs 1.1 ct, with VVS2 clarity. At $6,500 USD per carat, it is priced approximately 20 times less than its natural diamond counterpart. Such a huge price disparity creates a potential for fraud.

Fig. 3: These faceted synthetic blue diamonds were tested for this report: four CVD diamonds grown by Orion PDC (on top), four synthetic HPHT-grown diamonds from Chatham, AOTC, Tairus (middle), and one natural blue diamond (bottom). One HPHT crystal is not shown. Color and carat weights of these stones range from light blue to intense blue, and from 0.30 to 0.65 carats respectively.

Fig. 4: This HPHT synthetic blue diamond tested by an electrical conductance meter reveals considerable electrical conductance. Natural blue diamonds would show similar behaviour. The new blue CVD diamonds have been found to be non-conductive.

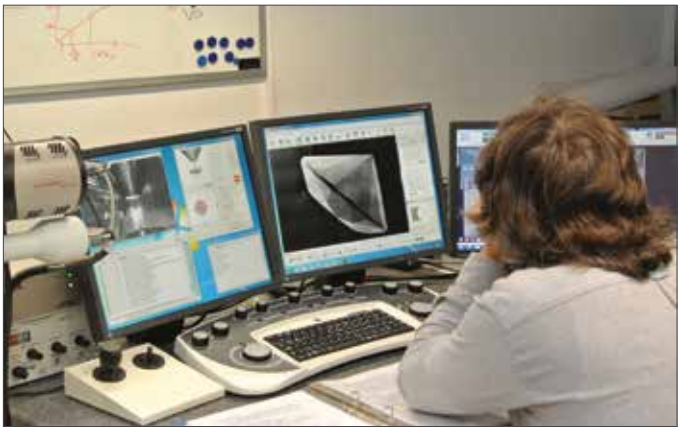

Fig. 5: A CVD blue diamond was exposed to an electron beam at low vacuum conditions in an Environmental Scanning Electron Microscope (Zeiss Evo 50 SEM) and a variable pressure secondary electron detector (VPSE) was able to produce images of differences in the charges located within the diamond (SEM-CC image), revealing details of the growth features. Operator PD Dr. Alfons Berger (in the picture). Results see Fig. 10-12.

A custom-built UV-VIS-NIR instrument using a quadruple-channel Czerny-Turner spectrometer and two broadband light sources recorded the spectra in the wavelength range from 240 - 1100 nm on all samples (Fig. 6, right side). This apparatus enabled the detection at liquid-nitrogen temperature (LNT) of very weak absorptions with spectral resolution better than 0.2 nm.

Photoluminescence (PL) of all samples was analysed at LNT using a custom-built spectrometer working with 405 nm and 532 nm excitation lasers. PL measurements were performed in a wavelength range from 408 to 1100 nm range (Fig. 6 left side).

Infrared absorption spectra were recorded in the mid-IR range from 400 - 7800 cm^{-1} (resolution 4 cm^{-1}) at room temperature using a Perkin Elmer Spectrum Two FTIR spectrometer equipped with a ZnSe beam splitter.

An ED-XRF instrument (FISCHERSCOPE XUV773) was used to examine the trace elements within the diamonds. 24 elements in the range from sodium (11Na) to uranium (92U) can be measured with this instrument. The conditions were optimized for testing heavy elements (results Tab. 1).

SEM-charge contrast (SEM-CC) images were taken on one sample (HRef0164) using a Zeiss Evo 50 SEM with a Gatan Mono CL 3 device available at the Institute of Geological Sciences Bern (Switzerland). The imaging was performed at acceleration voltage 20kV, sample current of 0.5 nA with VPSE detector at low vacuum mode (pressure 18Pa) (Fig. 5). The SEM-CC images of this synthetic CVD blue diamond are shown in Fig. 11. Chemical composition of the sample surface and inclusions located on the surface was analysed by EDX method (See Fig. 12) Exposure to electrons of the particular acceleration voltage is non-destructive. No alteration of color due to exposure to radiation is expected.

While these different methods were applied to all samples, only 2 synthetic blue diamonds (HPHT-grown and the new CVD-grown) have been selected to be measured by LA-ICP-MS analyses at the University (ETH Zurich) by Prof. Detlef Günther. One of the new synthetic blue CVD diamonds has been selected to be measured by SEM-CC at the University of Berne, Switzerland.

Results & Discussion

Visual characteristics

Visually, CVD diamonds grown by Scio Diamond and Orion PDC Diamond companies look very similar to natural diamonds. While colors of irradiated greenish blue and HPHT-grown deep blue diamonds look more intense or darker than their natural counterparts, the color intensity of CVD-grown blue diamonds varies from light to fancy, which is also common for natural greyish blue colored diamonds.

Most CVD-grown diamonds produced exhibit high clarity (VVS2-VS2). Based on this clarity it's not possible to distinguish them from similarly colored natural diamonds just by using a loupe or microscope. Colorless inclusions were present (Fig. 10b) and in certain directions , the growth features of the diamond could be seen (Fig. 10a). Similar features are observed by SEM-CC (Fig. 11b).

Examination in polarized light

The birefringence patterns of natural diamonds vary from type I (more intense interference colors) to type II (displaying a subtle 'tatami' pattern) and they are well recognized. The birefringence of synthetic diamonds, both HPHT-grown and CVD-grown, have distinct differences that assist identification of these diamonds [6]. All new blue color CVD samples are type IIa diamonds. Observed between cross-polarized filters, they produce two general patterns (see Fig. 7):

- A natural-looking pattern similar to 'tatami pattern' of type IIa natural diamonds (sample on the left), and
- Typical CVD pattern with stronger ADR reaction (samples on the right).

Fluorescence

A quick screening of loose and mounted diamonds is possible by using strong UV illumination in a darkened room. Some of our CVD-grown diamonds showed slightly stronger reaction to SWUV light than to LWUV light, but in most cases there was no noticeable reaction, both to LWUV and SWUV excitation.

The fluorescence test indicated that the new CVD material clearly contrasts to HPHT-grown synthetic diamonds (Fig. 8). HPHT synthetic blue diamonds show

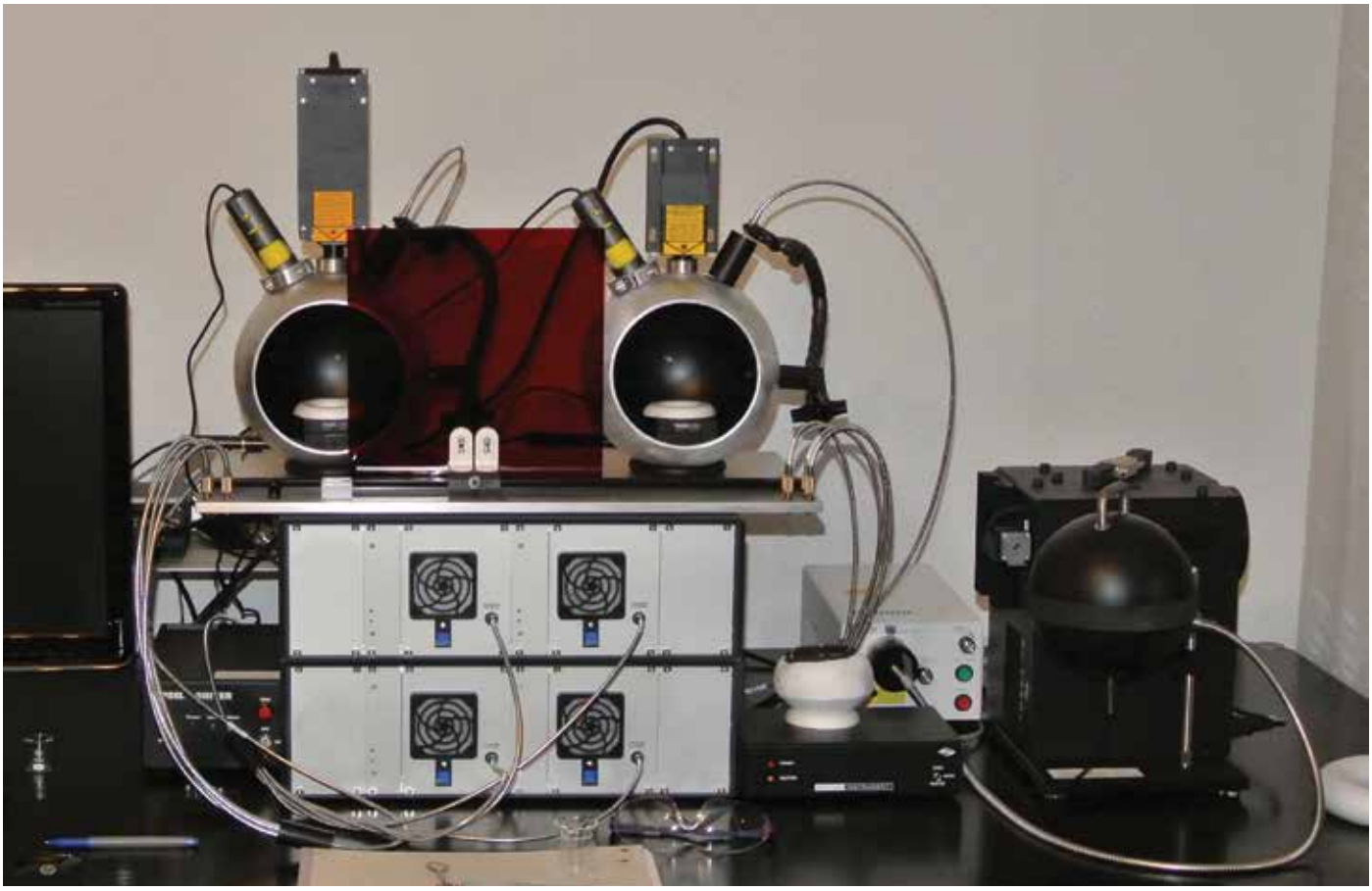

Fig. 6: An insider's look at the GRS diamond research laboratory instrumentation in Hong Kong and Switzerland. On the left side is the Photoluminescence analysis system with 2 Laser lights at 405nm und 532nm. The right side shows UV-VIS-NIR instrumentation. All measurements are conducted at liquid nitrogen temperatures. Results see Fig. 9a-9c.

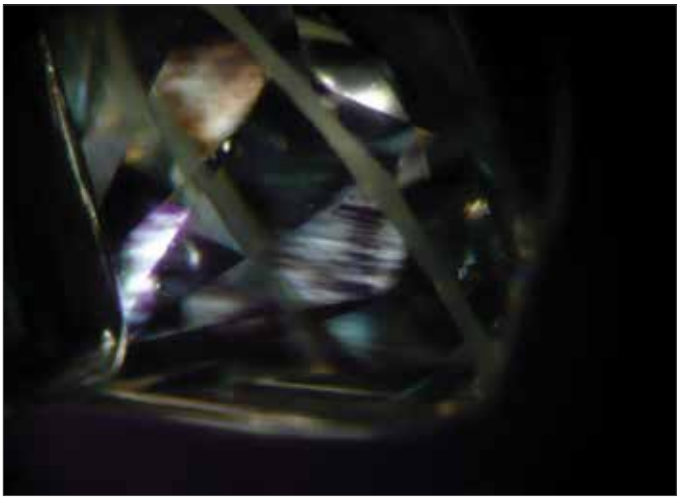

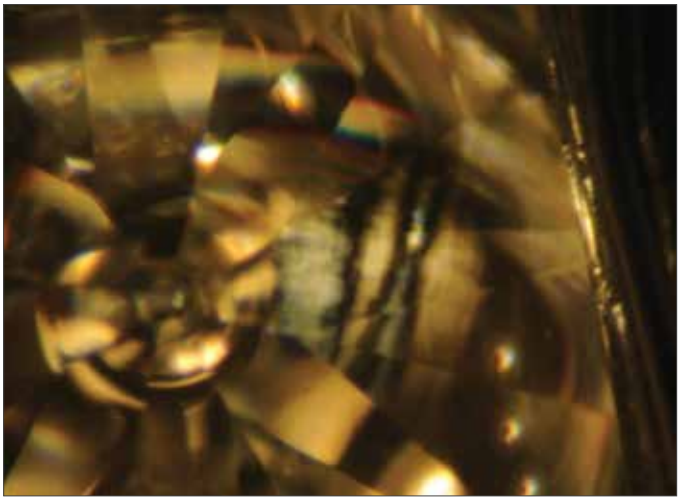

Fig. 7a, b: Birefringence pattern of two synthetic blue diamonds immersed in oil assisted by cross-polarizers under microscope.

weak to strong chalky yellow-green fluorescence under SWUV excitation. Much weaker fluorescence occurs when excited with LWUV light and weak to strong phosphorescence occurs under SWUV excitation. This typical reaction is well documented in literature [7]. The majority of Orion PDC blue CVD diamonds are inert under excitation with both wavelength 254nm and 365nm.

FTIR spectroscopy

The result of FTIR spectroscopy is shown in Fig. 9d. It appears that natural and HPHT-grown blue stones have typical spectra of type IIb diamond [8] with boron-related peaks at 1290, 2457 and 2802cm^{-1}. Intensity of these features is much stronger in HPHT-grown diamonds than in natural diamond, suggesting a much higher boron concentration. The CVD-grown blue diamonds reveal no presence of boron or nitrogen, thus they can be classified as type IIa. This is a common result for CVD diamonds [9, 10]. Non-commercial blue diamonds produced by CVD growth in the presence of boron have been documented in literature [11]. However, CVD diamonds from Orion PCD definitely do not owe their blue color to boron, but rather to some other defect. Although no optically active impurities with noticeable concentrations have been revealed by FTIR spectroscopy in blue CVD diamonds, traces of absorption of positively charged nitrogen (N^+ centre) could be detected in spectra (See Fig. 9d).

UV-VIS-NIR and PL spectroscopy

Four samples of CVD-grown blue diamonds have been thoroughly examined using absorption and photoluminescence spectroscopy at LNT (Fig. 9a-9c). Their spectra are compared to those of HPHT-grown synthetic and natural blue diamonds (Tab. 1).

Very intense SiV^- centre with zero-phonon line at 737nm (the most characteristic optical centre of CVD-grown diamonds [12]) was found as the dominating feature in both absorption and PL spectra. Although the absorption spectrum of SiV^- centre has a very complex multi-line structure, on average, its development over the visible spectral range is similar to that produced by boron. Absorption is the strongest in the red spectral range and it reduces towards UV spectral range. This results in preferential transmission of blue light and, consequently in blue body color. Yet, the silicon-related absorption has several specific features in the spectral range from about 490 to 540 nm (the main line at 546.6nm). The additional absorption in the green spectral range results in some greyish color modifier, as observed in the 0.65ct fancy greyish blue diamond (Tab. 2). This peculiarity differentiates the blue color of the studied CVD diamonds from the blue color of boron-doped type IIb natural and synthetic diamonds.

While the origin of these absorption features is unknown, we tentatively ascribe their origin to electronic transitions to the excited states with energy over 2.05 eV localized at negatively charged SiV^- defects. Since the energy levels of these states may lie in the conduction band [13] they are not visible in luminescence.

A number of sharp absorption lines in the spectral range from 830 - 950nm with the principal one at 946.3nm originate definitely from the SiV defects in neutral charge state (SiV^0) [14]. The SiV^0 defects are active in absorption only and they produce in PL spectra so-called 'negative luminescence' features (Fig. 9b and 9c). Thus based on these first results, we have strong evidence that blue color of the studied CVD diamonds is most probably caused by rather high Si-concentrations, either from the production process or by intention. Since SiV^- centre results from negatively charged SiV^- defects, its considerable stimulation may be achieved by co-doping with some donor-like impurities. Initial experiments indicate that co-doping with phosphorous and nitrogen even in a small concentration may considerably increase the intensity of SiV^- centre. It is quite possible that the N^+ centre detected in FTIR spectra results from the transfer of electrons from the residual donor nitrogen to SiV^- defects. Although no presence of other optically active impurities beside Si was observed in these diamonds, an intentional multi-species doping might nevertheless take place. For example, transition metals like Cr cannot be excluded. It is known that these impurities may produce optical centres similar to SiV^- [15].

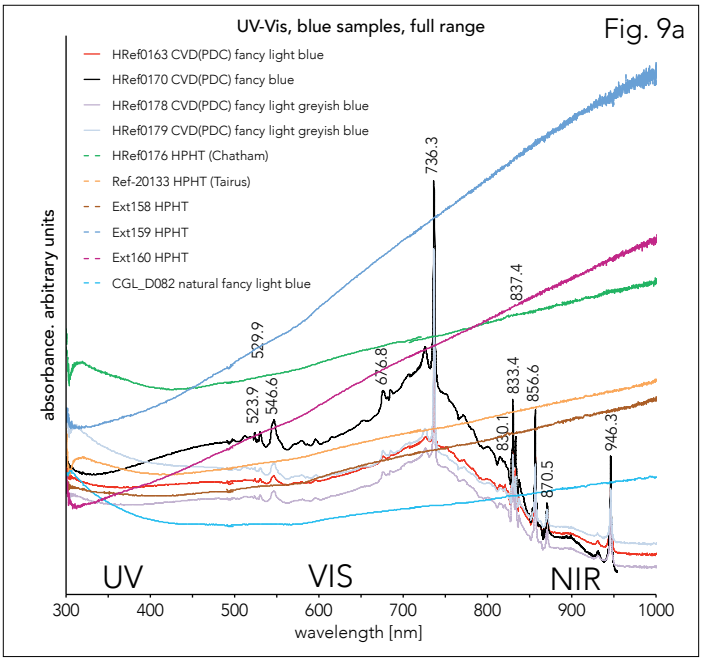

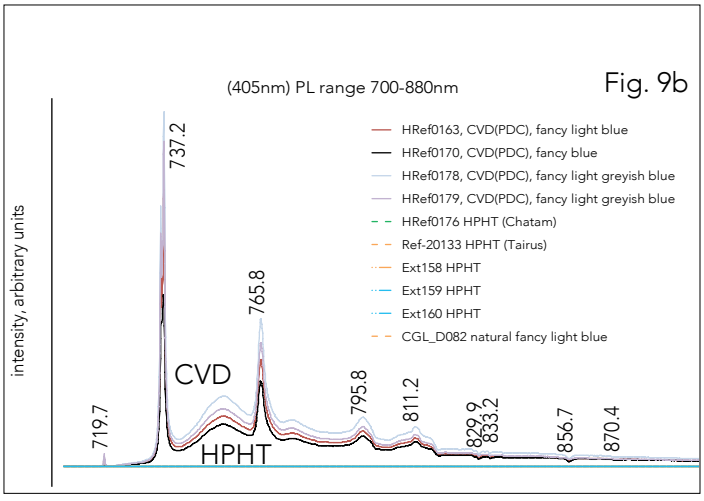

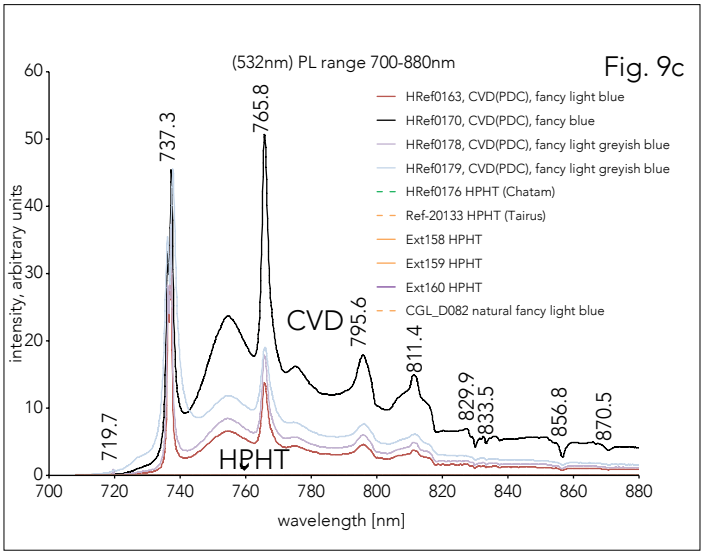

Fig. 9 a-c: UV-VIS-near IR absorption (a), PL (b, c) spectra of blue CVD diamonds. The SiV centre dominates in VIS absorption and PL spectra.

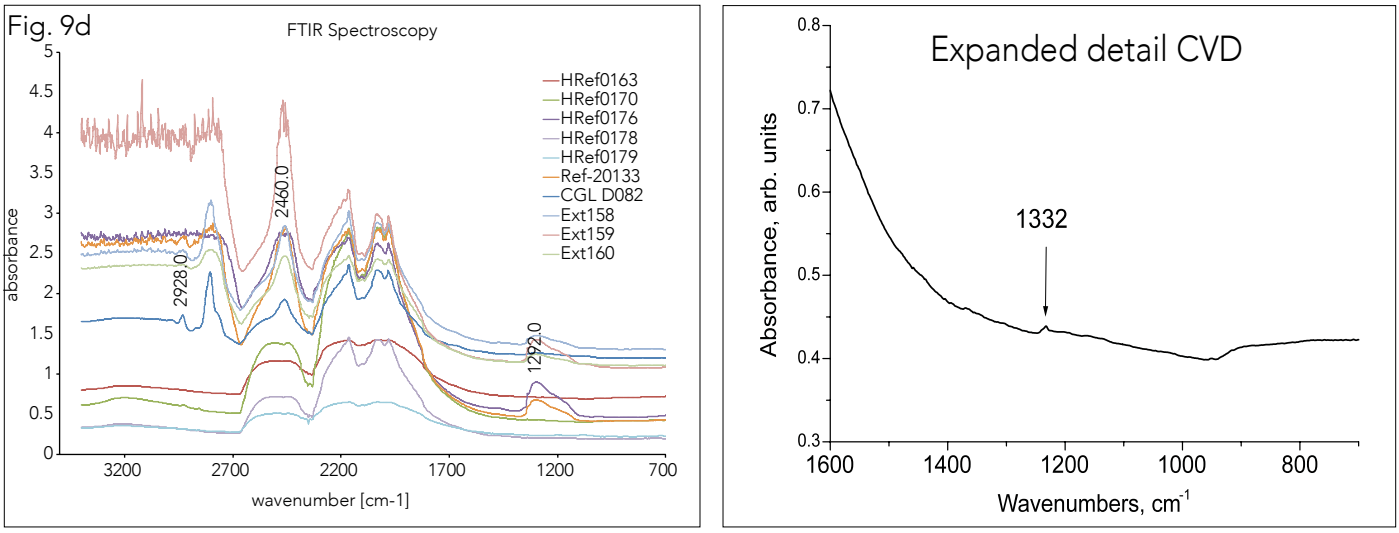

Fig. 9d: FTIR absorption spectra of blue CVD diamonds. Traces of boron are not detected in FTIR absorption spectra for the new synthetic diamonds as contrasted to their blue natural and HPHT-grown synthetic diamond counterparts (see legend). A trace concentration of N^+ centre (main feature at 1332 cm^{-1}) is detected in FTIR spectra of blue CVD diamonds.

Fig. 10a: Growth structure (striations) and color zoning in a CVD-grown blue diamond from PDC as seen through the microscope (100 mag. / fibre optic illumination). GRS collection (Sample No. HRef-0179). Photo AP.

Fig. 10b: Colorless inclusion in a CVD-grown blue diamond from PDC (100 mag. / darkfield / fibre optic illumination). GRS collection (Sample No. HRef-0170). Photo LH.

SEM charge contrast images revealed an interesting striation-like pattern of accumulated electron charge. Two sets of near parallel bands, the bands of one set being almost perpendicular to the bands of another set are seen (Fig. 11). Based on this first observation, we cannot produce a practical explanation for this structure, nor is it clear whether such a pattern is characteristic of CVD diamonds only. However, very tentatively, we ascribe this anomaly to some growth features developed during formation of diamond crystal in (100) plane.

SEM-ED-XRF analysis revealed the presence of particles on the surface of blue CVD diamonds inclusions containing Pb and Bi (Fig.12). The origin of these impurities is unknown. In order to determine if these elements were intentionally introduced during the growth phase, or whether they were captured in diamonds as contaminants of the growth medium, further investigation is required.

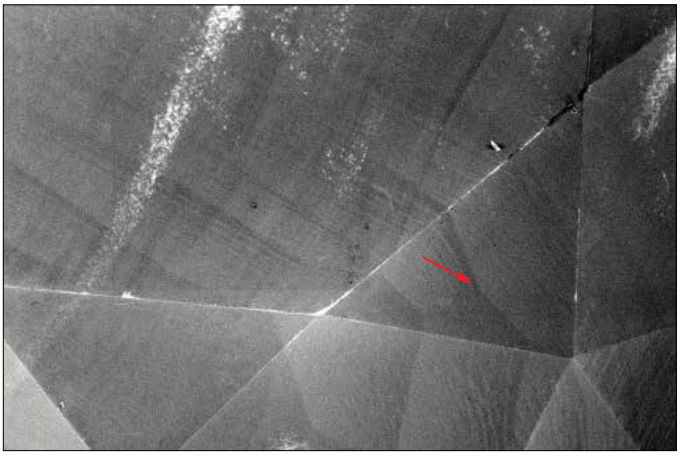

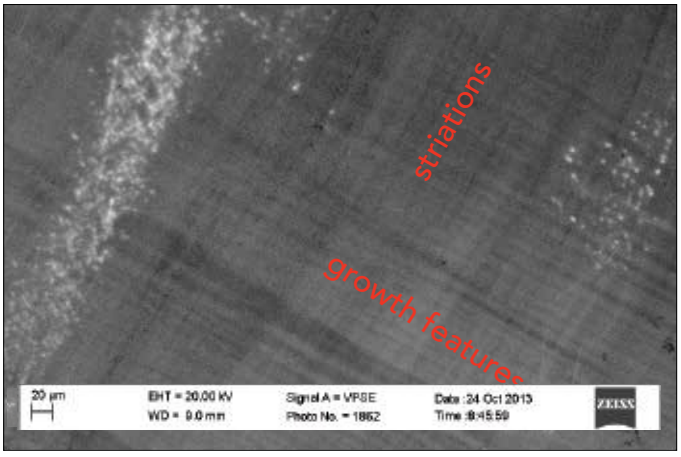

Fig. 11a, b: Two SEM-CC images exhibit assumed growth structure of blue CVD diamond. Fine bands of growth textures are observed outlining the shape (see red arrow) of the produced CVD crystal (Fig. 11a). In Fig. 11b, a detail of the growth features reveals these growth layers ranging from 5-20 microns wide. They are of varying thicknesses, slightly curved, and laterally discontinuing. Perpendicular to the zoning, a further feature (irregular striations indicated by different shades of grey tones) is visible and suggests irregularities in the diamond growth (picture on the right). These striations appearing throughout the diamond in the SEM-CC image could be related to different concentrations of an impurity which causes electrical contrast under electron excitation.

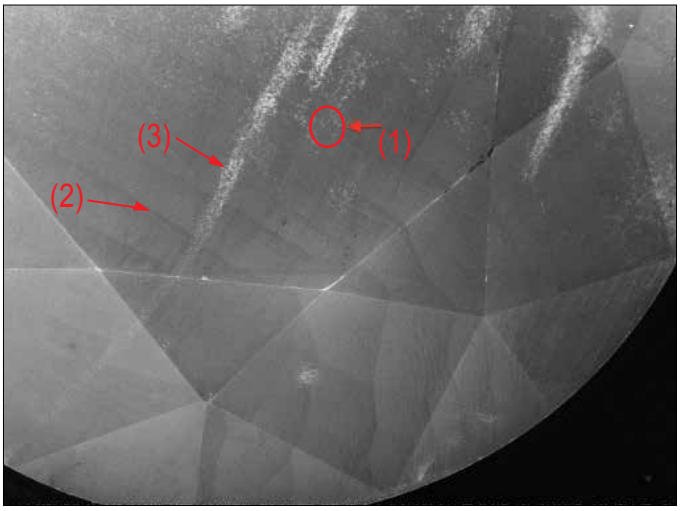

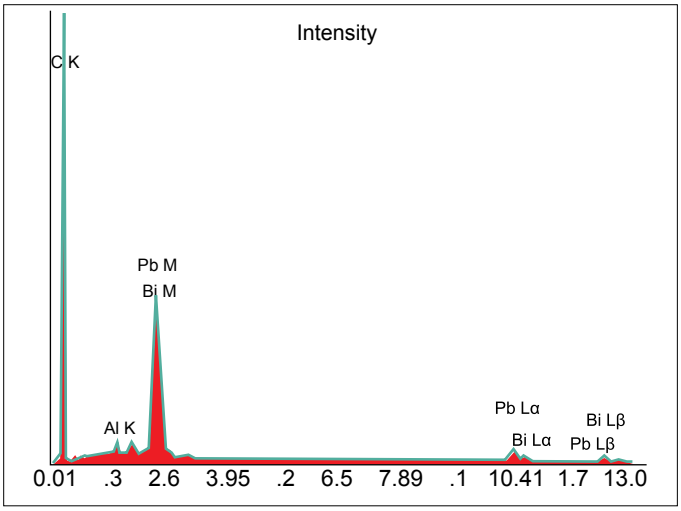

Fig. 12: SEM-CC image of a synthetic blue diamond produced by CVD (PDC Orion) shows the position of a sub-microscopic sized surface particle (1) that could be analysed (chemical spectra introduced). It was composed of Pb and Bi. Other features are also evident in the picture, such as growth structures (2) and bands of electric charges (3).

Laser Ablation ICP-MS Analasys

A set of three different synthetic CVD-grown diamonds were analysed for the trace element contamination, one HPHT-grown blue diamond, one Orion CVD-grown blue diamond as well as one Orion CVD-grown pink diamond. The measured element menu contained Li, Be, Bi, Mg, Si, S, Ti, Mn, Fe, Co, Cu, Sr, Zr, Nb, Ce, Tb, Ho, Hf, Ta, W, Pt, Pb, Bi and U. An ArF excimer laser ablation system (Resonetics, Resolution S155-LR) was coupled to an Element XR (Thermo Scientific, Bremen, Germany). The system was optimized for high signal intensities, a 232Th/238U ratio close to 1 and a 248ThO/232Th rate below 0.2% using a standard reference material from NIST (NIST SRM 612, National Institute of Standards and Technology, Gaithersburg, MD, USA). The settings for the laser ablation unit and the ICP-MS can be found in Table 1. The samples were analysed in low resolution (LR) (high sensitivity but mass resolution of 300) and medium resolution (MR) (typical only 10% transmission but higher mass resolution 4000). The LR allows measuring the sample with a high sensitivity but some of the transition elements (m/z 23 – 65) suffer from spectral interferences, thus those were re-measured in medium resolution to avoid those interferences.

Laser Ablation		ICP-MS	
Frequency	10 Hz	Nebuliser Gas	1.01 L/min
Crater	120, 172, 380 µm	Auxiliary Gas	0.97 L/min
Fluenz	10 J/cm^2	RF Power	1500 W
Helium	0.7 L/min	Scan Modus	Speed
		Pre Scans	3

Table 1: Settings for the Laser Ablation and the ICP-MS

Sample [nm/pulse]	120 µm	172 µm	380 µm	AVG
NIST SRM612	208	214	217	213
Blue Diamond HRef0163	51.4	44.7	48.1	48.1
Blue Splittered Diamond SRef50592		49.8	54.7	52.3
Pink Diamond HRef0161		54.7	53.1	53.9

Table 2: Ablation rates of the diamond sample and the NIST SRM612

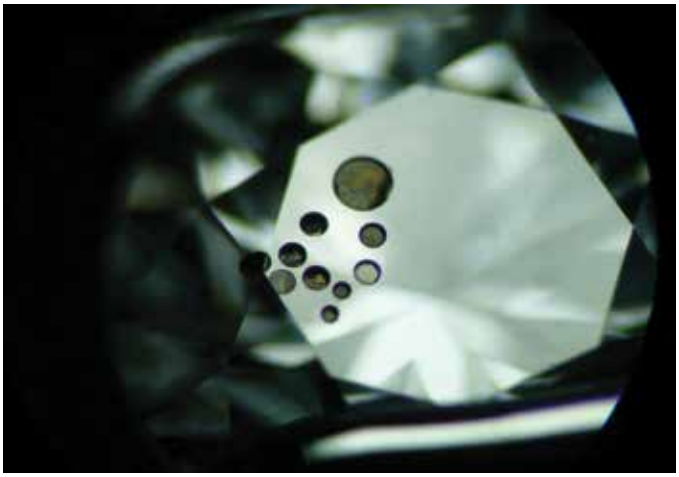

Fig. 13: 160 to 320 micron large LA-ICP-MS craters were produced during ablation of this synthetic blue CVD diamond from PDC. Traces of Bi and Pb were found in every measuring position and were located exclusively in certain internal layers within diamond.

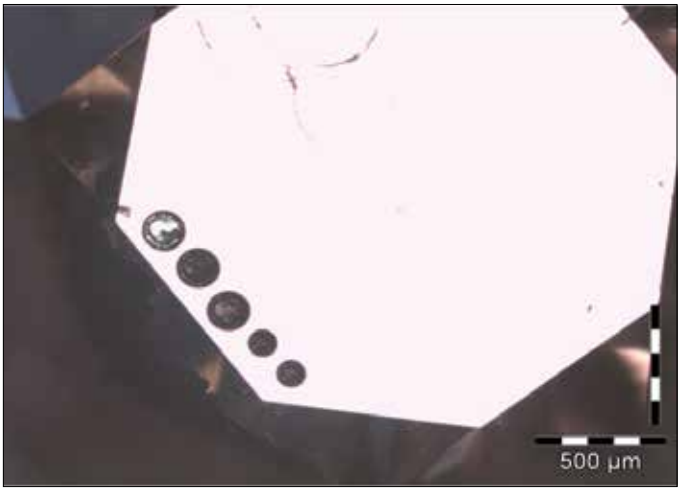

Fig. 14: Crater on the CVD-grown pink diamond sample. The same results were found during LA-ICP-MS (See Fig. 3) indicating that Bi and Pb are not causing the color in the CVD-grown blue and pink diamonds but are contamination products.

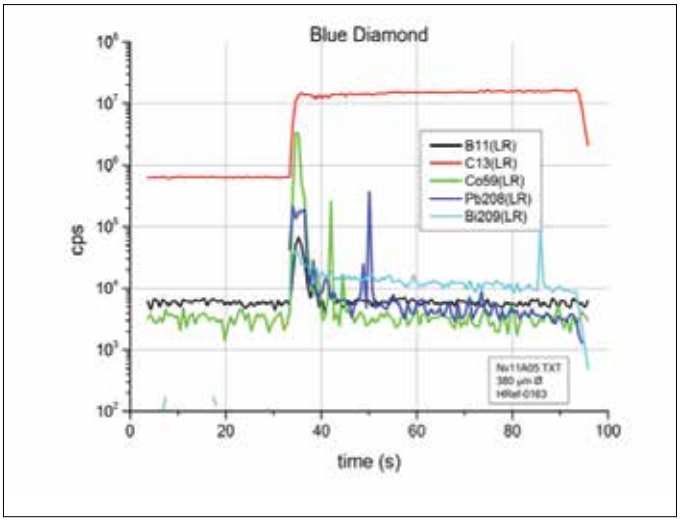

Fig. 15: The ablation characteristics of a CVD-grown blue diamond analysed with 380 µm crater showed Bi and Pb concentrations

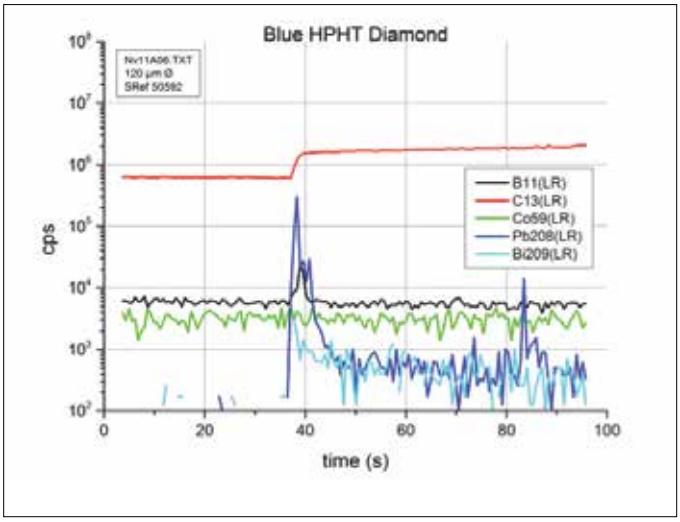

Fig. 16: The HPHT-grown blue diamond analyzed with a 120 µm crater revealed Bi and Pb concentrations.

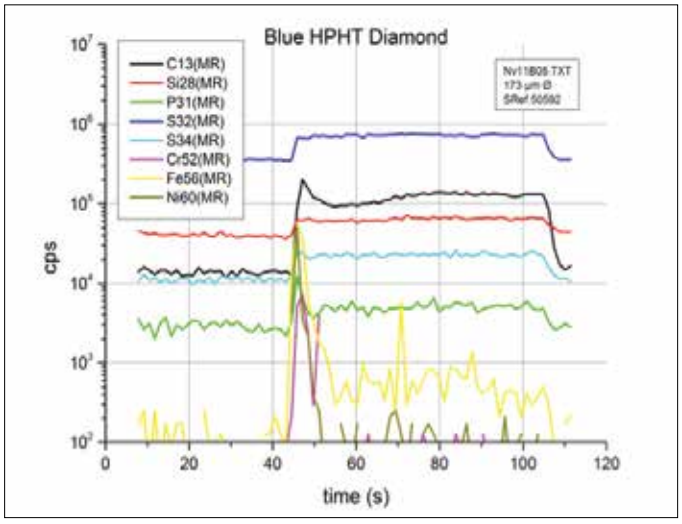

Fig. 17: The ablation characteristics of the HPHT-grown diamond showed concentrations of Fe.

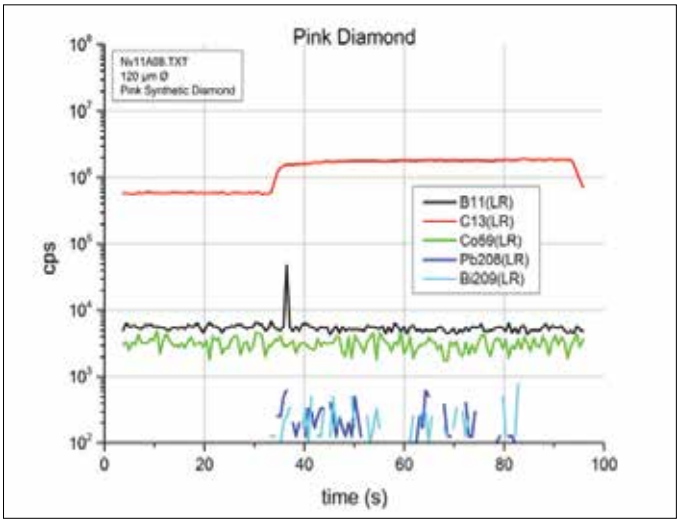

Fig. 18: CVD-grown pink diamond as analyzed with a 120 µm crater showed Pb and Bi- concentrations such as found in the CVD-grown blue diamonds (see Fig. 15)

Results

Ablation Rates

Diamonds and the NIST SRM612 glass do not have the same ablation rate; to have a comparison of the between the limits of detection and the sensitivity between the standard and the samples the crater depth after the ablation was determined using a petrographic microscope. The results are shown in Table 2.

Detected Elements

The blue CVD-grown diamond (HRef-0163) (shown in Fig. 13) has contamination of Pb and Bi. In MR no additional contamination was detected (see Fig. 15).

The blue HPHT diamond showed a slightly higher contamination with Pb and Bi than the blue CVD-grown diamond (Fig. 16), additionally an Fe contamination was detected in MR (Fig. 17).
The pink diamond showed only minor contamination of Pb and Bi, a slight elevation of Fe was detected in MR (Fig. 18).

Boron

No amount of boron was detected during the ablation of the diamond samples. The limits of detection was determined to be 2.4 and 0.34 ppm (µg/g) for 10B and 11B determined on NIST SRM612, this would translate to estimated limits of detection of 9.5 and 1.4 ppm respectively on the diamond samples.

The heavy elements Pb and Bi were detected above the background. The signal intensity was regularly recurring and indicated a layered structure to their occurrence in the sample. Based on the number of laser pulses and the total depth of the crater an estimation of their layers could be deduced. All replicates (n=5) showed a very similar structure with similar intensities. This phenomenon could be caused by the ablation of micro-inclusions. During SEM analysis, only a single Bi-Pb particle was found on the surface of the diamond. However, such particles were not homogeneously distributed over the diamonds' surface used for this analysis.

Therefore, it is unlikely that these signal intensities are caused by such inclusion-related effects. Furthermore, the variability in signal intensity of inclusions is much higher than those observed in our study. It seems therefore, that these two elements occur within different layers of the sample. The occurrence of the signals at nearly comparable distances indicates that these elements have been introduced into the sample either during production as impurities (due to the high volatility of these elements)

Conclusion

A new type of CVD-grown synthetic blue diamond has been discovered. We discovered that some of these CVD-grown diamonds can be identified by their characteristic strain-pattern under cross-polarized light conditions. These diamonds are inert to SWUV and LWUV illumination and reveal no specific phosphorescence characteristic of HPHT-grown and natural blue diamonds. Comparative analysis of new blue CVD diamonds with their HPHT-grown and natural counterparts using FTIR, UV-VIS and PL spectroscopy has revealed that these diamonds are of type IIa. They do not owe their blue color to boron impurities.

Because they are not doped with boron, the new blue CVD diamonds are not electrically conductive.

Thus, the new CVD-grown blue diamonds can be identified with the use of an electric conductivity tester for natural blue and HPHT synthetic blue diamonds which is available in the marketplace. This tester is useful for identification of irradiated blue natural diamonds which are of type Ia or IIa, and act as electric insulators.

The diamonds' blue color is attributed to a high intensity of the silicon-related SiV^- centre, which produces preferential absorption in the red spectral range. The SiV^- centre is so strong that it is the sole feature present in absorption and luminescence spectra taken in visible spectral range. By analysing the assembled data, we concluded that co-doping with silicon and some other impurity might be performed during the growth phase of blue CVD diamonds in order to stimulate efficiency of the SiV^- centre.

After conducting heat- and irradiation experiments on a CVD-grown grey-blue diamond from Orion (PDC) it can be clearly seen in absorption spectra, that the major SiV^- and SiV^0 centres do not change their intensity upon irradiation, suggesting that the concentration of SiV defects do not change either. Nevertheless the introduced radiation defects may considerably alter the position of Fermi level and hence alter the charge state of SiV defects. This result is quite obvious because the

formation of SiV defects requires annealing, during which vacancies become mobile and get trapped by Si atoms (see Appendix - Box 1)

Chemical analysis performed on the blue CVD diamond has identified the elements Pb and Bi as the major contributing impurities. Pb and Bi are heretofore unknown impurities in diamonds, so their influence on optical properties of diamonds has not been studied. Therefore at this stage, we cannot presume that these impurities were intentionally introduced in diamonds for the purpose of stimulating the SiV^- centre.

The trade and the public need to be made keenly aware of this discovery, particularly in light of the fact that the seller promotes this material as real diamonds in the marketplace [16]. Other types of synthetic blue diamonds (HPHT) are doped with boron corresponding to the trace elements found in nature. But they must be clearly described as lab-grown, and truthfully labelled as synthetic diamonds. This new generation of synthetic diamonds is different in that the origin of color is related to Si and possibly a dopant. Therefore, these new synthetic blue diamonds origin of color is not the same as is found in natural diamonds. Furthermore, they are synthetic and should not bear the conflicting misnomer of real diamonds. They may accurately be described as "CVD-grown blue diamonds", however.

Major lab-created diamond manufacturers such as AOTC, Chatham, Gemesis and Scio Diamond are transparent in their disclosure and cooperative within our trade. For example our suppliers of the Orion PDC diamond samples had to sign an agreement upon purchasing the samples that he discloses the fact that the purchased diamonds are man made in case he wants to re-sell them.

The majority of their diamonds are certified. Still, there are synthetic diamonds that reach laboratories undisclosed, and there are also synthetic diamonds brought in by individuals who bought them believing they are natural diamonds. Today, an increasing number of facilities grow diamonds, especially in Asia due to lower production costs. It appears that the CVD technology is increasingly employed to grow both near-colorless and colored diamonds. This development makes it imperative to screen melee and small colored diamonds parcels for determination of synthetic origin as well as for color origin, especially in the Asian markets.

Acknowledgements

We are grateful to Dr. A. Berger and Prof. K. Ramseyer of University of Berne for SEM-CC testing. Bill Vermeulen of CGL–GRS Swiss Canadian Gemlab and Diana Jarrett for editing the text and Lawrence Hahn for the inclusion photo.

Appendix - Box 1:

Heat & irradiation experiments with Orion (PDC) CVD-grown grey-blue diamonds

Heat-treatment experiment

An Orion (PDC) CVD-grown grey-blue diamond (HRef0179) was heated at a jewellery workshop in Vancouver, BC to approximately 900-1000 degrees °C with jewellery torch for 10 seconds in open air while diamond is protected by methyl hydrate from completely burning in air. Afterwards, the sample was boiled in acid to remove any surface marks from heating.

Fig. 19: 0.11ct Fancy grey-blue CVD grown diamond before (left) and after heating in air (right)

Results

The blue color very slightly modified to more grey but generally stayed the same, grey-blue, because SiV^- centres at 737nm (Si^-) is very stable and are not affected by this temperature (see below VIS spectra in absorption HRef0179 sample see Fig. 21). Heat did not remove color in the UV region of spectra. Spectra acquired by FTIR, UV-Vis, PL405 and PL532 before and after heat-treatment produced no distinctive differences. If a GR1-centre was present, it would have been annealed since it is not stable above 800 °C (Collins 1982). These results are consistent with heating experiment done at City University of New York (USA) by Prof Zaitsev when another CVD-grown Orion bluish grey diamond was heated at 700 °C for 2 hours in a graphite container under vacuum at about 1e-6 mbar and at 1400 °C. Again, grey-blue color of CVD-grown diamonds was not due to GR1-centre but rather is caused by the strong Si vacancy-centre at 737nm.

Irradiation experiment

Following the heat experiment, an irradiation experiment was conducted at College of Staten Island, City University of New York (USA) at the same Orion (PDC) CVD-grown grey-blue diamond (HRef0179) with the parameters of irradiation as following:

Electrons of energy 1.2 MeV at a dose of 1x1018cm^{-2} (1e18 cm^{-2}).

Heat & irradiation experiments with Orion (PDC) CVD-grown grey-blue diamonds

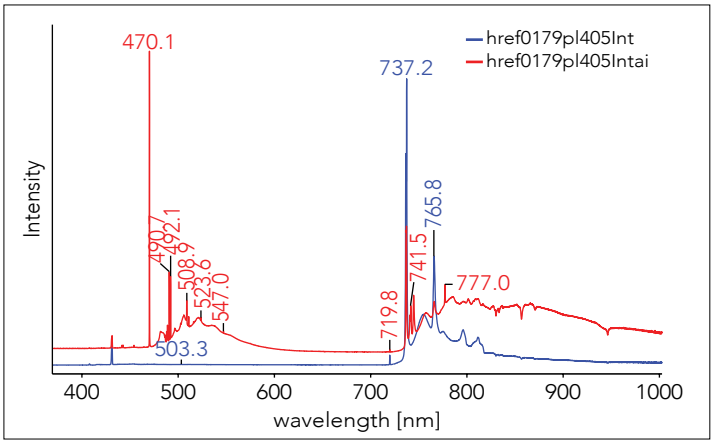

Fig. 20: Comparison of the PL spectra acquired with a 405nm laser before (blue spectra) and after irradiation (red spectra). Irradiation created many optical centres, the most intense of which are TR12 centre (ZPL at 470.1 nm) and GR1 centre (doublet ZPL at 741 and 744 nm). Less intense ZPL are at 490.7 and 492.7 nm. The peak at 503.2nm (H3-centre) was present before irradiation and absent after irradiation.

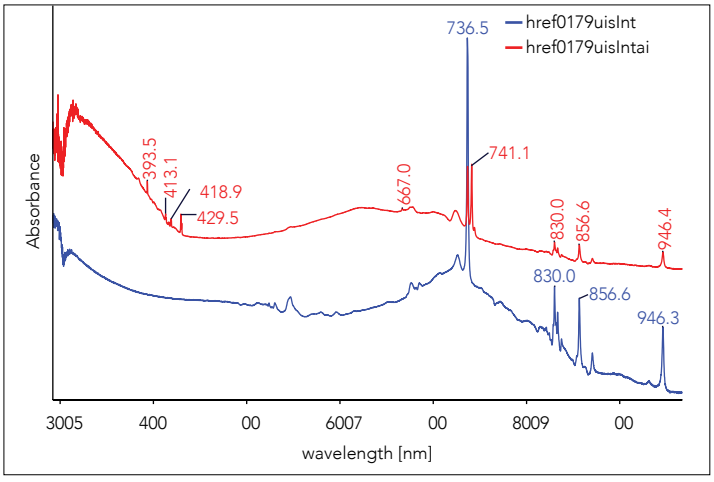

Fig. 21: Comparison of the UV-VIS spectra before (blue spectra) and after irradiation (red spectra). The main feature reveals a very pronounced peak at 741nm (GR1) after irradiation, which was absent before the experiment. Another feature are bands between 390 and 435nm (with main bands at 393.5 (ND1), 413.0, 419.0 and 429.5 nm) and very weak TR12 centre (ZPL at 470 nm). The SiV^+ centre with the main feature at 547 nm has reduced 4 times as compared with its intensity before irradiation. The SiV^- and SiV^0 centres have not changed their intensity after irradiation

Results

The color changed dramatically from light grey-blue to fancy dark blue after irradiation. Analysis of the UV-VIS and PL absorption spectra taken before and after irradiation of Si-doped CVD diamond illustrates this fact (Fig. 20 and Fig. 21).

Conclusion

After electron irradiation, Si doped CVD diamonds reveal many typical radiation centres in PL and UV-VIS absorption: GR1 (doublet ZPL at 741 and 744 nm, TR12 (ZPL at 470.1 nm), ND1 (ZPL at 393.5 nm). As it is clearly seen in absorption spectra, the major SiV^- and SiV^0 centres do not change their intensity upon irradiation, suggesting that the concentration of SiV defects do not change either. Nevertheless the introduced radiation defects may considerably alter the position of Fermi level and hence alter the charge state of SiV defects. This result is quite obvious because the formation of SiV defects requires annealing, during which vacancies become mobile and get trapped by Si atoms. As a result of the preliminary experiments on heating and irradiation carried out thus far, we believe that Orion grey-blue CVD-grown diamonds were not heat-treated or irradiated after growth.

Producer	CVD-grown - Orion PDC 4 samples	Natural 1 sample	HPHT synthetic - Chatham 1 sample	HPHT synthetic - Tairus 1 sample	HPHT synthetic 3 samples
Color	light blue, fancy greyish blue, fancy light greyish blue	very light blue	fancy blue	fancy blue	fancy blue
Clarity	VS1 to VS2	SI2	I1	I1	SI to I
Solid Inclusions (at 60x magnification)	transparent crystals, clouds and pinpoints	none	black metallic inclusions, feathers	black metallic inclusions	black metallic inclusions, feathers
ED-XRF	none	none	Fe, Co	Fe, Co	Fe, Co
SEM-EDS	Pb, Bi	not measured	not measured	not measured	not measured
Fluorescence SWUV (254nm)	inert	inert	medium to strong milky green; phosphorescence	medium to strong milky yellowish green; phosphorescence	weak chalky green; phosphorescence
Fluorescence LWUV (365nm)	inert	inert	very weak light orange	inert	inert
Cross Polarized Filters (CPF)	irregular pattern or "tatami pattern"	weak pattern	no pattern	no pattern (straining around black metallic inclusion)	no pattern
FTIR spectroscopy (absorption, cm^{-1})	type IIa, weak bands at 1340 and 1332cm^{-1}	type IIb, Boron related bands at 2455, 2802, 2928, small 1332 and 1303cm^{-1}	type IIb, very strong Boron related bands at 2455, 2802cm^{-1}, oversaturated above 2750cm^{-1}	type IIb, very strong Boron related bands at 2455, 2802, oversaturated above 2750, band at 1332 and 1292cm^{-1}	type IIb, very strong Boron related bands at 2455, 2802, oversaturated above 2750, band at 1332 and 1292cm^{-1}
UV-Vis-NIR spectroscopy at LNT (absorption)	prominent 737 band, peaks at 830, 833, 856, 870 and 946, additional peaks around 530 (523.9, 529.9, 546.6) and at 676.8nm	lack of sharp absorption bands, gradually increasing absorption towards near infrared (500 to 1000nm), slightly increasing towards the UV (420 to 300nm)	lack of sharp absorption bands, gradually increasing absorption towards near infrared (420 to 1000nm), slightly increasing towards the UV (420 to 300nm)	lack of sharp absorption bands, gradually increasing absorption towards near infrared (320 to 1000nm)	lack of sharp absorption bands, gradually increasing absorption towards near infrared (320 to 1000nm)
PL spectroscopy at LNT - 405nm	very strong 736 and 766 bands, peaks at 796 and 811; small to pronounced 719 peak; valley at 946nm	weak 741nm (GR1) due to natural irradiation	no PL features	no PL features	no PL features
PL spectroscopy at LNT - 532nm	very strong 736 and 766 bands, peaks at 796 and 811; small to pronounced 719nm peak	weak 741nm (GR1) due to natural irradiation	no PL features	no PL features	no PL features
Electrical conductivity	non-conductive	conductive	conductive	conductive	conductive

Table 3: Summary of tested natural and synthetic blue diamonds of different producers and synthesis methods including results of examinations.

References

[1] ZOHAR, E. 2012. Synthetics specifically made to defraud & exposing the fraudulent undisclosed synthetic diamond trail. Diamond Intelligence Brief

[2] http://www.business-standard.com/article/markets/demand-for-synthetic-diamonds-on-the-rise-113032300329_1.html 2013. Synthetic diamonds are gaining a foothold, Business Standard, India

[3] SHIGLEY, J.E., Ed., 2005. Synthetic Diamonds; Gems & Gemology in Review; Gemological Institute of America (GIA).

[4] DELJANIN, B., SIMIC, D., EPELBOYM, M. & ZAITSEV, A.M. 2006. Study of HPHT-grown diamonds by Advanced Optical Technologies Corporation (AOTC), Canada. International Research Conference, San Diego.

[5] DELJANIN, B. & SIMIC, D. 2007. Laboratory created diamonds – Guide to Identification of HPHT and CVD grown diamonds, GHI.

[6] SIMIC, D & DELJANIN, B. 2010. Identifying Diamond Types and Synthetic Diamonds with CPF (Cross Polarized Filters), D&S Gemological Service, 1st edition.

[7] SIMIC, D. & DELJANIN, B. 2007. Identification of Fancy Color Laboratory-grown Diamonds smaller than 0.09ct, De Beers Research Conference, Warwick.

[8] ZAITSEV, A. 2001. Optical properties of diamond. Springer-Verlag, Berlin, 227

[9] DELJANIN, B., HAINSCHWANG, T., FRITSCH, E., CHALAIN, J.P., KANDA, H., PONAHLO, J., SIMIC, D, KRZMENICKI, M., AKAISHI, M. & LINARES, R. 2004. Identification of CVD gem-quality, single crystal diamonds, as grown and HPHT-treated. ICNDST – Tokyo, De Beers Research conference, UK.

[10] WANG, W., D'HAENENS-JOHANSSON, U., JOHNSON, F.S.P., MOE, K. S., EMERSON, E., NEWTON, E. M. & MOSES, T. M. 2012. CVD synthetic diamonds Gemesis Corporation. Gems & Gemology.

[11] TALLAIRE, A., ISSAOUI, R., SILVA, F., MILLE, V., ACHARD, J.& GICQUEL, A. Growth of thick highly boron-doped diamond single crystals by CVD.

[12] VAVILOV, V.S., GIPPIUS, A.A., . ZAITSEV, A., DERYAGIN, B.V, SPITSYN, B. V. & ALEKSANKO, A. E. 1980. Fiz. Tekh. Polopruvodn. 14, 1811, (1980), sov. Phys. Semicond. 14, 1078.

[13] K. IAKOUBOVSKII, K & ADRIANSSENS G. J.2000. Phys. Rev. B 61, 10174.

[14] D'HAENENS-JOHANSSON, U. F. S., EDMONDS, A. M., GREEN, B. L., NEWTON, M. E., DAVIES, G., MARTINEAU, P. M., KHAN, R. U. & TWITCHEN, D. J. 2011. Phys. Rev. B 84, 245208.

[15] KIM, K. H., AKASE, Z., SUZUKI, T. & SHINDO, D. 2010. Charging Effects on SEM/SIM Contrast of Metal/Insulator System in Various Metallic Coating Conditions. Materials Transactions, 51, 1080-1083.

[16] www.gemresearch.ch/news 2013. Early Warning Alert: A new type of synthetic blue diamonds produced by CVD appeared on the market. GRS Gemresearch Swisslab.

New Generation of Synthetic Diamonds Reaches the Market

Part B: Identification of treated CVD-grown Pink Diamonds from Orion (PDC)

Deljanin B. [1]*, Herzog F. [2], Bieri W. [2], Alessandri M. [3], Günther D. [4], Frick D.A. [4], Cleveland, E. [5,] Zaitsev A.M. [6], Peretti A. [7]

[1]CGL-GRS Swiss Canadian Gemlab Inc., Canada
[2]GRS Gemresearch Swisslab AG, Switzerland
[3]GRS Lab (Hong Kong) Ltd, Hong Kong, China
[4]Laboratory for Inorganic Chemistry, ETH Zurich, Switzerland
[5]Delaware, USA
[6]The City University of New York, USA
[7]DR Peretti Co LTD, Thailand and GRS Laboratories

*Corresponding author: branko@cglworld.ca

Introduction

Natural pink diamonds, particularly those over 0.5ct and intense color are very rare, what makes them both highly precious and in great demand in the diamond market. Today, natural pink diamonds for the most part come from Australia, from the Argyle mine [1,2]. However, only 10% of all pink diamonds coming from that mine are larger than 0.2ct, so screening pink small and melee diamonds for treated and synthetic origin is a very important task of gem laboratories. One of the biggest challenges today in gem industry is to quickly identify the origin of color of pink diamonds - natural, treated or synthetic.

Nowadays the color enhancement is widespread and the aim of the color treatment is to provide stable changes in internal defect structure and produce pink color. The main technologies used for color enhancement of pink diamond include processing at high pressure and high temperature (HPHT), irradiation and subsequent annealing [3]. In the last decade we documented increased use of a new multistep method utilizing these three treatment techniques to produce rare pink colors and even large stones over 10ct were enhanced with this method [4]. Major gem laboratories have identified color surface enhancement processes (plasma deposition of hard ceramic coatings) with limited color stability that is observed primarily in pink diamonds in 2006 [5,6]. Laboratory grown yellow diamonds produced by HPHT process and brownish diamonds produced by CVD process are post-treated with irradiation/annealing to make pink color that became very popular and fashionable [7, 8]. Synthetic diamond producers like AOTC Canada and Scio Diamonds USA increased their production of pink lab-grown diamonds by 5-10 percent over the last 5 years to meet higher demand for more affordable but still stable color. As a consequence a new generation of pink CVD-grown diamonds, produced by "Orion PDC" and "Scio Diamond" were brought onto the market. They are of much more "natural looking" fancy colors (orangy pink and purplish pink) and higher clarity (VVS - VS); they are available in all sizes and harder to identify than HPHT-grown pink diamonds with standard instruments. The most widely used methods for separation of natural, treated and synthetic pink diamonds are optical methods (absorption and photoluminescence) that are used in our study as well to identify these stones as CVD-grown pink diamonds.

We concluded that it is possible to separate pink CVD-grown Orion (PDC) diamonds from natural pink diamonds (Argyle), from multistep treated pink and HPHT-grown pink diamonds by use of a combination of standard and advanced gemological instruments described in detail below.

Keywords: Synthetic, CVD-grown, pink diamond, type IIa, irradiation

Materials & Methods

GRS and CGL-GRS labs acquired 4 pink CVD-grown diamonds from a new producer Orion (PDC) in Hong Kong (see article on "Blue CVD-grown diamond", Part A, [9]), and compared them to pink diamonds of different origin from our research collection:

- 4 Natural pink diamonds, natural color from Argyle
- 2 Natural pink diamonds, natural color of unknown origin
- 1 Natural pink diamond, multistep treated (HPHT, irradiation and subsequent annealing) by Suncrest Diamonds, USA
- 2 CVD-grown, HPHT enhanced, irradiated and annealed diamonds by Scio Diamond, USA,
- 3 HPHT-grown and irradiated diamonds by Chatham, USA
- 1 HPHT-grown and irradiated diamond by Russian producer, USA
- 1 HPHT-grown and irradiated diamond by AOTC, Canada

The same methods were used as described in part A [9] and an additional luminescence microscope. A Zeiss Axioplan microscope with an external Mercury Short Arc HBO100 W/2 light source (excitation range: 395 – 440 nm) was used to produce luminescence images by UV Luminescence Microscopy.

Fig. 2a: This HPHT-diamond laboratory of Ziemer Swiss Diamond Art AG (Port, Switzerland) shows a recent example of an upcoming factory producing lab-grown diamonds by BARS split sphere technology. Compare with CVD-diamond factory (Part A, Fig. 1[12])

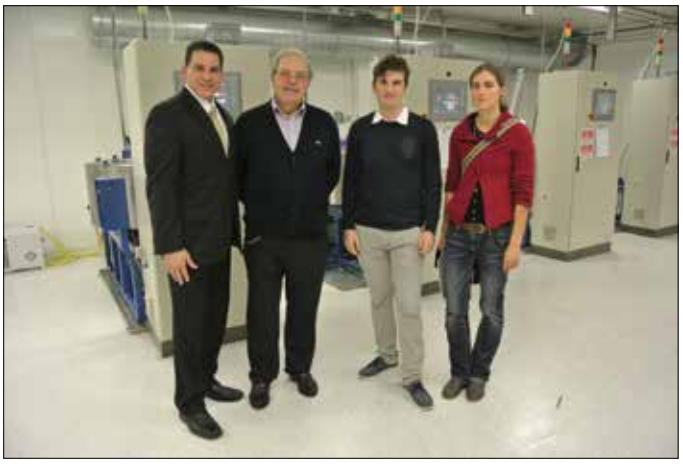

Fig. 2b: The expert group during the inspection of the HPHT laboratory in Switzerland from left to right: R.E. Chodelka (CEO and Chief Technical Officer of Ziemer Swiss Diamond Art AG, former technician at Gemesis Diamond Company, California), K. Ziemer (founder of the Ziemer Group AG) with GRS gemologists W. Bieri and F. Peretti.

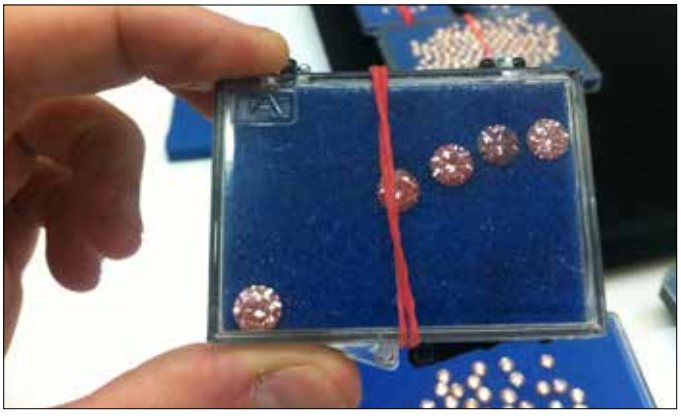

Fig. 1: A series of CVD pink diamonds from PDC Orion as offered on the market in September 2013 in Hong Kong. The CVD-grown diamonds are 1.2ct each.

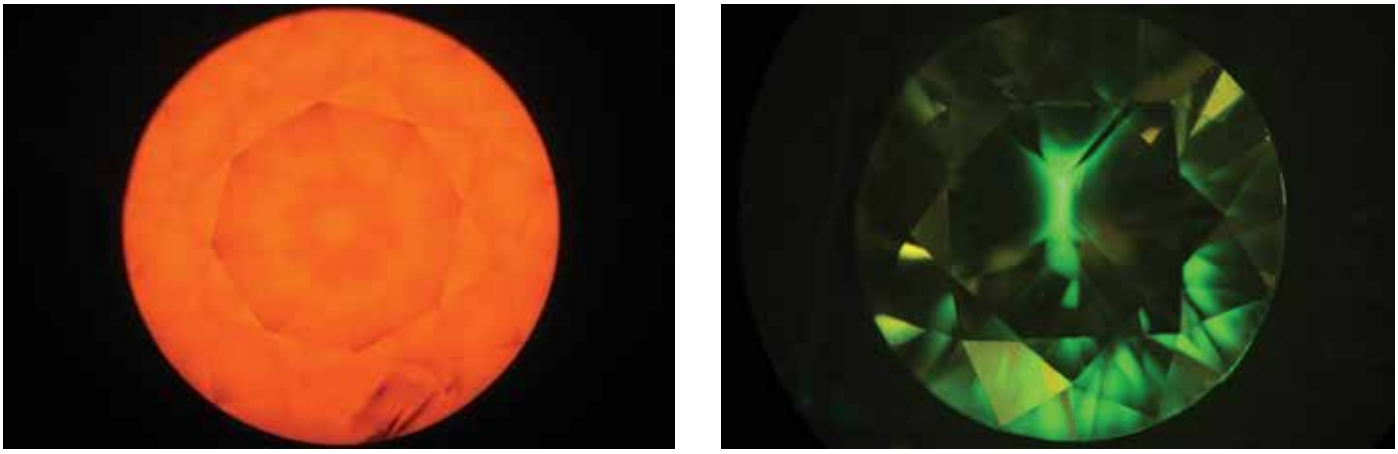

Fig. 3a-b: These 2 pictures were taken in the fluorescence microscope. A HPHT diamond of 0.70ct of the GRS collection showed a very characteristic geometric cubo-octahedral pattern under SW UV fluorescence and medium yellowish green reaction (right side). In contrast, the CVD synthetic pink diamond (left side) that was measured together with this sample in the same run showed strong pinkish orange uniform fluorescence reaction with no other structures than trails of black inclusions. (Photos WB).

Fig. 4: These faceted synthetic pink diamonds were tested for this report: four CVD diamonds grown by Orion PDC (on top), one CVD diamond grown by Scio Diamond, four synthetic HPHT-grown diamonds from Chatham, AOTC and Tairus (Russia). Color and carat weights of these stones range from Fancy light pink to Fancy intense pink, and from 0.05 to 0.60 carats respectively.

Results & Discussion

Visual characteristics

Visually, pink CVD-grown diamonds grown by Orion PDC Diamond companies look very similar to natural diamonds or Scio pink CVD-grown diamonds, mostly in Fancy color grade with orange or purple modifiers. HPHT-grown pink diamonds tend to have more nitrogen than CVD –grown diamonds and colors are usually darker, more intense and more purplish, and it's the similar case with natural diamonds that are multistep treated to make pink colors.

As in case with blue CVD-grown diamonds, most pink Orion PDC CVD-grown diamonds exhibit high clarity (VVS2-VS2). Based on this clarity it's not possible to distinguish them from pink natural diamonds just by using a loupe or a microscope. Yet, in some CVD stones, black inclusions (assumed to be non-diamond carbon) are visible and when located in one plane perpendicular to the direction of growth, they are a reliable indicator of the diamond's CVD origin.

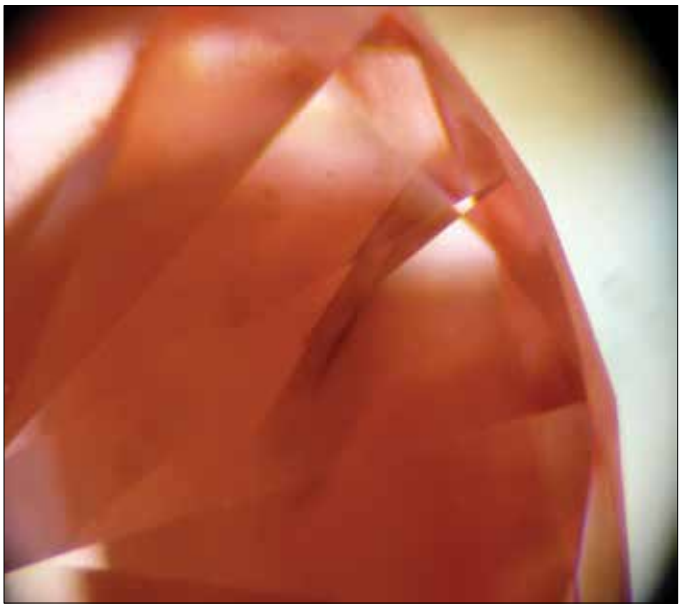

Fig. 5a: Blackish irregular clouds are found in this CVD-grown pink diamond from PDC (HRef0161-2)

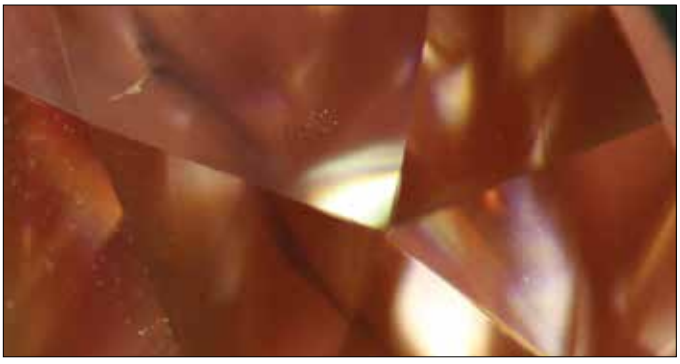

Fig. 5b: Blackish irregular clouds are found in this CVD-grown pink diamond from PDC (HRef-0172, 0.50ct, 80x, fiberoptic, L.H.)

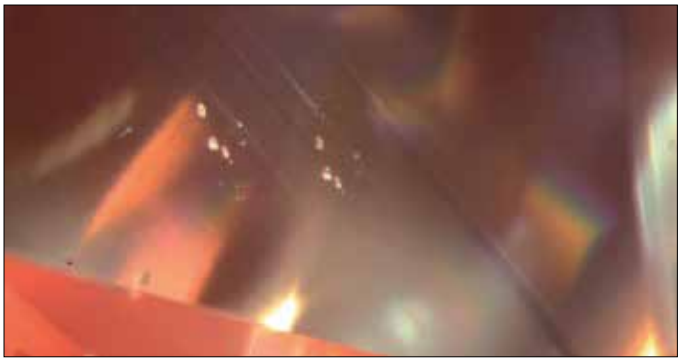

Fig. 5c: A blackish layer in a PDC CVD-grown pink diamond is accompanied by whitish particles and transparent crystals (HRef-0172, 0.50ct ,100x, fiberoptic, L.H.)

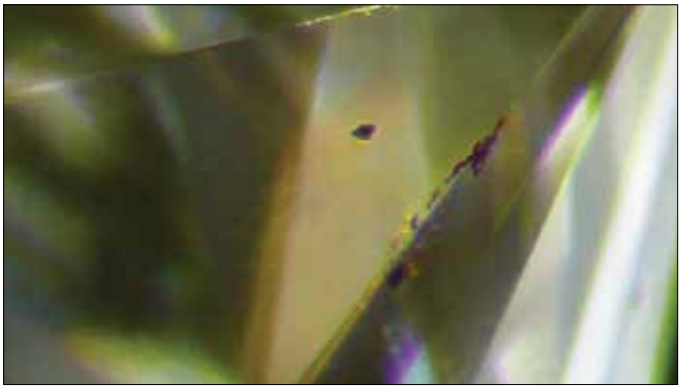

Fig. 6a-b: Black inclusion in a CVD synthetic diamond from Scio Diamond is assumed to be non-diamond carbon.

Examination in polarized light

The birefringence patterns of natural pink diamonds vary from type I (more intense interference colors) to type II (displaying a subtle 'tatami' pattern). The birefringence of synthetic pink HPHT-grown diamonds is not present and that assists with identification of these diamonds. All new-generation pink CVD samples are type IIa diamonds, low nitrogen diamonds. Observed between cross-polarized filters, they produce two general patterns:

- A natural-looking pattern similar to 'tatami pattern' of type IIa natural diamonds and
- Columnar pattern" typical for CVD–grown diamonds [10], see Fig. 7.

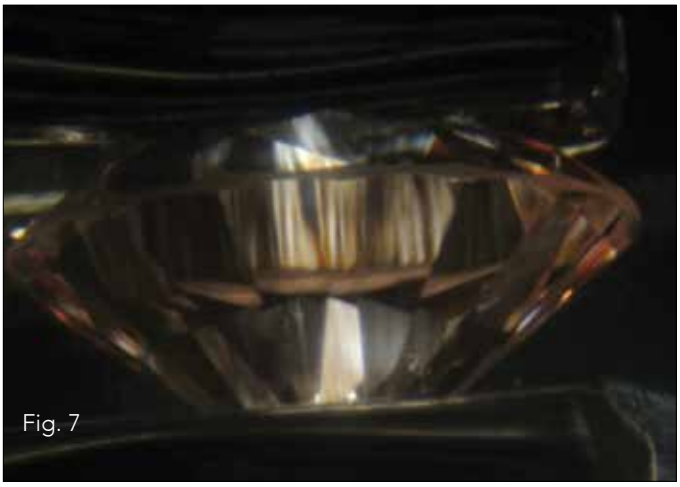

UV-Fluorescence

A quick screening of loose and mounted pink diamonds is possible by using strong UV illumination in a dark room. Natural Argyle diamonds studied for this project and by one of the authors (BD) in 2007 [5] are showing strong (LW) and weak (SW) blue florescence caused by N3 centre. On the contrary multistep treated natural [23] and irradiated and annealed HPHT-grown and CVD-grown samples from different producers are displaying characteristic medium to strong orange florescence in LW/SW light caused by dominant N-V0 centre (575nm). The fluorescence test indicated that the new CVD material show similar reaction to UV light as Scio CVD-grown and HPHT-grown synthetic diamonds (Fig. 8) and it is not possible or very difficult to separate these 2 categories of synthetic diamonds based on the fluorescence test only. A weak orange phosphorescence was observed in one of the CVD-grown pink diamonds (see Table 1).

Fig. 7: A parallel "columnar pattern" perpendicular to the table (which reveals direction of crystal growth) is a strong indication that these pink diamonds are CVD –grown, in this case by Orion (CPF HRef-0162, CVD from PDC).

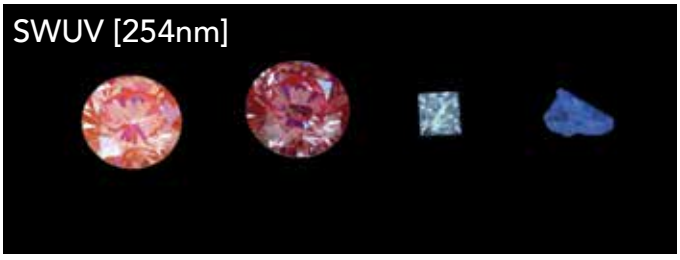

Fig. 8a-b: Comparison of fluorescence of synthetic and natural pink diamonds in Long Wave (LWUV) and Short Wave (SWUV) ultraviolet light. Note that a huge variety of color can be seen in fluorescence, blue typical for natural pinks, LW being stronger than SW. Synthetic pink diamonds show the same fluorescence in LWUV and SWUV in comparison to their natural counterparts.

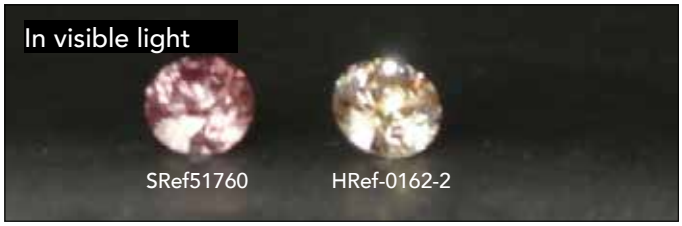

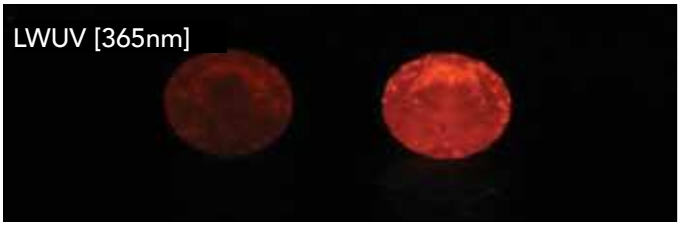

Fig. 9a-b: Synthetic HPHT-grown pink diamond and a brownish-pink CVD-grown diamond in day light and their fluorescence colors in Long Wave Ultraviolet (LWUV) light. Note the very strong pinkish orange fluorescence of the CVD-grown PDC diamond and strong orangy red fluorescence of HPHT-grown pink diamond caused by irradiation.

Box: Natural Pink and Red Diamonds from the Argyle Mine in Australia

The most prominent occurence of pink and red diamonds are known from the Argyle mine in Western Australia and a few examples of the color varieties, rough shapes are described below:

Fig. 10: Aerial view of Argyle mine, major source of pink diamonds since 1980's The Argyle mine located in the remote northwest of Australia first started producing diamonds 30 years ago and at its peak output produced 42 million carats from the lamproite pipe in 1994. Since then the output has dwindled to a recent low of 10 million carats, but with the current underground operation the annual output is expected to increase beyond 20 million carats. Argyle is the largest mine in the world by production, but produced mostly brown diamonds. Less than 0.1% of the production is pink diamonds, whereas almost three-quarters are brown hues popularly referred to as 'champagne', 'cognac' and 'chocolate' colors. Of it's total output, only a total of a few kilos of pinks are produced per year. These are mostly small diamonds and of that, only approximately 50 stones over 1 ct are found. These stones gain a lot of attention when sold in specially organized auctions (see Fig. 13a-d and Fig. 13a-b) / Fig. 10 - 14 Copyright Argyle Diamonds.

Fig. 11: The Argyle Mine is the world's only consistent source of Vivid Purplish Pink diamonds sold at breaking record prices at special tenders around the world, such as the one pictured.

Fig. 12: Variety of brown color crystals with one intense purple-pink crystal.

Box: Color Varieties of Natural Fancy Diamonds from the Argyle Mine, Australia

Fig. 13a: Variety of PURPLE colors.

Fig. 13b: Variety of Pinkish BROWN colors.

Fig. 13c: Variety of PINK colors.

Fig. 13d: Variety of Brownish PINK colors.

The Pink Diamond Tender 2000
Tokyo, Honk Kong, Sydney, New York, Geneva

Fig. 14a: 1.14ct GIA Fancy Deep PINK I1
HRD Fancy Intense Brownish PINK P1.

Fig. 14b. 1.66ct GIA Fancy Vivid Purplish PINK SI1
HRD Fancy Intense Purplish PINK SI2.

Fig. 14a-b: Same pink diamonds could receive different color and clarity grades from different gem laboratories, because grading of colored diamond is subjective and depends on color masters and grading standards used in various laboratories.

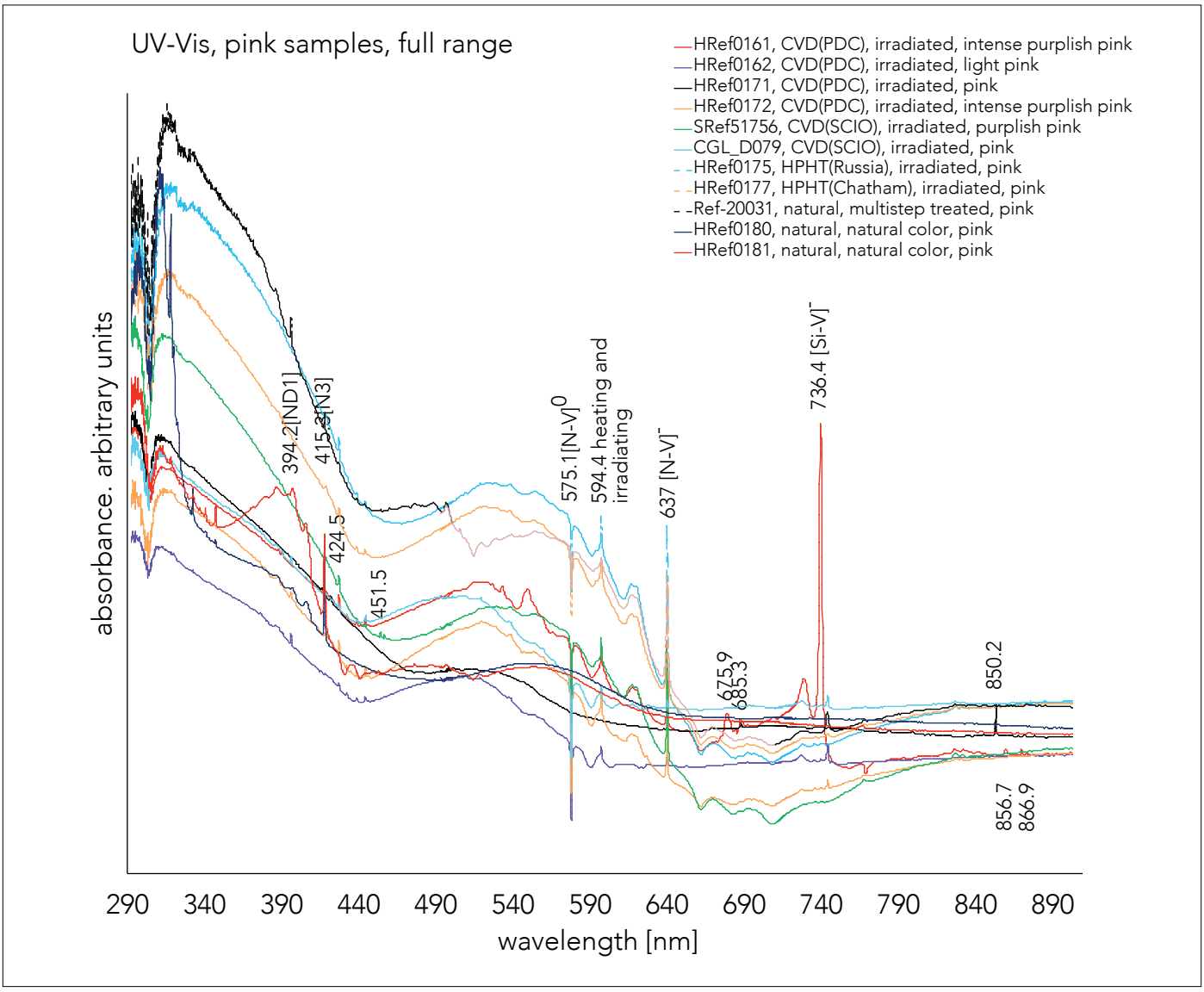

Fig. 15a: UV-VIS-near IR absorption of synthetic and natural pink diamonds as indicated. Spectra registered at Liquid nitrogen temperatures. For more details see the Fig 15b-d.

UV-VIS-NIR spectroscopy

The common dominating features of UV-VIS absorption spectra of the studied CVD pink diamonds are a broad band with maximum at about 520 nm, NV^0 (ZPL at 575 nm) and NV^- (ZPL at 637 nm) centres (Fig. 15b). Two diamonds also reveal strong presence of the silicon-related SiV^- centre with ZPL at 737 nm. The NV^0 centre is observed in the regime of luminescence suggesting its low efficiency in absorption, but high efficiency in luminescence.

Many weak absorption features have been found through the whole UV-VIS spectral range. In the spectral range of 380 to 460 nm, the studied pink CVD diamonds reveal numerous absorption features, the most common and obvious of which are lines at wavelengths 424.7, 436.4 and 441.9 nm. Traces of the 388 nm centre (a defect containing single nitrogen atom) and the ND1 centre (ZPL at a wavelength of 393.5 nm, negatively charged single vacancy) can be found in most Orion (PDC) too.

The main absorption feature distinguishing the studied natural pink diamonds from their CVD-grown and treated HPHT-grown counterparts is a pronounced N3 centre, which together with the 550 nm band ("Natural" Pink Band) and the 380 nm band are the dominating color centres (Fig. 15c). These two bands are among the most important optical centres. Indeed they come

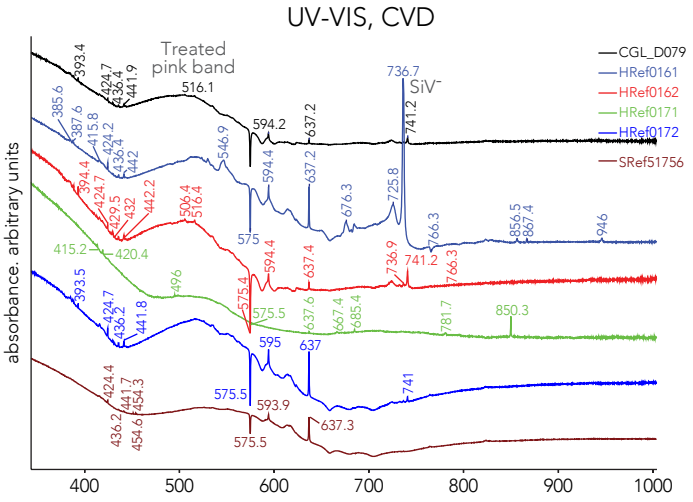

Fig. 15b

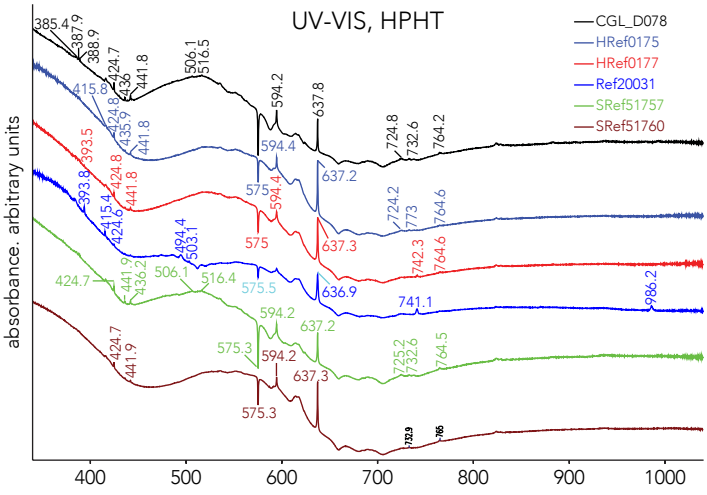

Fig. 15c

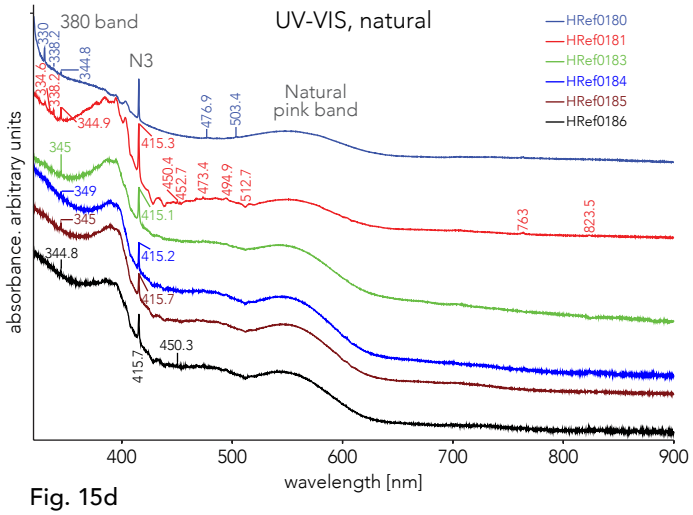

Fig. 15d

usually together in natural pinks, not in synthetic (both HPHT and CVD) pinks. Although their intensities do not correlate well, there is a tendency of stronger 380 nm bands in diamonds with a strong 550 nm band. Both bands are usually stronger in type I diamonds than in type IIa.

Thus it is quite possible that they originate from nitrogen-related defects. When the spectra of these bands are compared with the absorption spectra of nitrogen-related centres, it is seen that the spectral range of the 550 nm band coincides with that of the phonon sidebands of the NV^- centre, while the spectral range of the 380 nm band is almost the same as that of the N3 centre. Based on this match, one may come to an assumption that the 550 and 380 nm bands originate from defects similar to NV and N3 defects. The N3 centre is almost never seen in spectra of as-grown CVD diamonds. However traces of this centre can be detected in CVD diamond after HPHT treatment performed at temperatures high enough to cause aggregation of dispersed nitrogen atoms [12]. Very weak N3 centre has been found in absorption spectra of some studied CVD diamonds what suggests that these diamonds were subjected to high temperature annealing in their post-growth processing (Fig. 15b).

Fig. 15b-d: UV-VIS-near IR absorption spectra recorded at liquid nitrogen temperature (LNT) for the respective groups: CVD-grown, HPHT-grown and natural diamonds. Important features are highlighted. The synthetic (CVD, HPHT) diamonds were all irradiated. Apart from Ref20031 (natural, multistep treated) the natural diamonds show their natural (original) color. The ordinate shows the absorbance in arbitrary units. For better presentation the different spectra have been moved relatively to each other.

The well-known line at wavelength 594.4 nm (the 595 nm centre) has been found in all pink CVD diamonds. This centre is known as an evidence of irradiation followed by low temperature treatment [13]. In case of CVD diamonds, the generation of the 595 nm centre does not require the step of irradiation for they always possess high concentration of vacancies, which are required for the building of the defects responsible for the 595 nm centre. The presence of this centre is evidence that the studied CVD diamonds were not heated at temperatures over 1000°C at the last stage of treatment.

A weak GR1 centre is seen in absorption spectra of most CVD- and HPHT-grown pink diamonds (Fig. 15b-c). Conversely, GR1 centre has not been detected in spectra of natural pinks. GR1 centre together with ND1 centre strongly suggest that these diamonds were treated using irradiation followed by low temperature annealing. A multistep treatment HPHT + irradiation + annealing would be a possible procedure. In case of HPHT-grown diamonds, the standard procedure to achieve pink color via generation of high concentration of negatively charged NV^- defects is irradiation and low temperature annealing (Fig. 15c). In these diamonds, the NV^- centre band can be so strong that it is seen even with portable OPL spectroscope. In case of CVD-grown diamonds, which do not have the 520 nm absorption band strong enough to induce pink color, the generation of NV^- defects by multistep treatment is a reliable way to achieve the desired pink color.

The ND1 centre is almost always observed in absorption spectra of CVD-grown diamonds and treated HPHT-grown diamonds processed at low temperature. This centre, however, is rarely seen in spectra of natural diamonds (Fig. 15a). The ND1 centre is a negatively charged vacancy and its presence is an indication of an enhanced concentration of nitrogen C-defects, which are a common result of CVD growth and/or HPHT-growth. The broad band with maximum at about 520 nm present in absorption spectra of all studied pink CVD-grown and treated HPHT-grown diamonds deserves special attention (Fig. 15b,c). This band is most pronounced in synthetic and treated diamonds with pink-red color component and its spectral parameters differ from those of well known “Natural” Pink Band observed in natural pink diamonds at a wavelength of 550 nm (Fig. 15a,d). The spectral shape of the 520 nm band may vary from diamond to diamond and it can be considerably modified via interference with phonon side bands of the NV centres, when the latter are intense. The width of the 550 nm Pink Band is larger than that of the 520 nm band and the latter could be just a component constituting the 550 nm Pink Band. The 520 nm band may resemble the 550 nm Pink Band, however we assume that the origin of these two bands, although similar, are not identical. They both might originate from some vacancy clusters, which however could have different structure/size. Such a difference is quite expectable for diamonds grown in very different regimes: natural growth, under high pressure and epitaxial growth from gas at low pressure. Although vacancy clusters form in both natural and CVD-grown diamonds, the mechanism of their formation is substantially different: the plastic deformation of natural diamonds and a highly non-equilibrium, diffusion-limited formation of crystal lattice of CVD diamonds. A further difference between the 520 nm band and the Natural Pink Band is the 380 nm absorption band (Fig. 15d), which always accompanies the Natural Pink Band, but not the 520 nm band (Fig. 15a).

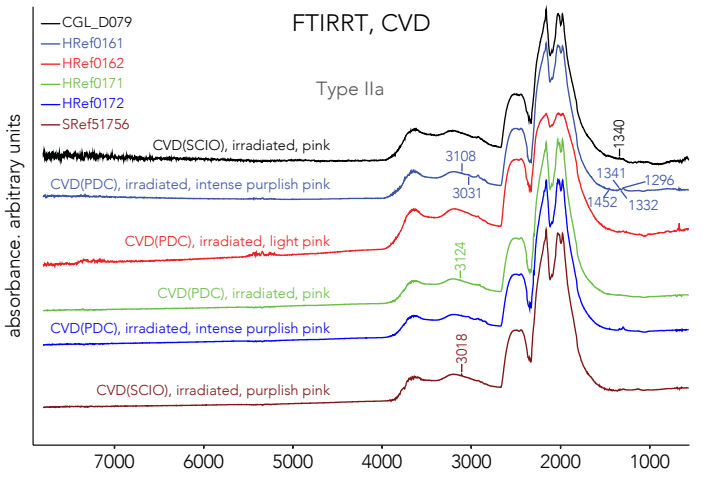

Fig. 16a

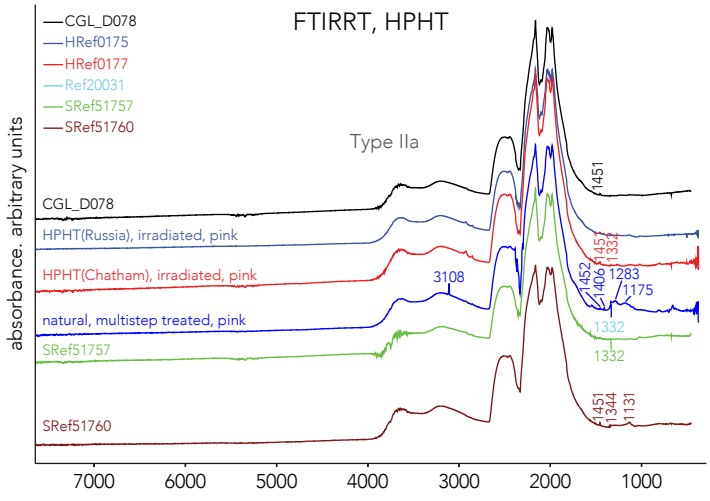

Fig. 16b

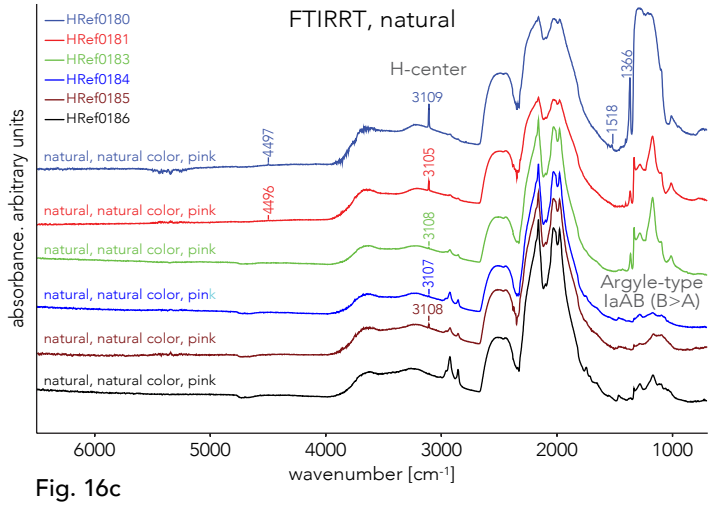

Fig. 16c

FTIR spectroscopy

All Orion PDC pink CVD-grown diamonds are of type IIa with negligible absorption in the range 1000 to 1500 cm^{-1}. Yet small peaks at 1503, 1450 (H1a centre), 1340 and 1332 (N+ centre) can be recognized. Two out of 4 stones display the peak at 3107 cm^{-1} related to hydrogen (Fig. 16a) [14]. Scio pink CVD-grown diamonds are also type IIa with FTIR spectra similar to those of Orion (PDC) pink CVD-grown samples (Fig. 16a). Type IIa natural pink diamonds are quite rare in nature (less than 2% of all natural pinks). Most natural pink diamonds come for Argyle mine and they are typically type IaAB with moderate to high nitrogen content and display the hydrogen-related peak at 3107 cm^{-1} (Fig. 16c). One of the characteristic "fingerprints" of Argyle natural pinks, as compared to non-Argyle" pinks, is that B aggregate concentration is higher than that of A aggregates [18, 19].

In case of HPHT-treated pink diamonds, Suncrest company uses low nitrogen type Ia diamonds and processes them by multistep treatment in order to get "natural looking" pink colors [11]. Producers of treated pink HPHT-grown diamonds from Russia, Chatham and AOTC also try to use type IIa or low nitrogen type Ib diamonds to obtain fancy pink diamond colors [17] (Fig. 16b). FTIR spectroscopy could be used as a preliminary screening technique for separation of treated pink diamonds based on their type, however further VIS absorption and PL spectroscopy is necessary to reliably identify them (Fig. 16a-c, Fig. 17a-c and Fig. 18a-d).

Fig. 16a-c: FTIR absorption spectra of pink diamonds for the respective groups: CVD-grown, HPHT-grown and natural diamonds. The spectra were taken at room temperature (RT). The synthetic diamonds (Fig 21a,b), which were all irradiated, are type IIa diamonds whereas the natural diamonds (Fig. 21c) are type Ia diamonds. The sample Ref20031 is a natural, multi-step treated diamond. The ordinate shows the absorbance in arbitrary units. For better presentation the different spectra have been moved relatively to each other.

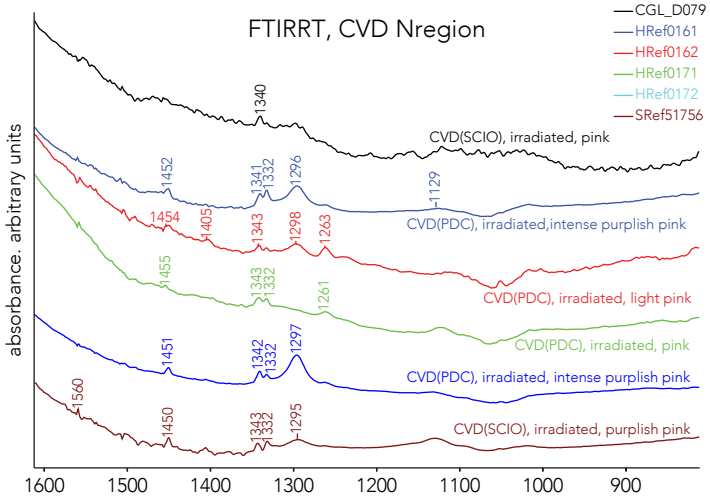

Fig. 17a

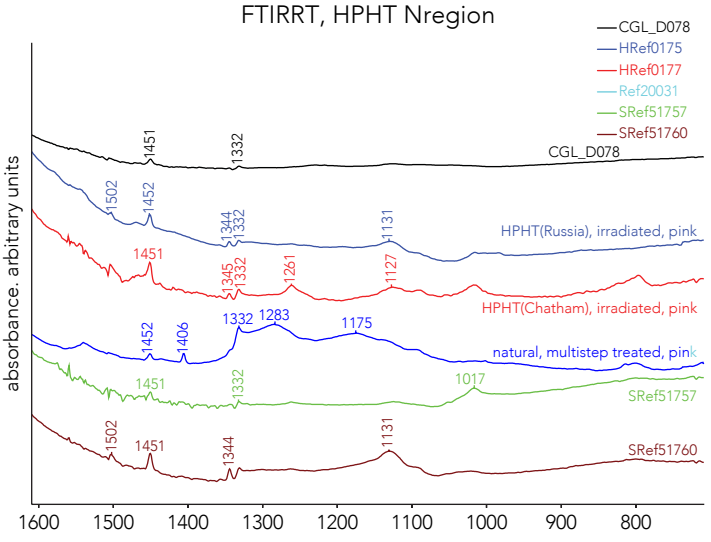

Fig. 17b

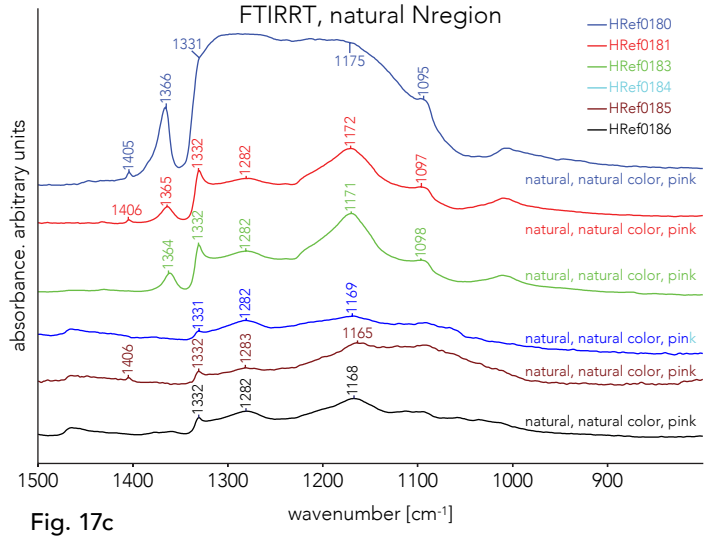

Fig. 17c

Other FTIR absorption features found in spectra of all studied pink CVD diamonds are peaks at 1292 and 1130 cm^{-1} (single nitrogen), which have been already reported for pink diamonds of CVD origin (synthetic) [18]. The 1292 cm^{-1} band is the main feature of the spectra of all but one CVD diamond (Fig. 17a). The origin of this band is unknown. However, since it is present in spectra of many synthetic pink diamonds, it is possible that the 1292 cm^{-1} band originates from defects common for these diamonds. Comparing the FTIR and VIS absorption spectra reveals some correlation of the 1292 cm^{-1} band intensity with the intensity of the short wavelength wing of the 520 nm CVD Pink Band, which probably originates from a broad band component with maximum at a wavelength of 480 nm.

Fig. 17a-c: FTIR absorption spectra of pink diamonds as seen in Fig 16-c, but zoomed into the N-region.

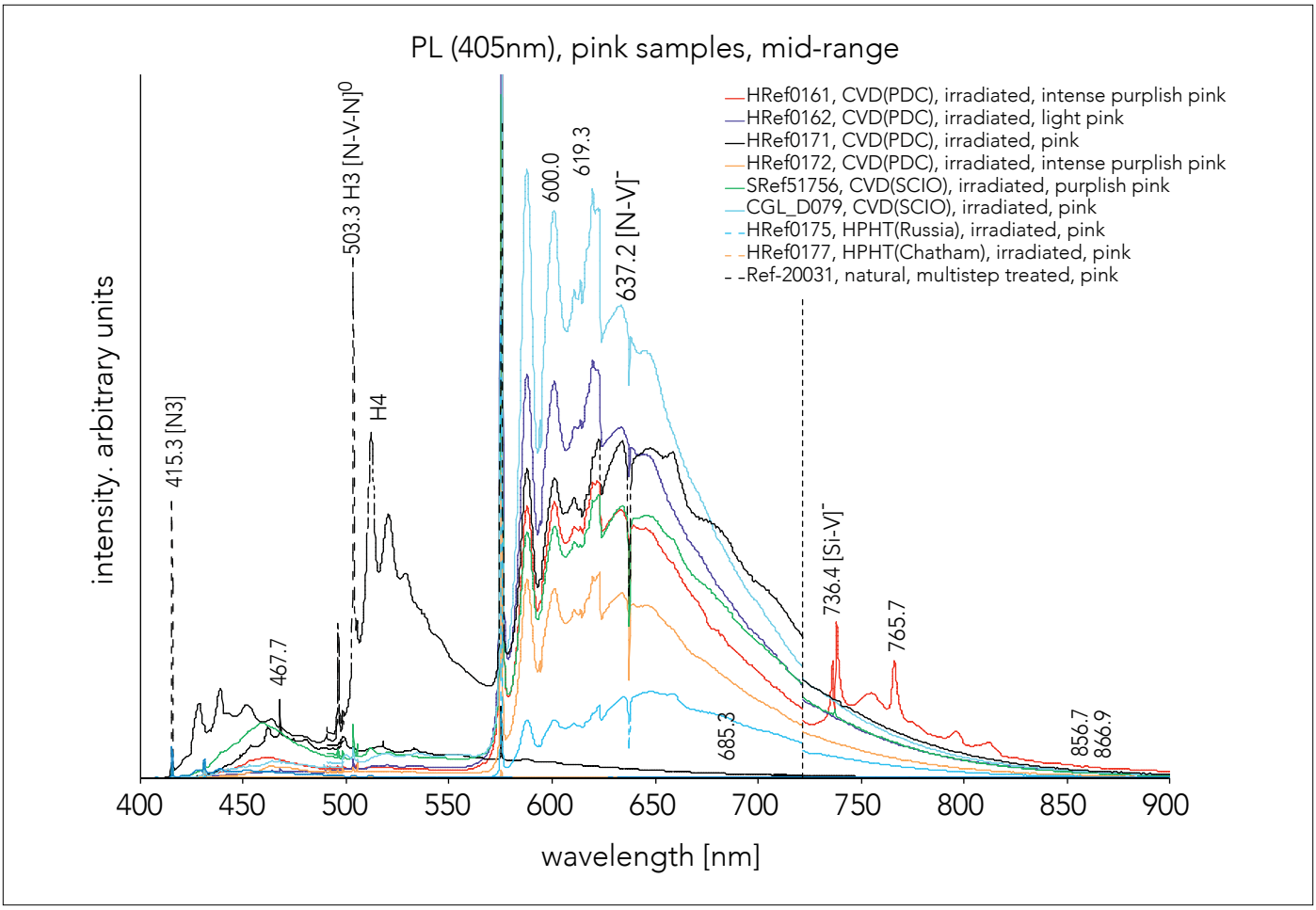

Fig. 18a: PL spectra of synthetic and natural pink diamonds as indicated. Spectra registered at Liquid nitrogen temperatures. For more details see the Fig. 18b-d.

PL spectroscopy

PL spectra of all studied diamonds are very complex revealing a few major centres and numerous week features over the whole visible spectral range (Fig. 18a). The most general feature distinguishing the natural pink diamonds from the CVD-grown, HPHT-grown and multistep treated pink diamonds is the different sets of dominating centres: the N3 and H3 centres in natural diamonds [19] and NV centres in synthetic and treated diamonds. This observation presents clear evidence that the aggregation of nitrogen even in type IIa diamonds is almost always close to completion, whereas is not at all in any laboratory-grown diamond even if it has been HPHT treated (Fig. 18b-c).

The behaviour of the NV centres in PL spectra depends considerably on the excitation wavelength. When excited with a wavelength of 405 nm, which does not fit into the excitation spectral range of the NV^- centre, the NV^0 centre always dominates and the NV^- centre is seen in the regime of absorption (negative luminescence) only (Fig. 18a-d). With excitation at a wavelength of 532 nm, both centres are excited in the regime of luminescence with comparable intensities (Fig. 19a-d). However, when the concentration of negatively charged NV defects is high, ZPL of the NV^- centre shows simultaneously luminescence and absorption resulting sometimes in a "doublet" line.

The SiV^- centre with ZPL at 737 nm [20], a feature manifesting the growth in a standard CVD reactor, has been found in some CVD diamonds only (Fig. 18a, b and Fig. 19a). None of the HPHT-grown and natural diamonds studied in this research have revealed even traces of this centre (Fig. 18b,c and Fig. 19b,c).

In PL spectra excited with a 532 nm laser, most of CVD

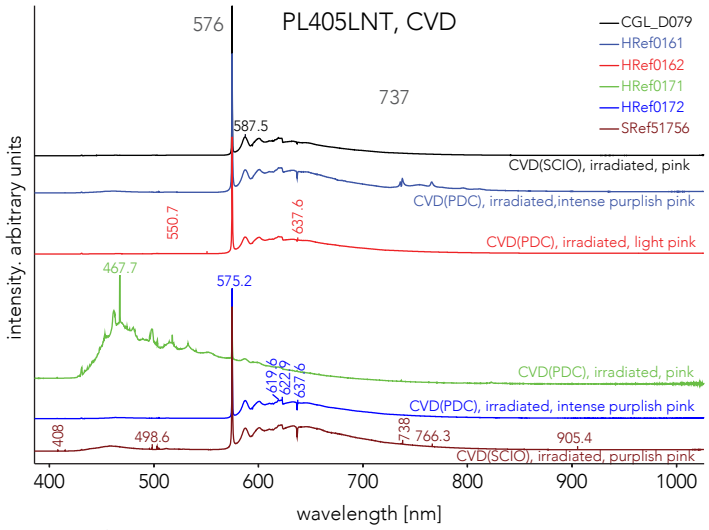

Fig. 18b

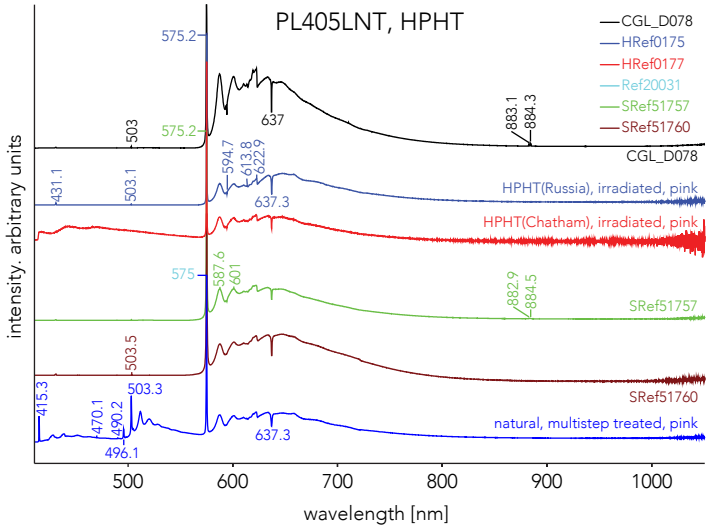

Fig. 18c

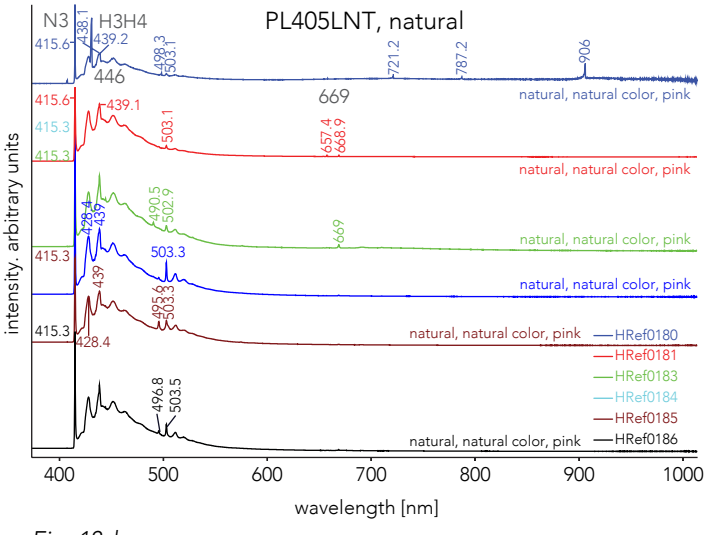

Fig. 18d

and HPHT-treated diamonds, as well as some of natural diamonds reveal the presence of weak GR1 centre (Fig. 19b-c). An unusual behavior of this centre is that in natural diamonds its ZPL is detected in the regime of luminescence only. All CVD and HPHT diamonds studied in this research exhibited the GR1 centre in the regime of absorption. Most of pink CVD-grown diamonds reveal in PL spectra (excitation at 405nm) the narrow lines at wavelengths 503.2 nm (H3 centre), 496.1 nm (possibly H4 centre) and 498.5 nm. Interestingly that in spectra of CVD diamond these lines are always accompanied by the lines at 505.2, 498.1 and 492 nm (Fig. 18b). In one HPHT diamond, the H3 and H4 centre are also accompanied by the lines 505.2 and 498.1 nm (Fig. 18c). The 505 and 498 nm centres were already reported [24, 13] and they were tentatively ascribed to H3 and H4 defects trapped into brown lamellae of natural diamonds. Both centres do not survive HPHT treatment. However, they can be well restored by following irradiation and conventional low temperature treatment [25, 17]. The present research reveals that these centres can be seen in pink synthetic diamonds (Fig. 18b,c).

All studied synthetic diamonds revealed in PL spectra "negative" luminescence (absorption) of a line at wavelength 594.4 nm, which originates from the well-known 595 nm centre) (Fig. 18b,c).

Fig. 18b-d: PL spectra (excitation 405nm) of pink diamonds recorded at liquid nitrogen temperature (LNT) for the respective groups: CVD-grown, HPHT-grown and natural diamonds. The synthetic (CVD, HPHT) diamonds were all irradiated. The sample Ref20031 is a natural, multi-step treated diamond. The ordinate shows the intensity (counts) in arbitrary units; for better presentation the different spectra have been moved relatively to each other.

A remarkable feature of the studied natural pink diamonds, like of almost any natural diamond of a color with the pink-brown component, is the presence in PL spectra excited with 532 nm laser at least traces of the 576 nm centre (Fig. 19c). The 576 nm centre is an evidence of plastic deformation and it is a very characteristic feature of natural untreated pink-brown diamonds. The 576 nm centre always anneals after HPHT treatment performed at temperatures over 1800C. Thus, with rare exception of low temperature HPHT treatment, the presence of the 576 nm centre is a reliable proof that diamond has not been HPHT processed [23]. Some other observations, which could be useful for separation of natural pink diamonds from their synthetic and treated counterparts, are the following:

(i) In PL spectra, natural pink diamonds frequently show a weak line at a wavelength of 444.6 nm, which is not seen in HPHT-grown and CVD-grown diamonds (Fig. 18d).

(ii) The spectra of natural pink diamonds do not show variety of many optical centres of measurable intensity over the whole visible spectra range like all studied pink CVD diamonds do (Fig. 15d).

(iii) In PL spectra, many natural pink diamonds reveal a centre with ZPL at 669 nm (Fig. 18d). Its position may vary from 669.0 to 668.6 nm [24]. Notwithstanding this variation, the 669 nm centre can be well recognized by its phonon replica at 690 nm. This centre is not the feature of pink CVD diamonds and HPHT-treated pink stones (Fig. 18b-c).

(iv) All pink CVD-grown (as well as most HPHT-grown) show the 1042 nm centre, which is another optical transition at NV defects [25]. This centre is always very weak and its presence is a proof of an enhanced concentration of the NV defects. Thus a clearly seen 1042 centre is a feature of lab-grown and treated diamonds (Fig. 19a-c).

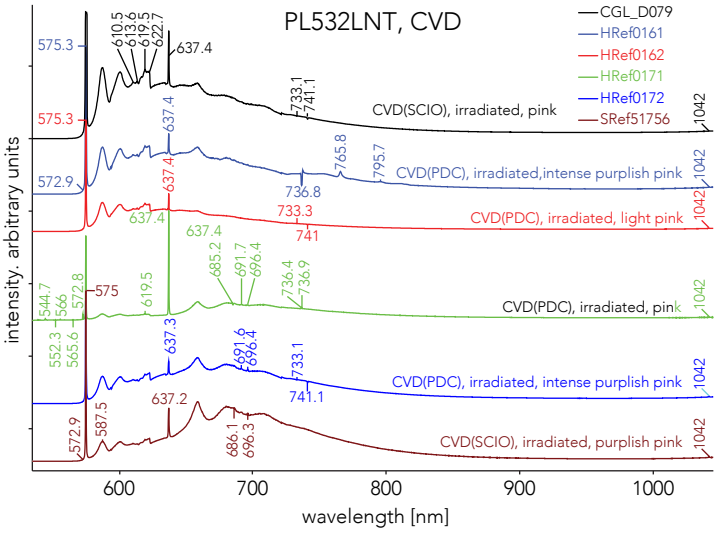

Fig. 19a

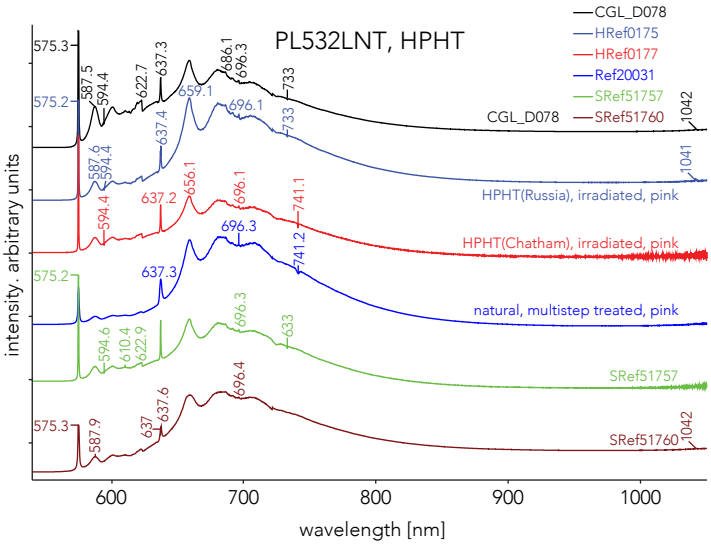

Fig. 19b

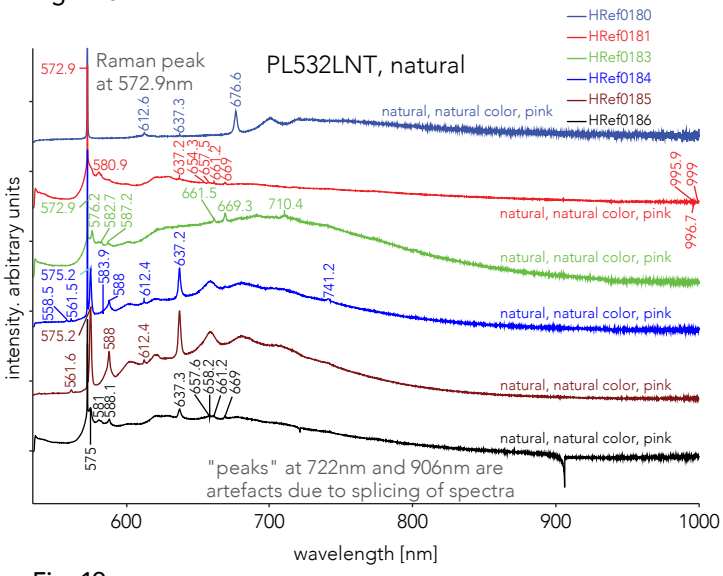

Fig. 19c

Fig. 19a-c: PL spectra (excitation 532nm) of pink diamonds recorded at liquid nitrogen temperature (LNT) for the respective groups: CVD-grown, HPHT-grown and Natural diamonds. The synthetic (CVD, HPHT) diamonds were all irradiated. The sample Ref20031 is a natural, multi-step treated diamond. The ordinate shows the intensity (counts) in arbitrary units; for better presentation the different spectra have been moved relatively to each other

Conclusion

We studied Orion PDC pink CVD–grown diamonds and compared them to natural, natural multistep treated, HPHT-grown and CVD-grown diamonds from other producers and similar pink colors (Appendix - Box 1). We found that screening with UV lamp is a useful test, especially convenient for melee and mounted pink diamonds. For pink diamonds a medium to strong orange fluorescence resulting from excitation by LW and SW-UV-light is a clear evidence, that this particular stone is NOT a Natural pink diamond with Natural color.The 520 nm absorption band is obviously the main reason of pink color of pink CVD-grown diamonds. The NV centres may also contribute to pink coloration, but their presence as the color centres in pink CVD-grown diamonds is not required. In this respect, pink CVD-grown diamonds resemble natural pink diamonds. Yet the spectral shapes of the Pink Bands in CVD-grown and natural diamonds are sufficiently different and their differentiation does not cause a problem.

PL spectroscopy is the most powerful technique in separation of natural untreated, natural treated and lab-grown pink diamonds. The major feature of PL spectra of natural untreated pink diamonds is the dominating N3 and H3 centres, whereas NV^- and NV^0 centres dominate PL spectra of treated and synthetic diamonds. Many other features uniquely present in spectra of either natural untreated, or natural HPHT-treated, or HPHT/CVD-grown diamonds also contribute to the reliable identification of color origin of pink diamonds.

The number of pink CVD-grown diamonds grows on the market in Asia, however their identification does not cause problems to the gem laboratories equipped with good VIS absorption and PL spectrometers. Nevertheless it is necessary to screen and test "natural looking" pink diamonds of different sizes in parcels of small and melee diamonds for their color origin: natural, treated or synthetic (HPHT-grown or CVD grown).

Acknowledgements

We are grateful to John Chapman for supplying the samples from the Argyle diamond mine. To Dr. A. Berger and Prof. K. Ramseyer of University of Berne, Switzerland for SEM-CC testing and Rio Tinto diamonds for the photos of the Argyle mine. Bill Vermeulen of CGL – GRS Swiss Canadian Gemlab and Diana Jarrett for editing the text.

Appendix - Box 1:

Comparison of Orion (PDC) CVD-grown blue and CVD-grown pink diamonds

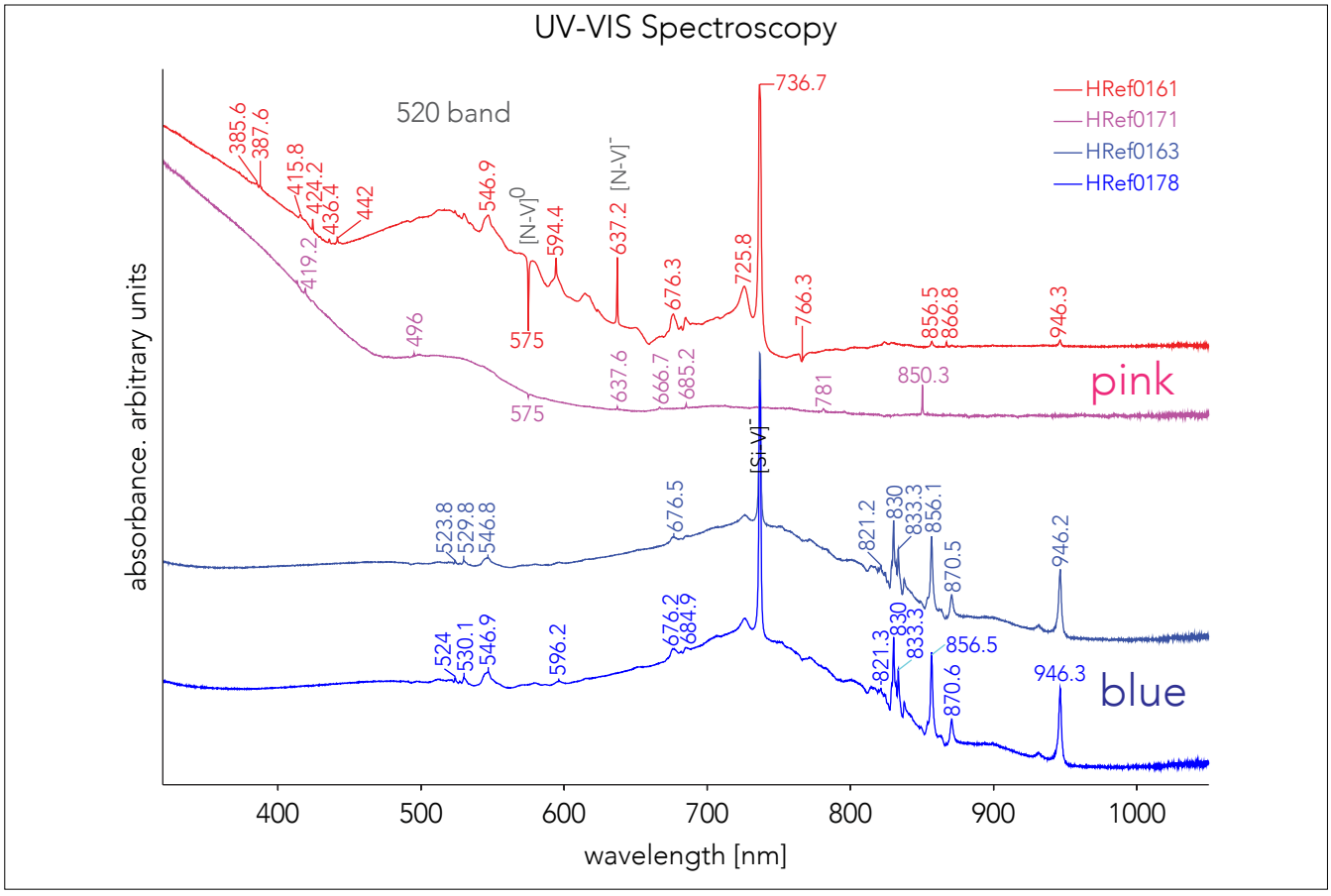

Perfect CVD diamonds, like perfect type IIa natural diamonds, are colorless. Introduction of certain impurities during growth and/ or activation of them by post-growth treatment produces color. Two colors characteristic of Orion colored CVD diamonds are pink and blue.

Pink color is produced by two color centres: a broad band centreed at a wavelength of 520 nm and the nitrogen-related NV^- centre. Both centres absorb in the green spectral range making these diamonds to transmit preferentially red and blue colors. A combination of these colors is seen as purple to pink. The 520 nm band and NV^- centre can be well induced in CVD diamond by doping with nitrogen, irradiation and annealing (e.g. HPHT treatment) and pink CVD-grown diamonds are becoming a pervasive synthetic gem material on the diamond market.

Blue color of CVD diamonds can be induced by doping with boron and, more recently, with silicon. Both impurities form optical centres absorbing preferentially the red and partially in green spectral ranges. Thus the boron- and silicon-doped diamonds have maximum transparency for blue light. The boron doped HPHT-grown diamonds are a perfect imitation of natural blue diamonds since the latter also owe their blue color to boron impurity. The blue color of the silicon-doped diamonds differs from that of the boron-doped ones. The reason is some additional absorption in a wide spectral range produced by silicon impurity. This absorption adds a grey-"steel" color modifier to the blue color of silicon-doped CVD diamonds. In contrast to pink CVD diamonds, blue CVD-grown diamonds are still relatively rare on the diamond market.

Producer	CVD-grown irradiated Orion PDC 4 samples	CVD-grown, irradiated Scio 2 Samples	HPHT synthetic, irradiated Chatham 4 samples	HPHT synthetic, irradiated Russia 1 sample	HPHT synthetic, irradiated AOTC 1 sample	Natural, multistep treated 1 sample	Nautral, natural color 2 samples	Natural, natural color Argyle 4 samples
Colour	fancy pink, fancy brownish orangy pink ("peach"), fancy intense purplish pink	fancy orangy pink fancy purplish pink	fancy intense pink to fancy intence purplish pink	fancy pink	fancy intense purple pink	fancy purplish pink	fancy light orangy pink	fancy light pink
Clarity	VVS1 to VS2	VS1, SI2	SI1 to I1	I2	IF	SI1	SI1 to I1	n/a (fragments)
Solid Inclusions (at 60x magnification)	dark cloud, crystals, feathers around girdle, dark blue staining in	graphitization of fracture	black metallic inclusions, small crystals forming a cloud	big crystal with associated feather	none	small feathers	feathers	n/a (fragments)
Fluorescence SWUV (254nm)	medium to strong orange, weak orange phosphorescence	strong orange	strong orange	medium orange	medium orange	medium orange	inert to weak blue	weak blue, none to weak blue phosphorescence
Fluorescence LWUV (365nm)	medium to strong orange, weak orange phosphorescence	strong orange	medium to strong orange	weak to medium orange	medium orange	strong orange	inert to strong blue	strong blue, none to weak blue phosphorescence
Cross Polarized Filters (CPF)	Irregular pattern OR "tatami" pattern	"Tatami" pattern	no pattern	no pattern	no pattern	patchy pattern		n/a (fragments)
FTIR spectroscopy (absorption, cm -1)	type IIa spectrum, small peaks at 1504, 1450 (H1a), 1340, 1332 (N+), 1296, 1263. Peak at 3107 (H-center). Two samples: no 3107 peak but 3123	type IIa spectrum sample 1: small peak at 1340 and 1406 sample 2: 1450 (H1a), 1342, 1331 (N+), 1295, 1128 (C-centers), peak at 3107(H)	type IIa spectrum, small H1a (1450) and N^+ (1332) peaks. Peak at 1560, sample 4: peaks at 1560, 1545, 1537, 1504, 1451 (with side band at 1470) 1344 and 1129 (C-center), 1332 (N+), broad peak at 766.4	type IIa spectrum, peaks at 1558, 1504, 1451 (with side band at 1470) 1344 and 1129 (C-center), 1332 (N^+)	type Ib with indications of C-centers (1344, 1130), peaks at 1560, 1502, 1450 and 1332.	type Ia of low nitrogen. H1a-center at 1450 and N^+ at 1331. A-aggregate at 1284, no signs of single nitrogen or B-aggregates. H-center related peaks at 3107 and 1405.	type IaAB, B>A, with a platelet peak at 1365, H-center related peaks at 4494, 3107 and 1405	type IaAB, B>A, platelet peak at 1362 (three samples only), H-related peak at 3108 and 1405; sample 4 shows no platelet but peaks at 1378 and 1359
UV-Vis-NIR spectroscopy at LNT (absorption):	small peaks at 415.8 (N3), 424.2, 436.4, 442.0 (radiation damage center), valley at 575 (NV0), peaks at 594.4 , 637.1 (NV-): 737 (Si-center), sample 2: no 415 sample 2 and 4: small peak at 741 (GR1)	peak at 393.5 (ND1), 424.8 (H6-center), 436.2 (A-band), 441.8 , valley at 575(NV0), peaks at 594 , 637.1 (NV-), 741 (GR1)	small peaks at 385.8, 387.9, 389.3, 416.2 424.7 436, 441.9 , 506.2, 516.5, 535, peaks at 575, 637 and 594.2 . Small peaks at 724.8, 732.6 and 764.6 sample 1 with doublet at 883.2/884.8; sample 4 with 741 (GR1)	small peaks at 385.4, 387.9, 415.8, 424.7, 436.4 and 441.8 , peaks at 637, 575 and 594	small peaks at 385.8, 387.9, 389.3, 416.2 424.7 436, 441.9 , 506.2, 516.5, 535, peaks at 575, 637 and 594.2	peaks at 393.8, 415.4, 424.9, dip at 575.5, peak at 637.0, small 741 peak	peaks at 315.6 (N6), 317.8, 320.1, 329.9, 338.2, 344.8 (N4). Clear 415 (N3-center "Cape"-line), small peaks at 477 (N2), 503.4 (H3), 763 and at 823.5 (very small)	small peak at 345 and clear N3-center at 415, peak at 450
PL spectroscopy at LNT - 405nm	peaks at 453.7, 462.3, 468.0, 496.1, 503.3, 503.8, 515.1, 517.8, small peaks at 533.1, 540.7, 575, 637.4, 658.2, 736.8 (Si), 767.5, 820.0, 823.0; sample 2 with small 441.9 and 594.4 peaks but no 737 ; sample 4 peak at 594.4	peaks at 496.0, 498.2 and 503.2, 505.1, peak at 575.2, sample1: valley at 637, small 737 -peak (Si), very weak 741 (GR1)	peaks at 438.4, 441.8 , 483.8, 489.4, 492.1, 503.5, 575.2, 637.3, small doublet at 882.9 and 884.6; sample 4 with peaks at 394 and 415	strong peaks at 575, 637, peaks at 431.1, 489.4, 503.1, 613.8 and a dip at 594	peaks at 489.4, 503.5, 575.2, 637.3	peak at 415.3 (N3), very small peak at 470.1. Peaks at 490.2 and 496.1, strong H3-peak at 503.3. Strong peaks at 575 and 637.3	415 peak (N3) with side bands at 421, 439, 452 and 463. H3-center at 503.2 with phonon side bands at 512 and 520, Small peaks at 657.4, 668.9	peaks at 415, 490, 496, 503.3, 575, 654.5, 657.9, 669.0, 679.6, 710.2, 802.5
PL spectroscopy at LNT - 532nm	575, 637 peaks, peak at 696.4, small valleys at 733.0 and small peak at 1041.6; sample 1 and 3: peak at 737 (SiV-) sample 2 and 4 valley at 741 (GR1)	575, 637 peaks, small 741 valley (GR1), sample 2 with peaks at 659 and 1041.8	peaks at 575, 594 , 610.4, 613.5, 619.5.t 622.7. Peak at 637. Further peaks at 696.4, and 1042, dip at 732.9, sample 3 with a valley at 741 (GR1)	strong (NV)-centers: 575, 637. small peak at 696.1 and dip at 733, small peak at 1041	peaks at 575 and 637, small peak at 1041.	peaks at 575 and 637, small peak at 1041. Peak at 741 (GR1)	Sample 1: peaks at 613.0, 637.5 and 676.6 Sample 2: peaks at 580.9, 637.2 and 669.2	Peaks at 588.2 and (NV)-center related peaks at 575 and 637, small peaks at 658.2, 669.2, Sample 2 with a small 741 (GR1)

Table 1: Summary of tested natural and synthetic pink diamonds of different producers and synthesis methods and results of examinations

References

[1] Hofer S.C., 1985, Pink diamonds from Australia. Gems & Gemology, Vol. 21, No. 3, pp. 145–155.

[2] Hofer S.C., 1998, Collecting and Classifying Colored Diamonds: An Illustrated Study of the Aurora Collection.Ashland Press, New York, 742 pp.

[3] Simic D., Woodring S., Deljanin B., 2004, Processed Pinks, Rapaport, November. www.diamonds.net/News/NewsItem.aspx?ArticleID=10740

[4] Simic D., Deljanin B., 2005, Provo Rose, rare 10ct pink diamond, the latest generation of processed pinks, Idex Magazine.

[5] Epelboum E., Zaitsev A., D., Deljanin B., 2006, Preliminary Study of New Generation of Coated Diamonds with Limited Color Stability, EGL Canada, www.eglcanada.ca/research.

[6] Shen A. H., Wang W., Hall M. S., Novak S., McClure S. F., Shigley J. E., and Moses T. M., 2007, Serenity coated colored diamonds: Detection and durability: Gems & Gemology, v. 43, no. 1, p. 16-34.

[7] Khan R. U. A., Martineau P. M., Cann B. L., Newton M. E., Dhillon H. K., and Twitchen D. J., 2010, Color Alterations In CVD Synthetic Diamond With Heat and UV Exposure: Implications For Color Grading and Identification: Gems &Gemology, v. 46, no. 1, p. 18-26.

[8] Wang W., Doering P., Tower J., Lu R., Eaton-Magana S., Johnson P., Emerson E., and Moses T.
M., 2010, Strongly colored pink CVD lab-grown diamonds: Gems & Gemology, v. 46, no. 1, p. 4-17.

[9] Peretti A. , Herzog F., Bieri W., Alessandri M., Günther D., Frick D.A., Cleveland, E., Zaitsev A.M., Deljanin B., 2013, New Generation of Synthetic Diamonds Reachesthe Market (Part A): CVD-grown Blue Diamonds. www.gemresearch.ch/news and Rapaport: http://www.diamonds.net/News/NewsItem.aspx?ArticleID=4 5256

[10] Simic D, Deljanin B., 2010, Identifying Diamond Types and Synthetic Diamonds with CPF (Cross Polarized Filters), D&S Gemological Service, 1st edition.

[11] Simic D., Zaitsev A.M., 2012, Characterization of diamonds color-enhanced by Suncrest diamonds USA, Analytical Gemology anf Jewelry Ltd, New York, p. 24

[12] Martineau P. M., Lawson S. C., Taylor A. J., Quinn S. J., Evans D. J. F., and Crowder M. J., 2004, Identification of synthetic diamond grown using chemical vapor deposition (CVD): Gems & Gemology, v. 40, no. 1, p. 2-25.

[13] Colins A., 1982, Color Centres in Diamond, Journal of Gemmology, Vol.18, No.1, 37.

[14] Zaitsev A., 2001, Optical properties of diamond, Springer-Verlag, Berlin

[15] Deljanin B., Simic D., Zaitsev A., Chapman J., Dobrinets I., Widemann A., Del Re N., Middleton T., Deljanin E., and De Stefano A., 2008, Characterization of pink diamonds of different origin: Natural (Argyle, non-Argyle), irradiated and annealed, treated with multi-process, coated and synthetic: Diamond and Related Materials, v. 17, no. 7-10, p. 1169-1178.

[16] Byrne K.S., Anstie J.D., Chapman J. &Luiten A.N., 2012, "Infrared microspectroscopy of natural Argyle pinkdiamond", Diamond and Related Materials, 23, 125-129

[17] Deljanin B., Simic D., 2007, Laboratory-grown Diamonds - Information Guide to HPHT-grown and CVD-grown diamonds, GHI, Mumbai

[18] Wang W. Y., Smith C. P., Hall M. S., Breeding C. M., and Moses T. M., 2005, Treated-color pink-to-red diamonds from Lucent Diamonds Inc: Gems & Gemology, v. 41, no. 1, p. 6-19.

[19] Chapman J., 2009, PL studies of pink and brown diamonds. De Beers Conference

[20] Wang W. Y., Moses T., Linares R. C., Shigley J. E., Hall M., and Butler J. E., 2003, Gem-quality synthetic diamonds grown by a chemical vapor deposition (CVD) method: Gems & Gemology, v. 39, no. 4, p. 268-283.

[21] Gaillou E., Post, J. E., Bassim N. D., Zaitsev A. M., Rose T., Fries M. D., Stroud R. M., Steele A., and Butler J. E.,2010, Spectroscopic and microscopic characteri

zations of color lamellae in natural pink diamonds: Diamond and Related Materials, v. 19, no. 10, p. 1207-1220.

[22] Dobrinets I. A., Vins V.G., Zaitsev A.M., 2013, "HPHT-Treated Diamonds, Diamonds Forever", Springer Series in Materials Science, Vol. 181, Springer Verlag.

[23] Shiryaev A. A., Hutchison M. T., Dembo K. A., Dembo A. T., Iakoubovskii K., Klyuev Y. A., and Naletov A. M., 2001, High-temperature high-pressure annealing of diamond - Small-angle X-ray scattering and optical study: Physica B-Condensed Matter, v. 308, p. 598-603.

[24] Iakoubovskii, K., and Adriaenssens, G. J., 2002, Optical characterization of natural Argyle diamonds: Diamond and Related Materials, v. 11, no. 1, p. 125-131.

[25] Rogers L. J., Armstrong, S., Sellars M. J., and Manson N. B., 2008, Infrared emission of the NV centre in diamond: Zeeman and uniaxial stress studies: New Journal of Physics, v. 10.

New Generation of Synthetic Diamonds Reaches the Market

Part C: Origin of Yellow Color in CVD-grown Diamonds and Treatment Experiments

Zaitsev A.M. [1]*, Deljanin B. [2], Peretti A. [3], Alessandri M. [4], Bieri W. [5]

[1]The City University of New York, USA
[2]CGL-GRS Swiss Canadian Gemlab Inc., Canada
[3]DR Peretti Co LTD, Thailand and GRS Laboratories
[4]GRS Lab (Hong Kong) Ltd, Hong Kong, China
[5]GRS Gemresearch Swisslab AG, Switzerland

*Corresponding author: alexander.zaitsev@csi.cuny.edu

Introduction

It's been a decade since Chemical Vapor Deposition (CVD) grown diamonds first appeared in the marketplace [Wang et al 2003, Deljanin et al 2003, Martineau et al. 2004]. But today it's a fast growing and increasingly important sector of the diamond trade.

The remarkable ascent of CVD-grown diamonds as a gem material followed the successful development of rapid growth CVD methods [McCauley and Vohra 1995; Yan et al 2002]. But behind those achievements is another reason for the swift market penetration of the CVD-grown diamond. There are critical advantages of CVD-grown diamonds as compared to those grown under high pressure and high temperature (HPHT). CVD diamond production is much simpler with more reproduction capability, and is fully automated without requiring qualified personnel to supervise the process. It also opens up the real potential of mass produced cheap synthetic diamonds.

Along with the advent of rapid growth methods of CVD, the technology provides for a considerably lower priced synthetic diamond; making their production a profitable one. Besides its technological efficiency, CVD-grown diamonds have another advantage, which is critical in its application to jewelry manufacture; the potential to control a broad range of diamond colors.

CVD growth commonly results in brown to colorless type IIa diamonds, whereas HPHT growth commonly results in yellow type Ib diamonds. Synthetic colorless diamonds are much more desirable than yellow ones. Moreover, brown to colorless type IIa diamonds are a much better foundation material for manipulation of their color than yellow type Ib diamonds.

To date, very little is understood with regards to CVD-grown diamonds as a gem material. Published reports have dealt mainly with the recognition of CVD-grown polished diamonds and their separation from natural ones. That is because data on CVD growth technology and methods of post-growth CVD-grown diamond treatment is proprietary and is never publicly disclosed. As a result, few publications have discussed the origin of color for CVD-grown gem quality diamonds. However, color is one of the key considerations of a gemstone. It is of particular importance for synthetic gem materials since, with improving growth technology, their structural perfection and size become increasingly less a matter of concern. Thus, color dominates the attributes of a gem material's attractiveness and impacts its value. By now, colorless, brown, grey, pink and blue colors are identified with commercial production of CVD diamonds (Fig. 1).

Perfect CVD-grown diamonds are colorless. They can be produced at a slow rate of growth, keeping colorless CVD-grown diamonds small and expensive. Rapidly grown CVD diamonds have brown or greyish-brown color. This undesirable brown color can be considerably reduced by standard HPHT treatment [Wang et al 2003]. However, a grey component is much more stable and cannot be easily removed; producing non-colored CVD-grown gem diamonds in a color grade not higher than K, faint, very light to light grey.

Blue was the first fancy color produced in CVD-grown gem diamonds [Fritch et al 1989; Martineau et al. 2004]. Its color was achieved through boron doping. Although blue color boron-doped CVD-grown diamonds have been known to exist for decades, they did no appear commercially as a gem product. Recently,

non-boron-doped CVD-grown diamonds with dominating a blue color component were discovered in the marketplace [Peretti et al. 2013]. The color's origin is a strong absorption of optical SiV^- centre, which is common for CVD-grown diamonds. Its high intensity can be produced via heavy doping of silicon with the growing diamond. SiV^- centre absorbs preferentially in the red spectral range and makes diamonds transparent preferentially in the blue spectral range. Along with the SiV^- centre, silicon produces other optical centres active in the green spectral range. It is this additional absorption that produces the greyish color component of the silicon-doped CVD-grown diamonds.

Pink was the first commercial color of fancy colored CVD-grown diamonds [Wang et al. 2010]. The pink results from strong absorption of nitrogen-related NV^- centre, which absorbs in the green spectral range. Pink diamonds artificially colored via NV-centre are very well known in diamond trade [e.g. Simic et al 2014, Dobrinets et al 2013]. To produce stones with pure pink color, low nitrogen type Ib diamonds containing preferentially single nitrogen atoms (C defects) are used. The presence of other nitrogen defects (e.g. A-, B- and N3 defects) is undesirable since they produce optical centres over the entire visible spectral range, resulting in dark and dull colors. So the CVD-grown diamond is ideal for this purpose. It can be lightly doped with nitrogen during growth. The introduced nitrogen forms exclusively single atom defects.

Recently, we have found that CVD-grown gem diamonds can be produced in a straw yellow color. Yellow is not one of the more expensive colors, yet it is much more attractive than the greyish colors of non-colored CVD diamonds. The CVD-grown yellow diamonds have not appeared on the market yet, but Scio Diamonds occasionally produces this color. However, there is strong commercial potential for them along with the pink and blue colors. The goal of this research is to present a first account of optical properties for yellow CVD-grown gem diamonds and to discuss possible methods of their production. In addition to this we compare our own produced CVD-grown yellow diamonds with a CVD-grown yellow diamond from Scio Diamonds to identify possible similarities in treatment that result in the yellow color.

Fig. 1: These faceted CVD-grown diamonds comprise 4 different colors. Colorless, blue, pink and yellow of around 0.4 ct in weight, imitating the colors of their natural counterparts.

Materials & Methods

Three CVD-grown, brilliant cut diamonds of very light grey color were converted in yellow and studied by spectroscopic methods. For comparison, some other CVD-grown diamonds of a different color and different treatment history were studied too. These samples were purchased from third parties. Direct information with regards to the technology of their growth, or post-growth treatment was not available. However, considering the common light grey color most CVD-grown gem diamonds present, we assumed that after growth, the diamonds were HPHT annealed.

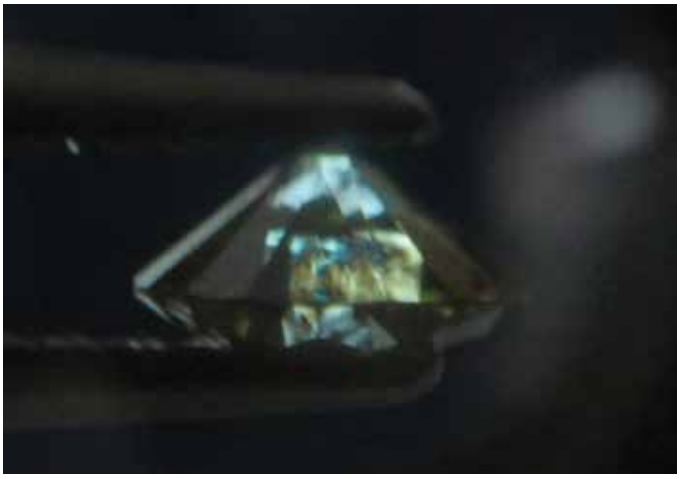

Fig. 2. CPF pattern of "low nitrogen" CVD-grown diamond with "parallel needle-like and patchy pattern".

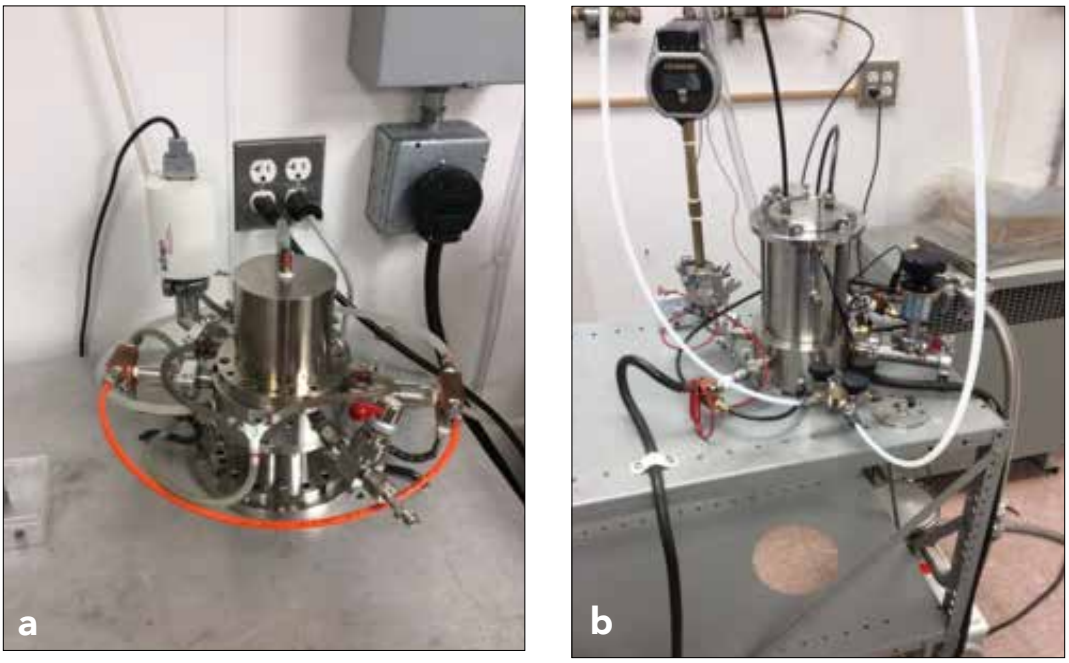

Fig. 3: High temperature graphite furnaces used for annealing of diamonds in this research: (a) vacuum furnace, (b) gas furnace

In order to achieve a yellow color, we performed different treatments including electron irradiation at room temperature with energy 1 MeV and annealing at different temperatures and in different atmospheres. Total dose of the electron irradiation could differ from sample to sample. However, according to the intensity of blue color, all diamonds received about 10^{18} cm^{-2} electrons.

Annealing in vacuum was performed in a home-made all-graphite furnace operating at a temperature range of 50 to 2000°C at a residual pressure of 10^{-5} mbar (Fig. 3a). Temperature in the sample container was measured with W-Re thermocouple and could be set with an accuracy of 10°C. The thermocouple was calibrated against melting points of pure elements (Al, Au, Si, Pt, Rh). The annealing time (the time diamonds are kept at the nominal temperature) could vary from 1 minute to several hours. Length of time for heating up and cooling down did not exceed 3 minutes each.

Annealing in argon, nitrogen and hydrogen was performed in another home-made all-graphite furnace designed for annealing in gas atmosphere (Fig. 3b). The furnace chamber was filled with gas (ultra-high purity grade) at a pressure in the range 300 to 1000 mbar. Prior to filling, the chamber was evacuated to a residual pressure of 10^{-3} mbar. Like in the vacuum furnace, temperature in the sample container was measured with a calibrated thermocouple. Temperature range of the gas furnace was 500 to 2700°C. Although, for annealing of diamonds, in order to avoid bulk graphitization, the maximum temperature did not exceed 2200°C. Accuracy of maintaining the nominal temperature and the time parameters of annealing were the same as for the vacuum furnace.

The measurements of optical absorption and photoluminescence (PL) were performed at room temperature (RT) and liquid nitrogen temperature (LNT) using home-made setups. A custom-built UV-VIS-NIR absorption instrument using a quadruple-channel Czerny-Turner spectrometer and two broadband light sources recorded the spectra in the wavelength range from 240 – 1100 nm. This apparatus enabled the detection at LNT of very weak absorptions with spectral resolution better than 0.2 nm. Photoluminescence spectra were measured using a custom-built spectrometer working with 405 nm and 532 nm excitation lasers. PL measurements were performed in a wavelength range from 408 to 1100 nm range.

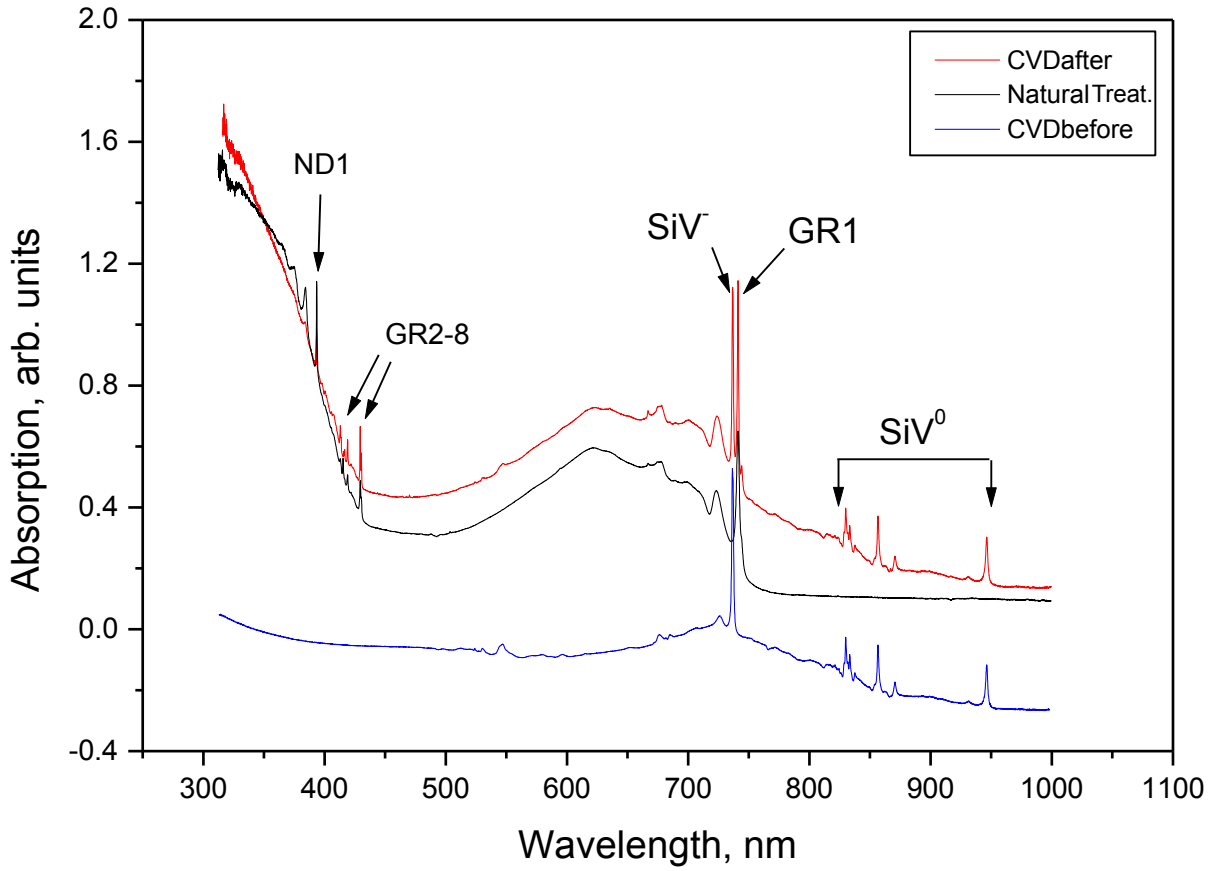

Fig. 4. Absorption spectra of electron irradiated natural type IIa irradiated diamond (black curve) and Si-doped CVD-grown (red curve) diamonds after irradiation. The spectra were taken at LNT. The dominant feature of both spectra is the GR1 centre. SiV centres retain their intensity in the CVD diamond after irradiation. Blue curve shows the spectrum of the CVD-grown diamond before irradiation. All spectra were measured at LNT.

Annealing of greyish CVD-grown diamonds

Annealing of greyish CVD-grown diamonds in vacuum, argon and nitrogen to a temperature of 1600°C for a few hours, in hydrogen up to a temperature of 2100°C for one hour, or in hydrogen at a temperature of 2200°C for 1 minute did not result in noticeable color changes. This suggests that high temperature annealing at low pressure, even at a temperature as high as 2200°C, does not activate the defect transformations in CVD-grown diamonds previously subjected to HPHT treatment.

Electron irradiation

Three CVD-grown diamonds were irradiated with electrons as detailed in description "Materials & Methods". In the as-irradiated state, all diamonds revealed intense blue color with a greenish component normally associated with natural electron-irradiated diamonds. There was no noticeable difference between the blue color of an irradiated natural diamond and that of the irradiated CVD-grown diamonds except for the weak grey modifier of the CVD-grown diamonds. Optical absorption of all irradiated diamonds is qualitatively identical in the visible spectral range (Fig. 4).

The dominant feature is the GR1 centre with zero-phonon line (ZPL) at 741 nm. Yet, in the near infrared spectral range, the spectrum of the CVD-grown diamond differs from that of the natural one through the presence of a set of narrow lines in the wavelength range from 820 to 960 nm and an absorption continuum with intensity rising towards shorter wavelength. These narrow lines have previously been reported in [Peretti et al. 2013] and interpreted as absorptions on silicon-related SiV^0 centre.

The absorption continuum is responsible for the grey color of HPHT-treated CVD-grown diamonds [Wang et al. 2003; Martineau et al. 2004]. This result suggests that electron irradiation does not affect the optical centres of grey color and the grey color is retained as a color component of the irradiated CVD-grown diamonds. The SiV^- centre, ZPL is very prominent in the spectrum of a CVD-grown diamond. But it has no remarkable influence in the diamond color because the intensity of

its vibrational side-band is weak and completely overlapped by the intense vibrational side-band of the GR1 centre.

Annealing upon irradiation

Absorption

Two of the irradiated diamonds were annealed in vacuum at a temperature of 1500°C for one hour. Both diamonds produced a yellow color, which was a somewhat unexpected result. In order to determine whether the color was specific to these two diamonds, a few more irradiated CVD-grown diamonds were annealed under the same conditions. None of them received yellow color, but some stones became a light greyish-pink color. The CVD-grown diamonds with pink were found to have an elevated concentration of nitrogen (a few ppm) as compared with those of yellow color. Thus, the pink color was produced by the generation of NV^- centre. This suggests that the outcome of annealing irradiated CVD-grown diamonds will depend on the kind of impurities within them.

The third irradiated diamond was annealed in hydrogen atmosphere at varying temperatures from 600°C up to 2200°C. After the first annealing at 600°C, the diamond retained its overall blue color component, but added a stronger grey color. After annealing at 1000°C, the color changed to greyish-yellow with a dominant yellow component. Further annealing at 1300°C resulted in addition of an orange component, and the diamond became greyish-orangish-yellow. Next annealing step at 1600°C converted the diamond color to brownish grey. After annealing at 1800°C, the CVD-grown diamond lost spectral colors and appeared light grey. Subsequent annealing at 2100°C and 2200°C for 1 minute each resulted in no visible change in color.

Comparing these results, we observe that the yellow color is stable at temperatures over 1500°C when heated in vacuum, but it is destroyed at these temperatures when heated in hydrogen. We may conclude that the different color changes occur either from the influence of hydrogen atmosphere on the defect transformation in diamond, or because of the different impurity content. Unfortunately, we did not record the spectra after every annealing step. However, taking into account the color changes and the final absorption spectrum obtained after 2200°C annealing, we can speculate about the possible changes of the major color centres in the studied CVD-grown diamond during annealing.

The absorption spectra of the finally annealed CVD-grown diamonds are shown in Fig. 5. The principal attribute of the spectra of the CVD-grown diamonds annealed in vacuum is the SiV^- centre. Although having identical phonon side-bands in the range from 600 to 737 nm, this centre has been found to have different spectrum in the range of ZPL for different diamonds. In one diamond, ZPL of the SiV^- centre has a usual spectrum: a narrow sharp line at a wavelength of 736.8 nm, whereas in another one ZPL is broad and strongly suppressed in intensity. The further narrow lines are at wavelength 637 (NV^- centre), 594.4, 575.4 (NV^0 centre), 516.5, 506.4, 425 and 389 nm. ZPL of the NV^0 centre is seen in the luminescence mode, or negative absorption, which is common for this centre measured in absorption spectra in the regime of full spectrum excitation.

The 389 nm centre is well-known and always present in diamonds with strong NV^0 centre. Like NV defect, the defect responsible for the 389 nm centre contains single nitrogen atom. Much weaker NV^- centre as compared with the NV^0 centre suggests that the concentration of nitrogen C-defects in these diamonds is very low. The line at 594.4 nm is almost always observed in any natural or synthetic diamond after irradiation and annealing. It is probably the well-known 594.2 nm centre present in nitrogen containing natural diamonds after irradiation and annealing at temperatures below 1100°C [Collins et al. 2005]. However, very high temperature stability of the centre in our CVD-grown diamonds does not allow us to declare definitively that we are talking about one and the same centre. A complex set of lines with prominent ones at wavelengths 475.7, 478.7, 506.3 and 516.5 nm was found in spectra of other CVD-grown and HPHT-grown diamonds after irradiation and annealing. Nothing is known as to the origin of these optical centres.

The absorption spectrum of the diamond annealed in hydrogen at 2200°C is actually without structure. An absorption continuum rising towards shorter wavelength is the dominating feature. In its background, a weak H3 centre (ZPL at 503.3 nm) and vanishingly weak NV^0 and NV^- centres are seen. No trace of other centres present in the spectra of CVD-grown diamonds annealed in vacuum at 1500°C can be recognized. The SiV^- centre has been annealed too, suggesting that it is not a centre of high-temperature stability. The centre withstands low temperature HPHT treatment [Crepin et al. 2012], but anneals out completely at tempera-

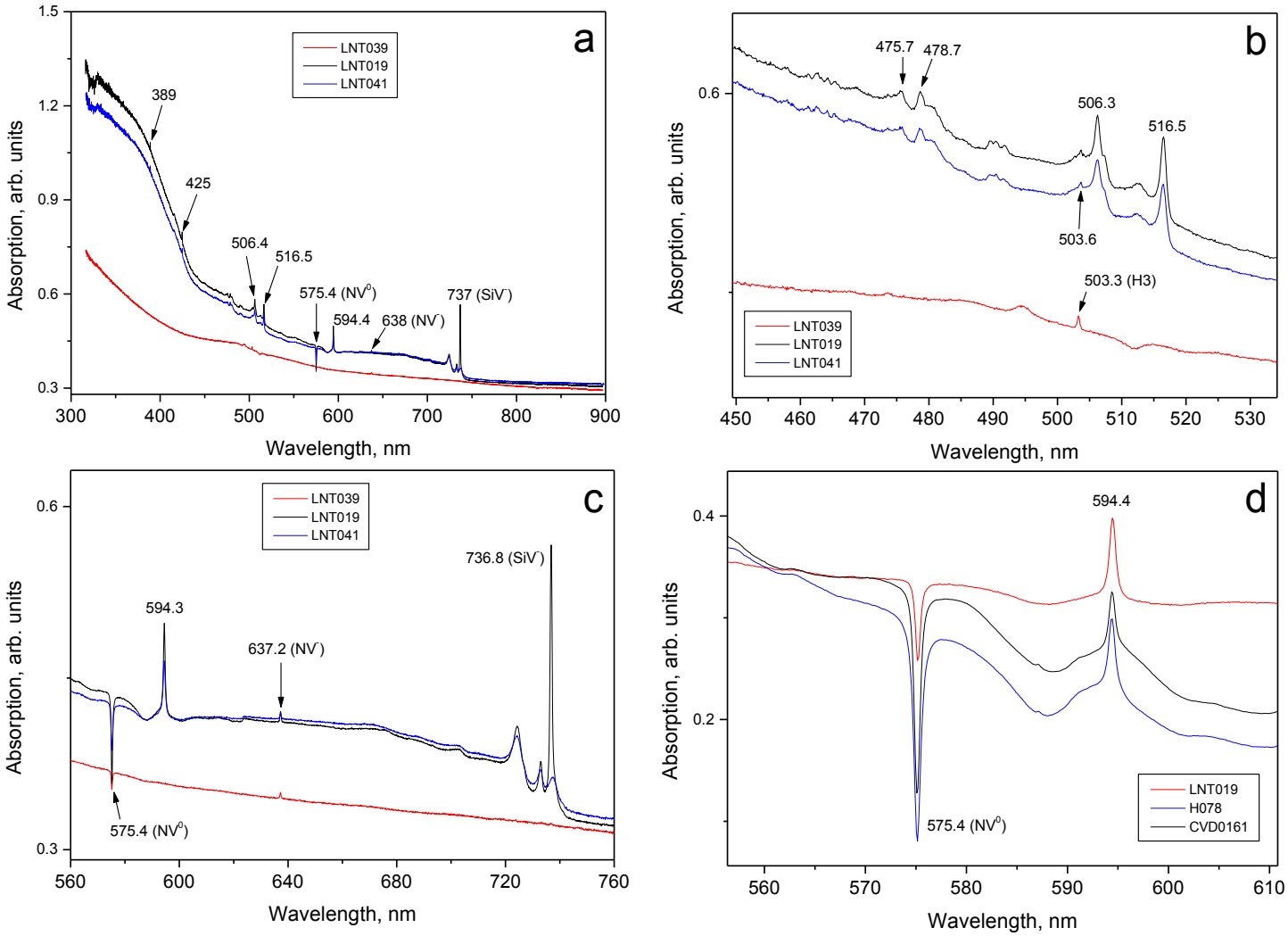

Fig.5. (a) General absorption spectra of the yellow CVD diamonds in the spectral range from near UV to near IR measured at LNT. (b) Part of the spectra showing spectral structure of the unknown optical centres with main lines at 506.3 and 516.5 nm. (c) Spectral range of absorption of SiV- centre. Annealing at 2200°C removes the SiV- centre completely. (d) Comparison of absorption spectra of ZPLs of 594.4 nm centre and NV0 centre measured at LNT in irradiated and annealed synthetic diamonds: yellow CVD-grown diamond annealed at 1500°C (red), pink CVD-grown diamond annealed at a temperature below 1000°C (black) and pink HPHT-grown diamond annealed at a temperature below 1000°C (blue).

tures above 2000°C.

The spectral features, which determined color transformations in yellow CVD-grown diamonds, are the featureless absorption continuum, intensity of which increases from near IR to UV with a sharp increase at a wavelength of 430 nm, GR1 centre produced by irradiation and SiV- centre. Before irradiation, the CVD-grown diamonds were grey because the grey continuum dominated and the SiV- centre was not intense enough to contribute to blue color. After irradiation, the GR1 centre becomes the dominating one with absorption in the red, yellow and green spectral ranges and this absorption makes diamonds blue.

The spectral features, which determined color transformations in yellow CVD-grown diamonds, are the featureless absorption continuum, intensity of which increases from near IR to UV with a sharp increase at a wavelength of 430 nm, GR1 centre produced by irradiation and SiV- centre. Before irradiation, the diamonds were grey because the grey continuum dominated and the SiV- centre was not intense enough to contribute to blue color. After irradiation, the GR1 centre becomes the dominating absorption in the red, yellow and green spectral ranges and this absorption makes diamonds blue.

Annealing at 600°C partially reduces the GR1 centre resulting in greyer diamonds. Annealing at 1000°C makes single vacancies mobile and destroys the GR1

centre. The mobile vacancies may be trapped by Si atoms and form additional SiV defects, thus strengthening the SiV^- centre. The stronger SiV^- centre produces preferential absorption in the red and orange spectral range, creating a transparency window in the yellow spectral range. Thus the diamonds acquire yellow color. The SiV^- centre remains stable at temperatures up to 1600°C. Annealing in vacuum at this temperature has no effect on the yellow color. However, annealing in hydrogen may affect SiV defects even at temperature as low as 1300°C and a CVD-grown diamond annealed this way may reduce absorption of SiV^- centre resulting in an orange tint to its color. Annealing in hydrogen at 1600°C further reduces intensity of the SiV^- centre. This extends the transparency window in the red range creating a brownish diamond. Higher temperatures anneal SiV^-centre out completely and the remaining absorption is that of the unstructured continuum. The CVD-grown diamond becomes grey again.

The absorption spectra of the three yellow CVD-grown diamonds after final annealing are shown in Fig. 6. The CVD-grown diamonds annealed at 1500°C in vacuum have two elevated absorptions in the spectral ranges from 600 to 750 nm (SiV^- centre) and 460 to 520 nm (uncertain origin) which leave preferential transparency in the yellow spectral range. CVD-grown diamond annealed in hydrogen at 2200°C reveals only the grey absorption continuum and a weak absorption of H3 centre (a small hump with maximum at 480 nm).

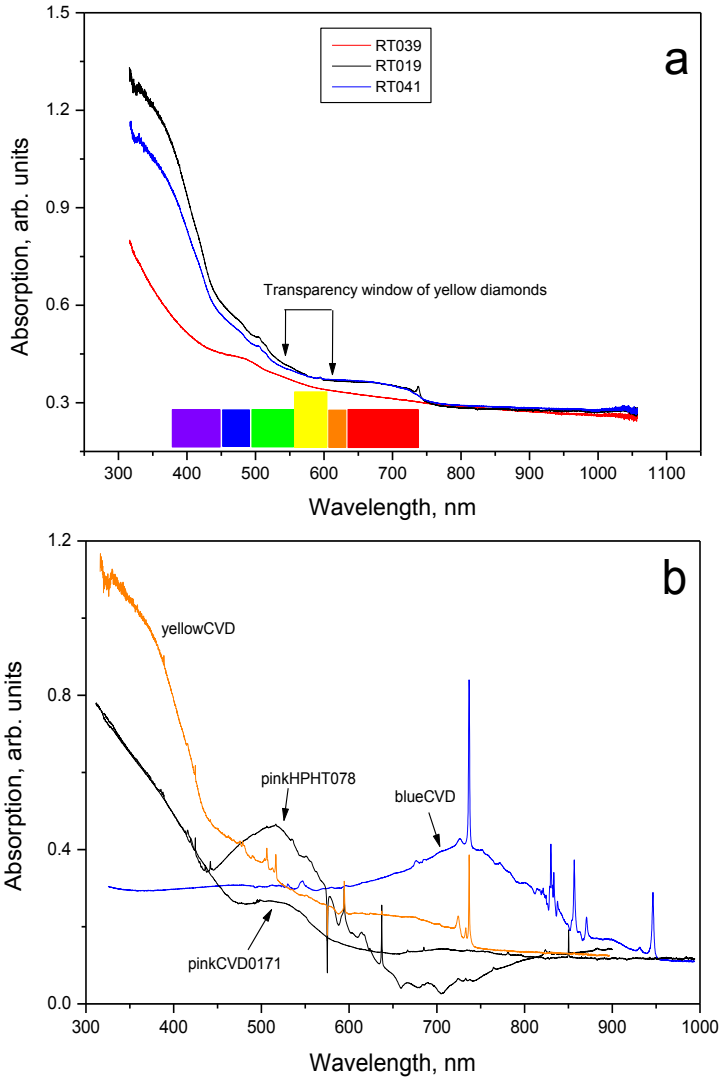

Fig. 6. (a) Absorption spectra of the yellow CVD-grown diamonds recorded at RT after final annealing. The optical transparency window determining the yellow color is indicated by arrows. (b) Comparison of absorption spectra of synthetic diamonds of different color: greyish-blue silicon-doped CVD-grown, pink nitrogen-doped HPHT-grown, pink CVD-grown with 520 nm band, yellow silicon doped CVD-grown.

Luminescence

The samples annealed in vacuum exhibit in spectra excited with 405 nm laser an intense NV^0 centre with ZPL at 575.2 nm, very weak H3 centre with ZPL at 503.5 nm and in addition also SiV^- centre with ZPL at 736.9 nm in one diamond and 738.2 nm in another (both in regime of luminescence), as well as the 441.8 nm centre of trace intensity (Fig. 8a). No sign of the NV^- centre was detected with 405 nm excitation.

The sample annealed at 2200°C reveals a very different PL spectrum when excited with 405 nm laser. The spectrum looks very similar to an irradiated and annealed low nitrogen type Ia natural diamond with all major nitrogen-related centres (Fig. 8b). The dominant feature is the H3 centre. There is an intense NV^0 centre and also the N3 centre (ZPL at 415.2 nm) of significant intensity. The spectrum also shows very weak luminescence of the SiV^- centre and a centre with ZPL at 467.6 nm.

The 467.6 nm centre shows dominating electron phonon coupling with 72 meV vibrations, Huang-Rhys factor is about 2. Temperature quenches the 467.6 nm centre strongly. No sign of it was detected in spectra recorded at RT. These data suggests that we observed the centre previously reported [Field 1992; Zaitsev 2002]. Low energy phonon side-band of the 467.6 nm centre is similar to that of the 389 nm nitrogen-related centre, which is ascribed to a defect containing interstitial nitrogen atom [Zaitsev 2000]. Tentatively, we can assume that the 467.6 nm centre originates form a nitrogen-re-

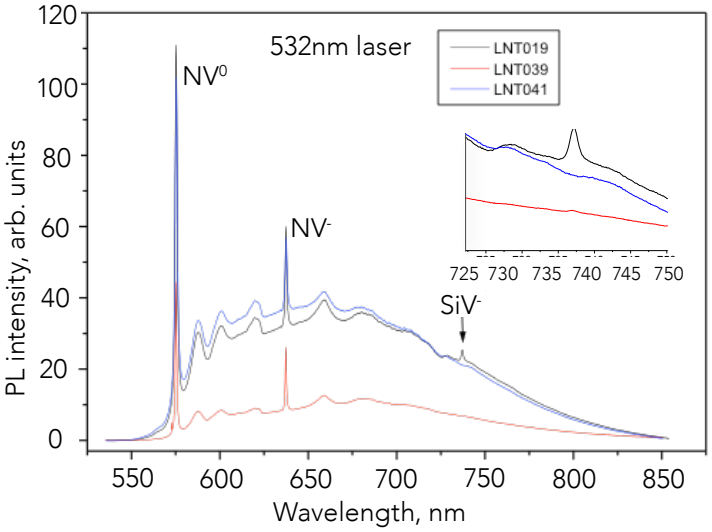

Fig. 7. PL spectra of the yellow CVD-grown diamonds recorded at LNT with 532 nm laser excitation. The insert shows the spectra of ZPLs of SiV- centre. Vanishing and weak ZPL of this centre is recognized in the CVD-grown diamond annealed at 2200°C.

lated defect, atomic structure of which is similar to that of the 389 nm defect; e.g. they both contain a single interstitial nitrogen atom.

The presence of H3 and N3 defects in the diamond annealed in hydrogen is an evidence of aggregation of nitrogen. This result suggests that annealing at low pressure at temperatures over 2000°C is comparable with HPHT annealing.

When excited with 532 nm laser, all three CVD-grown diamonds reveal NV^0 and NV^- centres of comparable intensity, yet the NV^0 centre being stronger than NV^- for both samples (Fig. 7). Stronger NV^0 centre suggests that the concentration of single substitutional nitrogen atoms (C-defects) is very little, and NV defects remain preferentially in a neutral charge state.

All CVD-grown diamonds also show traces of SiV^- centre, which however, in CVD-grown diamond with atypical SiV^- centre, is seen in regime of absorption (negative luminescence). The presence of the SiV- centre in a CVD-grown diamond annealed at 2200°C suggests that SiV defects are actually very temperature-stable and can survive commercial HPHT treatment.

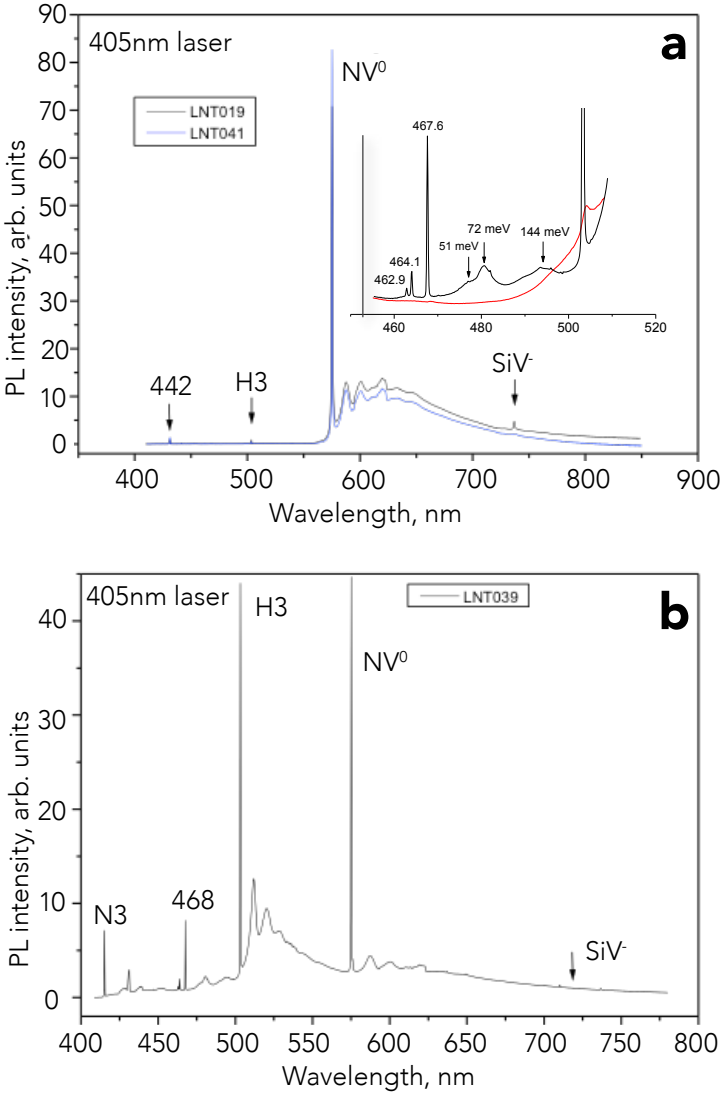

Fig. 8. PL spectra of yellow CVD-grown diamonds measured at LNT. (a) Samples annealed in vacuum at 1600°C. The insert shows the spectra of ZPLs of SiV^- centre. (b) CVD-grown annealed in hydrogen at 2200°C. A very weak SiV^- centre can be detected. Spectrum of its ZPL is identical to that shown with the black curve in (a). The insert shows the vibrational side-band of the 467.6 nm centre. No trace of this centre could be detected at RT (red line).

GR1 and SiV$^-$ centres

Analyzing absorption spectra of different CVD-grown diamonds with GR1 and SiV centres formed the following conclusions:

Spectrum of GR1 centre is very similar to that of SiV$^-$ centre in both terms of position of ZPL and structure of vibrational side band (Fig. 9). Both centres reveal dominant interaction with quasilocal vibrations. For GR1 centre, the energy of these vibrations is 41 meV. For SiV centre, the energy of the quasilocal vibrations could range from 25 meV and 29 meV. Distinctive features account for the interaction with lattice phonons. For GR1 centre, they are: 675.1 nm (1.837 eV, 164 meV, on optical phonon at the edge of the Brilloin zone), 678.2 nm (1.828 eV, 155 meV, maximum density of optical phonons), 689.3 nm (1.799 eV, 126 meV, maximum density of acoustic phonons) and a broad plateau-like band from 699 to 713 nm (1.773 to 1.739 eV, 100 to 66 meV, maximum density of long wave optical phonons). All these features coincide very well with calculated energies of high density phonons in diamond lattice [Windle et al. 1993; Zaitsev 2001].

In spectra of SiV$^-$ centre, some of the above mentioned spectral features can be recognized too. Their relative intensity with respect to the intensity of ZPL is about five times weaker. A striking difference of vibrational spectra of GR1 and SiV$^-$ centres is a very low intensity of the low energy acoustic phonon of SiV- centre as compared with those of GR1 centre. This strong electron-phonon interaction with acoustic phonons on GR1 centre produces the intense absorption band from the wavelength range from 500 to 730 nm and is the reason of very small Debye-Waller factor of GR1 centre. Qualitative similarity of the phonon side-bands of GR1 and SiV$^-$ centres supports their atomic models as defects involving single vacancy and suggests that the electron-vibrational interaction occurs mainly on the vacancy.

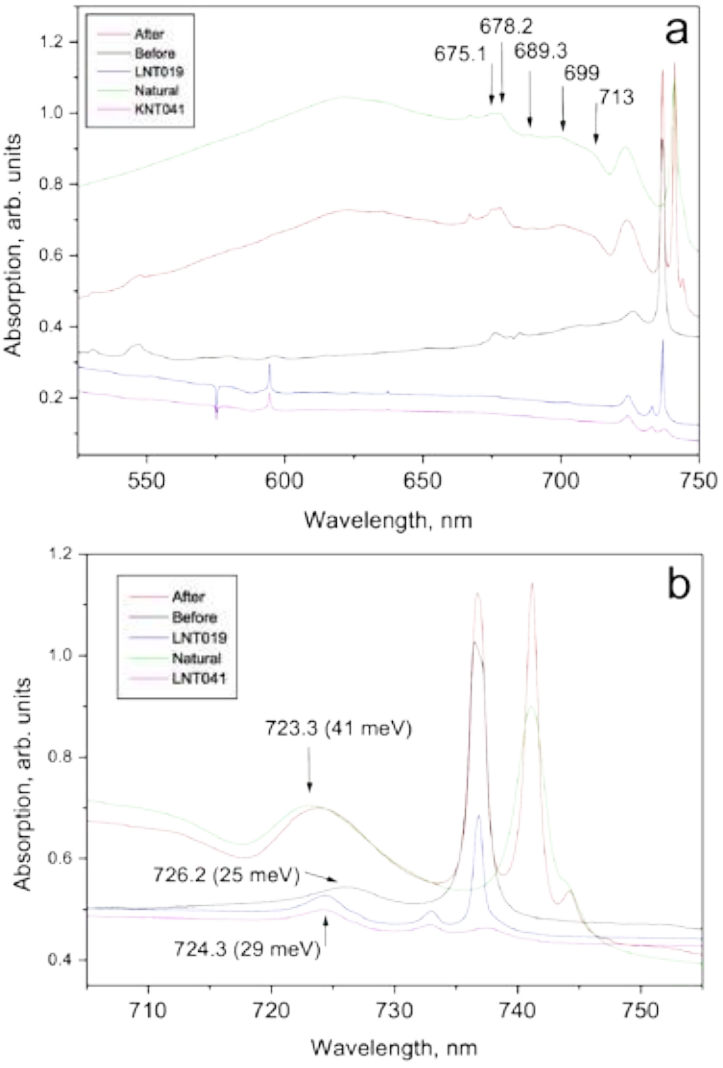

Fig. 9. Comparison of absorption spectra of GR1 and SiV$^-$ centres recorded at LNT. The main phonon features of GR1 centre are indicated. Vibrational band of the atypical SiV$^-$ centre in sample 041 (pink curve) is identical to that of 'normal' SiV$^-$ centre. However spectra of their ZPLs are quite different. (b) Detailed spectra in the range of ZPLs and quasilocal vibrations for GR1 and SiV$^-$ centres. Spectral positions and energies of the quasilocal vibrational bands are indicated.

Broad vibrational features at wavelengths of 723.3 nm (for GR1 centre) and 726.2 nm (for SiV centre) are most probably quasilocal vibrations with energies of 41 and 25 meV respectively. The energy of quasilocal vibrations directly corresponds to the vibrating mass and the strength of the interatomic interactions within the defect. Assuming that both features originate from the same type of quasilocal vibration, the ratio of their energies can be considered as energies of harmonic oscillators. In this case it should follow the inverse ratio of the square root of the vibrating masses. Indeed, the ratio $h\omega_{SiV}/h\omega_{GR1} = 0.61$ is close to the ratio $(m_c/m_{si})^{0.5} = 0.65$. Thus we deem that the explanation of these vibrational features as quasilocal vibrations on vacancy makes sense. The small difference between the two numbers can be logically explained by the different force constants driving C-C and C-Si vibrations. The above considerations suggest that vacancy in the diamond lattice may form similar optical centres when being captured by different impurity atoms. This simi-

larity is in the close spectral position of ZPLs and dominant interaction with quasilocal vibrations. It's likely that many impurity-related centres with ZPLs in the spectral range close to the wavelength 740 nm originate from this type of defect. Besides SiV^- centre, they could be the 812 nm Xe-related centre [Martinovich et al. 2003], the 805 nm Ni-related centre and a number of centres with ZPLs about 740 nm ascribed to Cr [Aharonovich et al. 2009; Aharonovich et al. 2009a; Aharonovich et al. 2010; Steinmetz et al. 2010]. Given this assumption, one may speculate that different species may produce similar optical centres with ZPL close to 740 nm. It might be that the atypical SiV^- centre seen in spectra of one of the studied yellow diamonds does not actually originate from Si, but some other impurity. Thus its spectrum is somewhat different as compared with that of real SiV^- centre.

This theory of the possibility of the creation of different vacancy-related optical centres may have critical technological implications for CVD diamonds grown for jewelry application. Indeed, these centres could be conveniently created by corresponding doping during growth followed by irradiation and subsequent annealing. Although these centres are expected to absorb preferentially in the long wave visible spectral range; yet they could have various absorption spectra and various temperature stability. Therefore choosing appropriate regimes of doping and annealing, one could produce CVD-grown diamonds of different colors and create "rainbow of diamond colors" as more affordable alternative to natural fancy colored diamonds.

FTIR spectroscopy

It can be seen that the sample from Scio has more prominent peaks at 1344 and 1332cm^{-1} than the three diamonds used for the annealing and irradiation experiments. We can assume that yellow color in Scio diamond is due to higher concentration of single nitrogen than studied 3 samples. However, all peaks at 1344 and 1332cm^{-1} are too small for quantitative analysis (see Fig. 10).

FTIR Spectroscopy

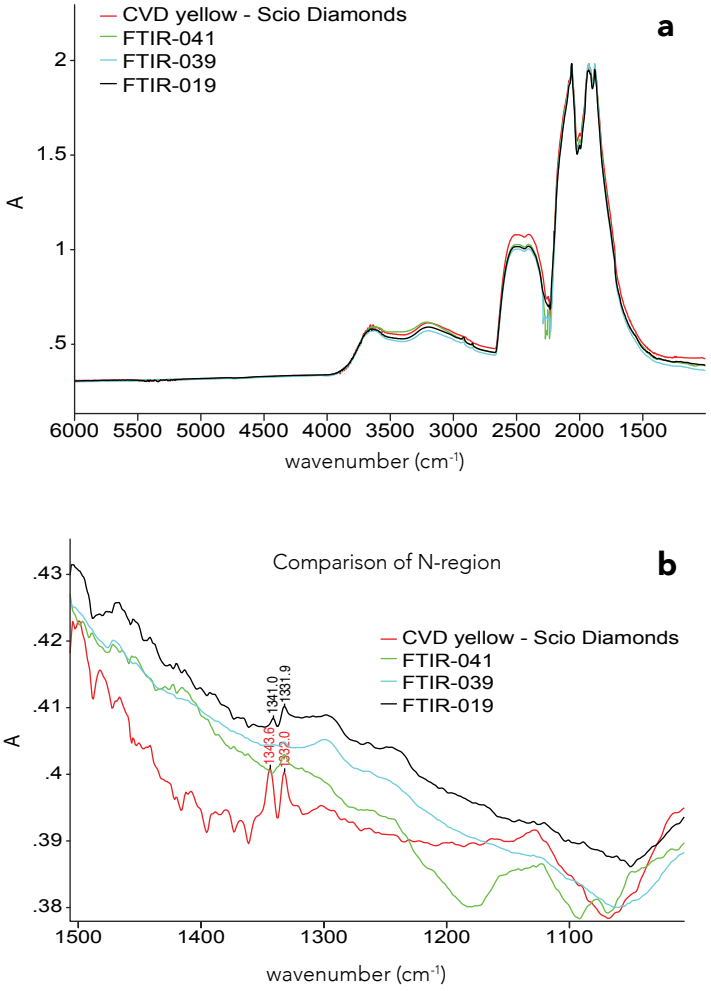

Fig. 10: Comparison of FITR spectra of the three CVD-grown irradiated and annealed yellow samples with a CVD-grown yellow diamond available on the market, produced by Scio Diamonds (ex Apollo).

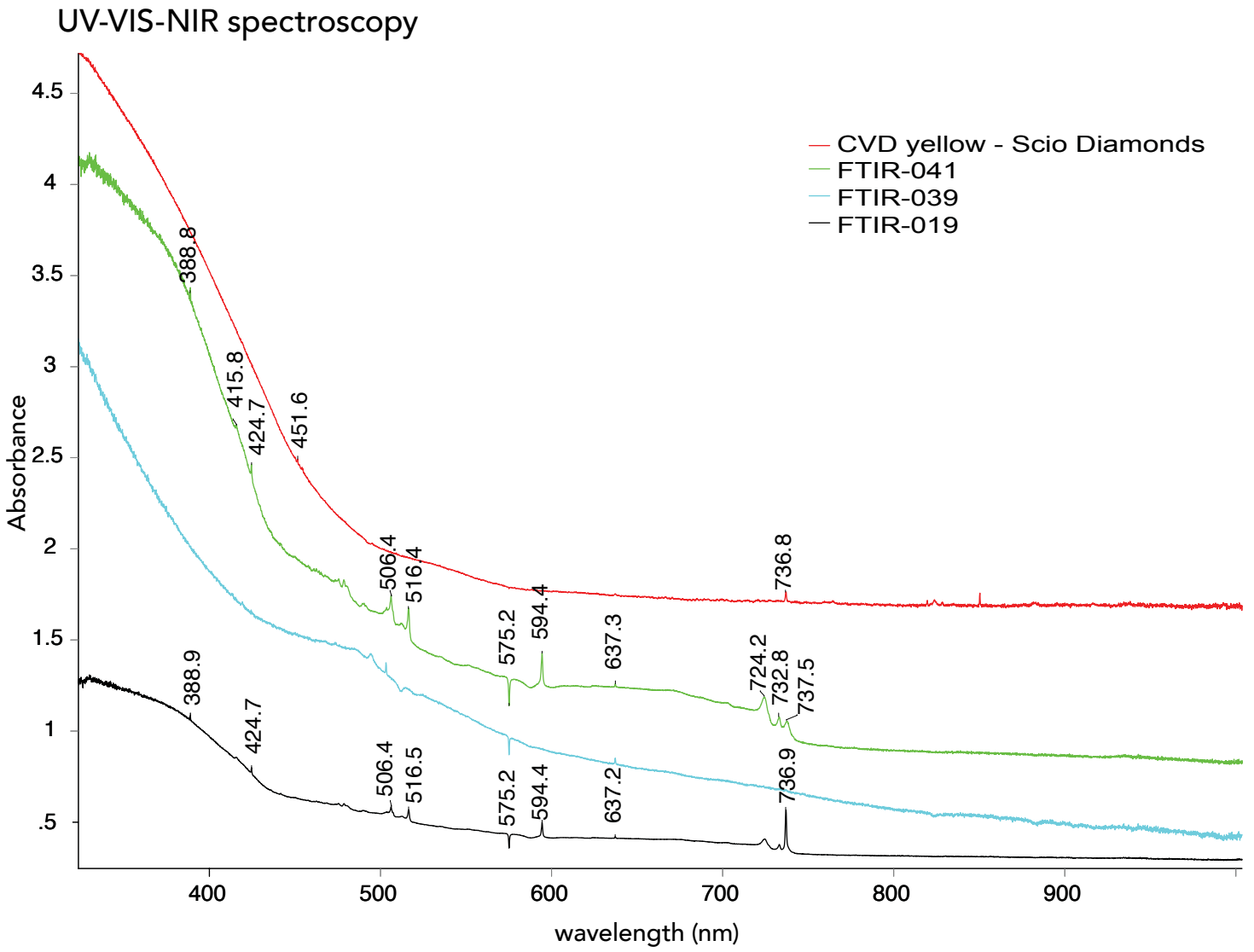

Fig. 11: Comparison of UV-VIS-NIR spectra of the three CVD-grown irradiated and annealed yellow samples with a CVD-grown yellow diamond from Scio Diamonds (ex Apollo).

UV-VIS-NIR spectroscopy

Clear differences between the Scio sample and the three CVD-grown irradiated and annealed are visible. The Scio sample only shows the Si-peak at 736nm. The NV-centres at 575nm (NV^0) and 637 (NV^-) are not identifiable. In contrast to the three CVD-grown anneald and irradiated samples, where the NV-centres and the M1-centre at 516.4nm (radiation centre) are clearly visible. Equally to the radiation centre at 595nm and the Si-centre that can also be seen in these three samples.

The cause of yellow color in the experimentally derived diamonds is a combination of the grey continuum and SiV^- centre absorption. In the case of the Scio diamond, it is a reduction in absorption of the the grey continuum at a wavelenght of around 600nm.

PL 405nm

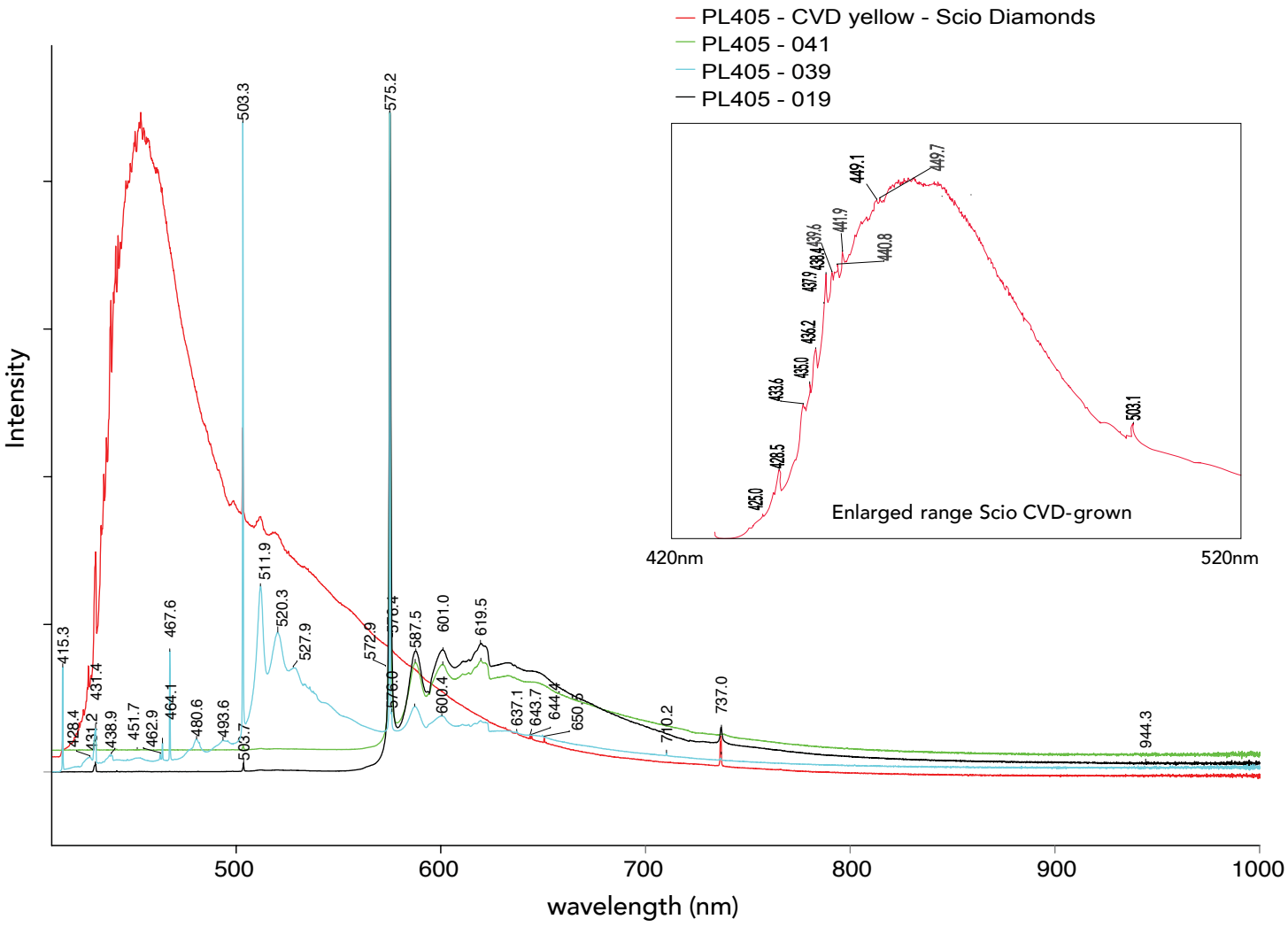

Fig. 12: Comparison of PL 405nm spectra of the three CVD-grown irradiated and annealed yellow samples with a CVD-grown yellow diamond from Scio Diamonds (ex Apollo).

Photoluminescence 405nm

The PL405nm spectrum from the Scio CVD-grown yellow diamond clearly differs from the other three spectra of the CVD-grown irradiated and annealed stones. Along with the Raman-peak (431nm) only the H3-centre (503nm), the NV^0-centre (575nm) and the Si-centre (737nm) are clearly visible in the spectrum of the Scio CVD-grown yellow diamond. The NV^- -centre is very small and accompanied by small peaks at 643, 644 and 650nm. Besides the peaks, the full spectrum has the shape of an asymmetrical bell curve, with a long tail towards the higher wavelength -region.

All other samples do not exhibit this asymmetrical bell curve shape. Sharp peaks at 575nm and 637nm (637nm < 575nm) are present. The H3-centre is only developed clearly in sample 039 (blue curve). Overall this sample shows more structure than the other two CVD-grown irradiated and annealed yellow diamonds. The Scio diamond has many low intensity PL lines throughout the entire visible range. The most probable explanation of such many low intensity PL lines is doping with heavy transition metals and/or rare earth elements. Rare earth elements in diamonds are an absolutely unknown science and could be something to onset a new era in optical applications of diamond.

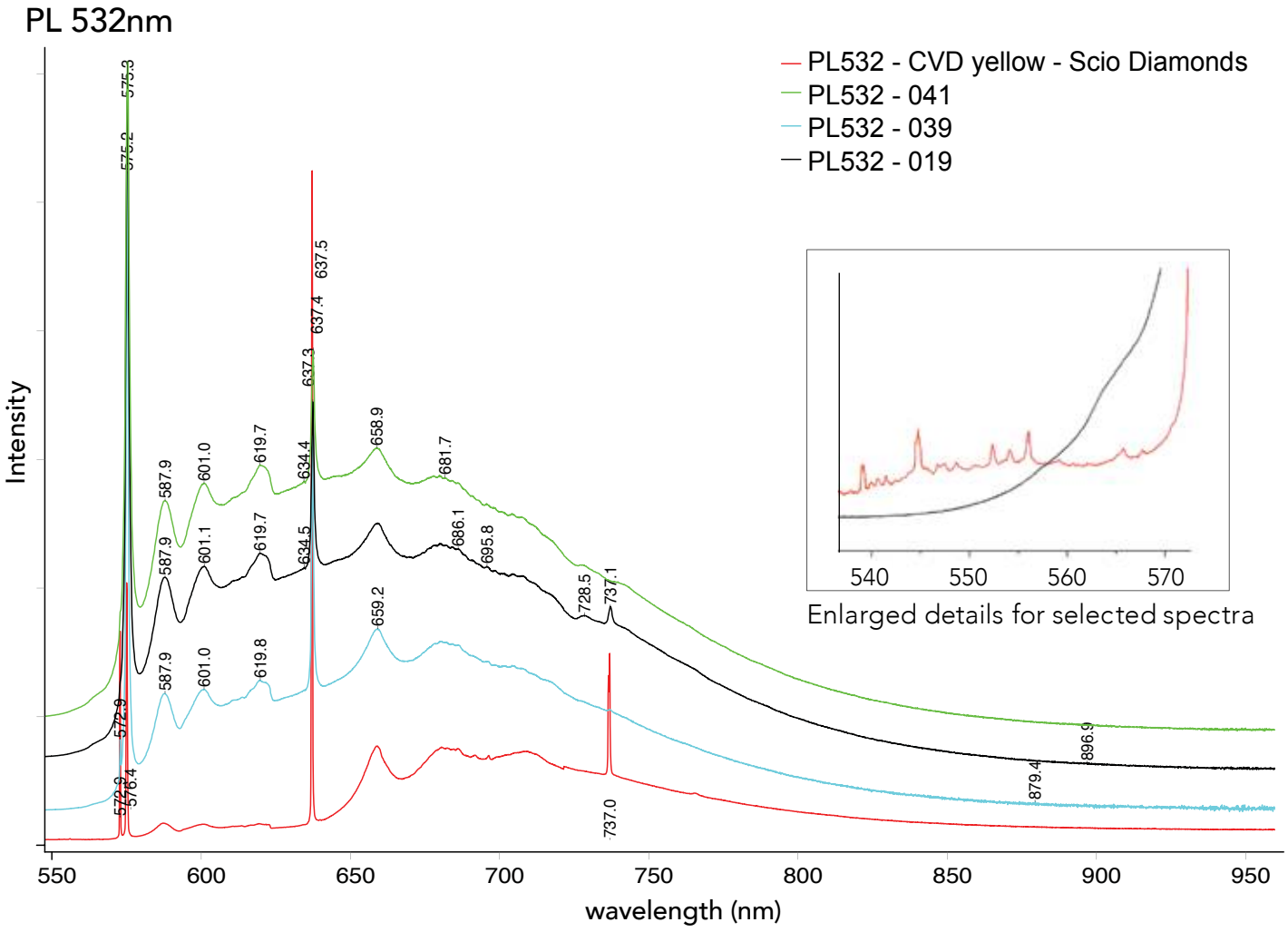

Fig. 12: Comparison of PL532nm spectra of the three CVD-grown irradiated and annealed yellow samples with a CVD-grown yellow diamond from Scio Diamonds (ex Apollo). The inserted graph shows many low intensity PL lines between 540nm and 570nm for the Scio CVD-grown (red line) diamond but not present in the experimentally created CVD-grown yellow diamonds (black line). Interpretation see conclusion.

Photoluminescence 532nm

When exposed to 532nm laser irradiation, the spectra of all CVD-grown yellow diamonds resemble each other, although the Si-peak at 736nm is more prominent for the CVD-grown yellow diamond from Scio and 637nm is stronger than 575nm as well. This ratio (typical for HPHT treatment of natural diamonds) indicates that HPHT treatment could be responsible for creation of single nitrogen and yellow color.

Conclusion

We present here the first comprehensive data on CVD-grown gem quality diamonds of yellow color, that is produced commercially by HPHT treatment (Scio Diamond) and experimentally by our research team by multistep annealing and irradiation process at different conditions. Based on this data we deduce that the reason for experimentally produced yellow is strong absorption of the silicon-related SiV-centre in the red spectral range and an absorption continuum in the green and blue spectral ranges. The absorption continuum is a very temperature-stable feature and it cannot be removed from CVD-grown diamond by commercial HPHT treatment of heating in hydrogen at temperatures up to 2200°C. The SiV^- centre has lesser

temperature stability and it can be considerably destroyed by heating at temperatures over 1600°C.

This study proofs that the cause of yellow color in the CVD-grown diamond available on the market (Scio Diamonds) differs to the cause of color in our experimentally derived multistep treated yellow CVD-grown diamonds. The Scio CVD-grown yellow diamonds may possibly involve the doping of additional, currently unknown elements such as heavy transition metals and/or rare earth elements (see Fig. 12, inserted spectra), as we were not able to reproduce its color with multistep treatment experiments. Most probably pure yellow color is produced by other treatments not applied by us, such as HPHT treatment. We have contacted Scio Diamonds (personal communication with CEO) and it is confirmed that HPHT treatment was applied on request of Scio Diamonds, but the stone was grown by Apollo and without any records of previous growing and treatment conditions.

Since 1600°C is much higher than temperatures that diamonds can be exposed to during cutting and jewelry manufacture, the described yellow color is permanent. This is very important because stable color lab-grown diamonds are graded with same or similar terminology as natural colored diamonds at most major laboratories as well as at GRS and CGL laboratories.

Analyzing the spectra of GR1 and SiV^- centres and comparing them with existing published data, we conclude that silicon might be not the sole impurity providing absorption in the red spectral range. Other impurities, like Xe, Ni or Cr may produce this result. Spectral variations of these new centres and possibly different temperature stability of the corresponding defects might be an effective means of achieving other colors in CVD-grown gem diamonds.

Fig. 13: Overview of all tested samples from left to right. The first three samples are the experimentally created, multistep treated CVD-grown yellow diamonds.
The sample on the right is a CVD-grown yellow diamond from Scio Diamonds, available in the market. For more details see Table 1.

Acknoledgements

We are grateful to Dusan Simic (Analitical Gemology and Jewelry, USA) for providing the research-samples.

References

[1] Collins A. T., Connor A., Ly C. H., Shareef A. and Spear P. M. (2005) "High temperature annealing of optical centres in type I diamond", J. Appl. Physics, Vol. 97, p. 083517.

[2] Crepin N., Anthonos A. and Willems B. (2012) "A study of multi-treated CVD synthetic diamonds", Proc. 63rd Diamond Conference, Warwick, UK, p. O3.1-O3.3.

[3] Deljanin B., Simic D., Linares R. (2003). "New challenge for jewelry industry: Laboratory-grown CVD gem-quality diamonds", Material Research Science Conference, Boston abstract.

[4] Dobrinets I. A., Vins V. G. and Zaitsev A. M. (2013). "HPHT-Treated Diamonds", Springer Verlag, pp. 257.
Field J. E. (ed.) (1992) "The Properties of Natural and Synthetic Diamond", Academic Press, London.

[5] Fritsch E., Conner L. and Koivula J. I. (1989) "A preliminary gemological study of synthetic diamond thin films", Gems & Gemology, Vol. 25, No. 2, pp. 84–90.

[6] Martineau P. M., Lawson S. C., Taylor A. J., Quinn S. J., Evans D. J. F. and Crowder M. J., (2004), "Identification of synthetic diamond grown using chemical vapor deposition (CVD) Gems and Gemology, Vol. 40. p. 2–25.

[7] McCauley T. S. and Vohra Y. K. (1995) "Homoepitaxial diamond film deposition on a brilliant cut diamond anvil ", Appl. Phys. Letters. Vol. 66, p. 1486-1488.

[8] Peretti A., Herzog F., Bieri W., Alessandri M., Günther D., Frick D.A., Cleveland, E., Zaitsev A.M. and Deljanin B. (2013) "New Generation of Synthetic Diamonds Reaches the Market (Part A): CVD-grown Blue Diamonds", Contributions to Gemology, No. 14, p.1-14.

[9] Simic D, Woodring S, Deljanin B.; "Processed Pinks", Rapaport, Nov. 2004.

[10] Wang W., Moses T., Linares R. C., Shigley J. C., Hall M. and Butler J. E. (2003) "Gem-quality synthetic diamonds grown by a chemical vapor deposition (CVD) method", Gems and Gemology, Vol. 39, p. 268–283.

[11] Windl W., Pavone P., Karch K., Schutt O. and Strauch D. (1993) " Second-order Raman spectra of diamond from ab initio phonon calculations", Phys. Rev. B, Vol. 48, p. 3164-3170.

[12] Wang W., Doering P., Tower J., Lu R., Eaton-Magaña S., Johnson P., Emerson E. and Moses T. M. (2010) " Strongly colored pink CVD lab-grown diamonds", Gems and Gemology, Vol. 46, No. 1, pp. 4–17.

[13] Yan C. S., Vohra Y. K., Mao H. K. and Hemley R. J. (2002) "Very high growth rate chemical vapor deposition of single-crystal diamond", Proc. Natl. Acad. Sci. Vol. 99, p. 12523–12525.

[14] Zaitsev A. M. (2000) "Vibronic Spectra of Impurity-Related Optical Centres in Diamond", Phys. Rev. B, Vol. 61, p. 12909-12922.

[15] Zaitsev A. M. (2001) "Optical Properties of Diamond: A Data Handbook", Springer Verlag, Berlin-Heidelberg-New York, pp. 502.

[16] Aharonovich I., Zhou C., Stacey A., Treussart F., Roch J-F. and Prawer S. (2009) "Formation of color centers in nanodiamonds by plasma assisted diffusion of impurities from the growth substrate", Appl. Phys. Lett., Vol. 93, p. 243112.

[17] Aharonovich I., Zhou C., Stacey A., Orwa J., Castelletto S., Simpson D., Greentree A. D., Treussart F., Roch J-F. and Prawer S. (2009a) "Enhanced single-photon emission in the near infrared from a diamond color center", Phys. Rev. B, Vol. 79, p. 235316.

[18] Aharonovich I., Castelletto S., Johnson B. C., McCallum J. C., Simpson D. A., Greentree A. D. and Prawer S. (2010) "Chromium single-photon emitters in diamond fabricated by ion implantation", Phys. Rev. B, Vol. 81, p. 121201.

[19] Martinovich V. A, Turukhin A. V., Zaitsev A. M., Gorokhovsky A. A. (2003) "Photoluminescence Spectra of Xenon-Implanted Natural Diamonds", J. of Luminescence, Vol. 102/103, p 785-790.

[20] Steinmetz D., Neu E., Meijer J., Bolse W. and Becher C. (2010) "Single photon emitters based on Ni/Si related defects in single crystalline diamond", arXiv:1007.0202.

Producer	CVD-grown- Scio Diamonds HPHT treated by Suncrest (as indicated by producer) 1 sample - 0.19ct HRef-0165	CVD-grown - Unknown producer irradiated + annealed in vacuum at 1500°C for 1h 1 sample - 0.41ct HRef-0263	CVD-grown - Unknown producer irradiated + annealed in hydrogen atmosphere at 600°C up to 2200°C 1 sample - 0.39ct HRef-0264	CVD-grown - Unknown producer irradiated + annealed in vacuum at 1500°C for 1h 1 sample - 0.19ct HRef-0265
Color	fancy yellow	fancy deep brownish yellow	light greyish yellow	fancy brownish yellow
Clarity	VVS1	VS1	VS1	VS1
Solid Inclusions (at 60x magnification)	fingerprints, pinpoints	black pinpoints, internal graining, feather	black pinpoints, internal graining, feather	black pinpoints, internal graining, feather
ED-XRF	none	none	none	none
Fluorescence SWUV (254nm)	strong yellowish green	weak orange	weak yellow	weak orange
Fluorescence LWUV (365nm)	weak green	medium-strong orange	weak-medium yellow	medium orange
Cross Polarized Filters (CPF)	net-like pattern	parallel needle-like and patchy pattern	parallel needle-like and patchy pattern	parallel needle-like and patchy pattern
FTIR spectroscopy (absorption, cm^{-1})	type IIa, no features in ZPR, except two very small peaks at 1332 and 1344 cm^{-1}	type IIa	type IIa	type IIa
UV-Vis-NIR spectroscopy at LNT (absorption)	Si-centre (737), 850, otherwise feature-less	peaks at 389, 415, 424, 506, 516, 575 (emission), 594, 637 and Si-related peaks	peaks at 506, 575 (emission), 637	peaks at 389, 424, 506, 516, 575 (emission), 594, 637 and Si-related peaks
PL spectroscopy at LNT - 405nm	peaks at 425, 428.5, 433.6, 435, 436.2, 437.9, 438.4, 439.6, 440.8, 441.9, 449.1, 449.7, sharp 503 peak (H3-centre), 575 sharp peak, very small 637, Si-"doublet" at 736.5, 736.9	small peak at 503, very sharp peak at 575	peaks at 415, 467, very sharp ones at 503 and 575, peaks at 710nm and doublet at 736nm	small peak at 503, very sharp peak at 575, Si-peak at 736
PL spectroscopy at LNT - 532nm	very sharp peaks at 575 and 637 (637 > 575, about a factor of 3), Si-"doublet" at 736.5, 736.9	sharp peaks at 575 and 637 (575 > 637)	sharp peaks at 575 and 637 (575 > 637)	sharp Peaks at 575 and 637 (575 > 637) and Si-Peak 737
Electrical conductivity	non-conductive	non-conductive	non-conductive	non-conductive

Table 1: Summary of tested CVD-grown yellow diamonds and results of examinations. Sample HRef-0165 is a CVD-grown and HPHT treated yellow diamond available on the market from Scio Diamonds. Samples HRef-0263 to HRef-0265 are experimentally produced, multistep treated CVD-grown diamonds.
Note: The unidentified lines found in sample HRef-0165 in the visible range with PL405 at LNT are possibly related to doping with rare earth elements (see discussion page 54 and Fig. 12).

Record-breaking Discovery of Ruby and Sapphire at the Didy Mine in Madagascar:

Investigating the Source

Scan QR codes to watch corresponding video

By Dr. Adolf Peretti, FGA FGG and Lawrence Hahn, GG
GRS Laboratories (http://www.gemresearch.ch/video/Didy5.htm)

In May 2012, the GRS lab in Bangkok received two very large, high-quality rough ruby crystals (Fig. 1A) for testing from a client who had flown straight to the lab from Madagascar.

The concerned client had heard rumours swirling about in Madagascar that the crystals were synthetic, and that he needed confirmation of their authenticity before his group would proceed with further investments.

Laboratory testing with ED-XRF, FTIR, UV-VIS, Raman and microscope of the specimens confirmed that the huge crystals were indeed natural and unheated. To link these crystals to the mine in question for their client, the authors undertook a perilous field trip to the source of the crystals for a first-hand inspection of the mine site. By documenting the gemstone rush on video and collecting rock and mineral samples from the site for comparison, they would be able to decode the geological conditions under which this corundum deposit was formed.

Fig. 1A, B: A gem-quality rough of over 60 carats from Didy (Madagascar) is faceted into an over 26 carats of magnificent ruby (right). World record prices were paid for such magnificent rubies, initiating an enormous buying rush. All pictures are by the authors Peretti and Hahn and copyrighted by GRS if not otherwise noted.
(http://www.gemresearch.ch/video/Didy4.htm)

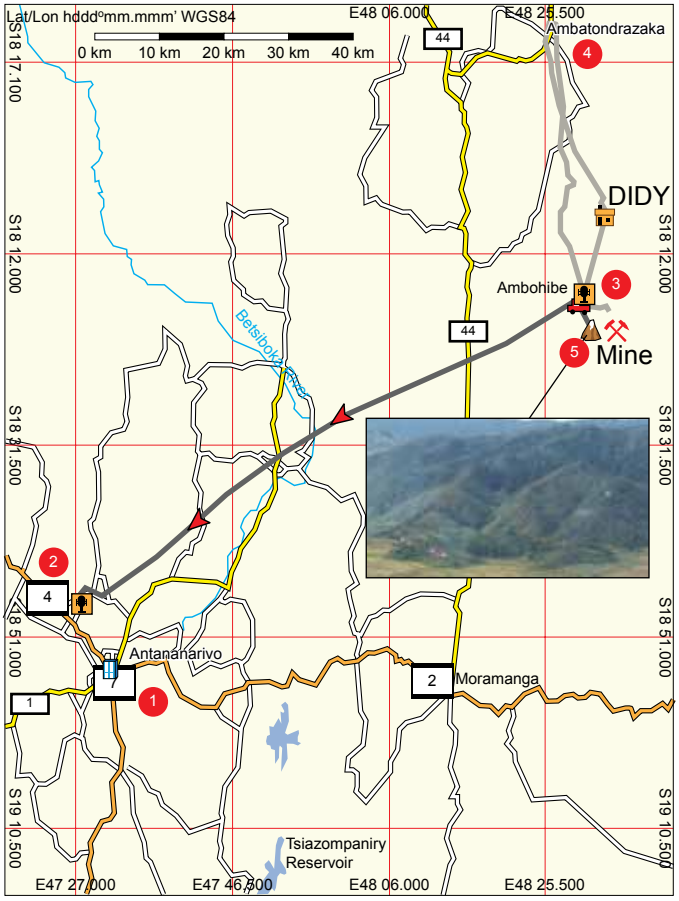

Fig. 2: A section of the detailed flight map to the mine by helicopter as recorded by our own GPS; 3-4 Good weather flight from Ambohibe to Ambatondrazaka navigated by Peretti when the board computer crashed. (Fig. 5) 4-3 Bad weather flight following terrain to Ambohibe without use of GPS; 3-2 return flight to the capital bypassing the rainforest (1 is the capital Antananarivo).

Fig. 3: A memorable snapshot of the authors Peretti (left) and Hahn (right) after returning from the expedition to the Didy mine. The expedition material exceeding 150kg that returned back included a portable gem lab and camping equipment. The authors are barefoot after the strenuous16.5-hour jungle walk to the mine and back; their feet are sore and the mountain boots are drenched by mud. (Photo: Cushman. © GRS.)

They would also acquire critical ruby and sapphire samples for further study (Fig. 7A and cover page). Every field trip like this one in Madagascar carries safety risks, logistical challenges and often, delicate negotiation with local residents and the government. Getting there was the first of a series of challenges. As Peretti recalls, "It entailed 12 hours by car to Ambatondrazaka (Amba) followed by a 3- to 5-hour drive to Didy, weather permitting; finally, foot travel for at least a day. Still there was no guarantee of success in this unknown territory in the midst of a seemingly protected and impenetrable rainforest to the north-east of the capital." Hence, Peretti determined that air travel was the better option, and enlisted a former local gem dealer to arrange for a helicopter flight out of Antananarivo over the apparent national park to locate the mine and plot definitive GPS coordinates. They would determine the nearest landing site, continue to Didy for authorization from the local government for clearance to the destination, and then commence the journey somehow. A 400-liter re-fueling deposit in Amba was organized by the aviation company. They were accompanied by a helicopter technician in the 12-hour drive to Amba in tandem with their departure from Antananarivo (Fig. 2)

Excerpts taken from Peretti's expedition diary reveal the spellbinding drama that unfolded during the field trip.

Monday, May 14, 2012

Late information reached the GRS Laboratory that the mine, with an estimated 30,000 miners, was sealed off for non-locals by the government, and that it is a 3-hour walk from the nearest village. Roadblocks set up by locals or government authorities, heavy rains or adverse road conditions would have compromised our road trip, which requires nearly a 15-hour drive from Antananarivo, known as Tananarive Capital, to Didy the nearest town to the mine.

Wednesday, May 16, 2012

Zahamena-Ankeniheny, the forest corridor where the mining was supposedly occurring, is not yet a national park but has been proposed for protection. Referred as a national park, it is earmarked for such classification to prevent its desecration like the protected areas.

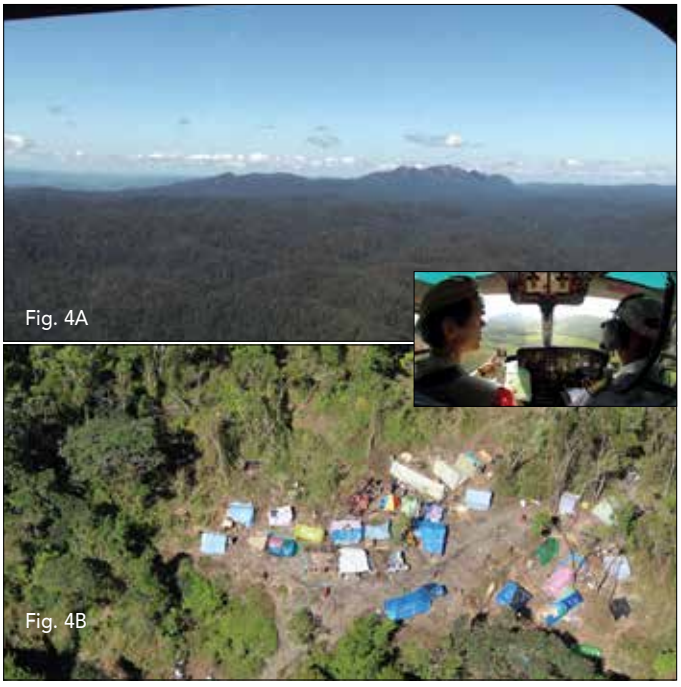

Fig. 4A: Granite rocks 10km south of the mines form a mountain range (more resistant to weathering). (See Fig. 17 for geology).
Fig. 4B: An aerial photo by GRS from the mining camp at Didy (Madagascar) when overflying the protected forest of Zahamena-Ankeniheny (inserted picture, Peretti taking over the navigation as onboard GPS computer crashes).

FLYING OVER THE NEW MINES

http://www.gemresearch.ch/video/Didy1.htm

Soaring over steep cliffs blanketed by rainforest. The panorama was breathtaking (Fig. 4A). After 40 minutes of flying, the pilot announced that we had reached our GPS coordinates. An assembly of people on the ground came into view (Fig. 4B). The sapphire area called Didy is officially named Ambatovolona.

Circling the mining area following a riverbed, miners were seen digging and washing. Almost everyone on the ground stopped working to stare at the helicopter. A second smaller place we spied suggested that miners were expanding to different areas now. Witnessing hundreds of blue tents, we wondered how many miners were actually there. It did not appear to be a 30,000-miner campsite as previously speculated; but more like 5,000 to 10,000 miners. This was no organized mining effort. It was a first-come, first-served operation led by a large number of individuals.

After circling several times, Peretti signaled the pilot to abandon the area. The images and video footage captured were sufficient, and we did not want to disturb the miners any further. We looked for the closest landing site. Past some small mountains, the mine spanned about 5km to 10km inside the rainforest, and yet, no landing site near the mine seemed possible. Then we spied small groups of cars parked at the forest edge, most likely gemstone buying agents. Then we discovered a small hill with a steep road surrounded by a half dozen houses, like a medieval village fortified on a hilltop. We called it the Eagle's Nest, and later found out that it's actually named Ambohibe.

The nearest possible landing site was about an 8-minute flight from the mine next to the Eagle's Nest. We discovered a harvested rice field with hardened earth and a few cows. We made a test landing there, saving the GPS coordinates for reference. There, we studied the environment before going on to Didy.

Landing at Didy, a throng of charming children met us and a large crowd appeared relatively subdued. They acted respectful and obedient to the local elders. Surely, it was the first time these kids had seen a helicopter. The village mayor explained that all able-bodied men were now mining in the forest, leaving the hard work at the rice paddies to the women, resulting in a low harvest this year. We negotiated an important written permission by the local government to visit the mines.

Then arriving in Ambatondrazaka, a reliable source that had been contacted before the trip offered us a fine lot of small rubies and sapphires for our reference collection. When we examined some large ruby and sapphire specimens using a portable lab (Fig. 24), we realized the mine does exist, and was producing large, unheated vibrant stones. Our anxiety grew as we contemplated being able to make it to the mine. That may be too much to hope for we thought. "Single-day trips to mines are never enough for serious geological field work, and would this mine prove to be a short-lived flash instead of a real rush?" We received a valuable tip, "Buy cigarettes for the miners." Peretti had recalled that the miners in Ilakaka, working far from civilization, always asked the same question, "Cigarettes?" especially when being photographed or filmed. They expected royalties.

Thursday, May 17, 2012, 8am

FACING A HOSTAGE SITUATION After circling around low clouds, we finally made it to a landing spot. Locals on the ground seemed dangerously hostile, grim-looking folks. They had encircled us and their Land Cruisers had blocked our exit route. A non Malagasy national dealer said, "The local 'chief' is asking US$1,000 for landing rights and US$2,000 as passage tax," disregarding our authorization letter from Didy. We were already there with the helicopter and completely surrounded. We agreed to not comply with their "offer." Further negotiations reduced the "offer" to US$1,000, breaking the impasse. We started our march from a point we christened the "Car Drop-off;" the furthest point a vehicle could reach (Fig. 5). This parking outpost gathered various 4-wheel drives, crewed by an assembly of local

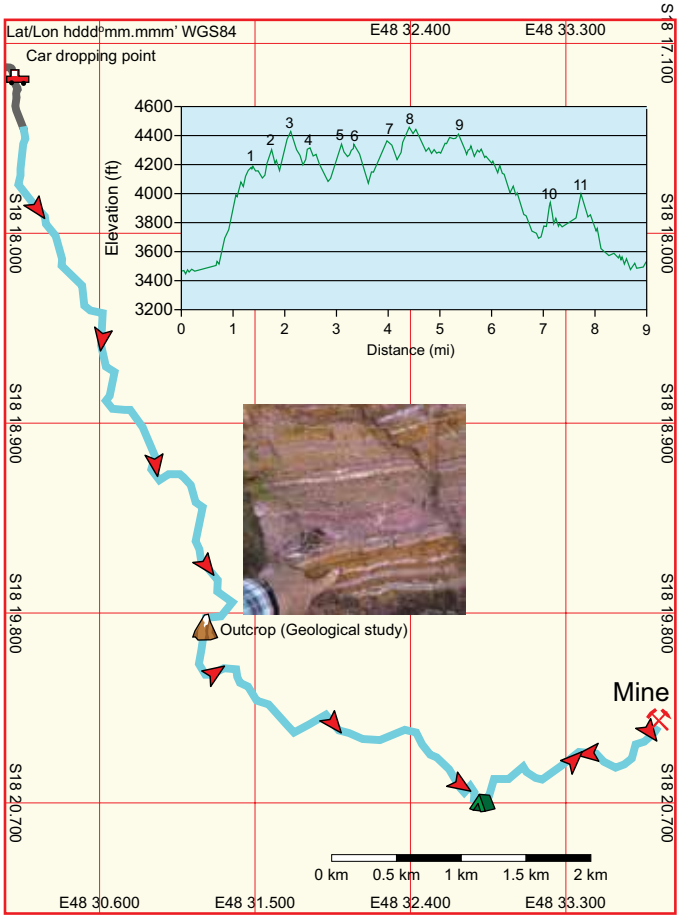

Fig. 5: GPS tracking of the walking route through the jungle to the mine, including the marched elevation profile. Note first steep climb and the crossing of about 14 small mountain peaks (hills) on the way to the mine. Red arrows mark stops for drinking water and eating in approximate one-hour intervals. Trail inserted in geological map (Fig. 17)

gemstone buying agents. We were met with hostile and sullen stares until they realized we were non-threatening. A driver we pre-arranged to pick us up there the next day disappeared, never to be seen again.

THE EXPEDITION ON FOOT We commenced our 16-and-a-half-hour walk after programming the coordinates of the mine and this landmark entry point into our GPS. We also took a guide and four porters for our equipment containing tents, food reserves and water, but we carried our camera equipment.

At first, we covered a good distance, moving at about 6km per hour. We gained confidence, following a small stream running through the valley bordering on rice paddies. Further along, the path became more densely overgrown. We crossed two men carrying a massive wooden log, probably rosewood, and walking the opposite direction towards Eagle's Nest. The log looked like it had been stripped and formed in a factory within the protected rain forest, prepared and hand-carried for exportation. These illegal wood loggers had (probably) also discovered the gems in the first place.

Eugene, the guide, doubled as a bodyguard. Our hired staff needed some energy and prepared themselves by stopping for a rice and fish bowl at a nearby hut. This entry point to the protected rainforest had another group of buying agents that seemed unfit for the brutal walk, relaxing with radios in an improvised hut. We would endure seemingly endless mountain climbing; 200 meters up and down repeatedly. Eugene brought up the rear, ensuring that nobody got lost or injured. The mountain path went up and down, the overall tendency being upwards (Fig. 5 elevation chart).

UNAUTHORIZED PROMOTIONAL HELI FLIGHT 11:34am, Ambohibe

Upon returning home and studying the pilot's logbook, we discovered that 2 hours after leaving the landing spot, the helicopter crew boarded with an unknown person on the aircraft.

Fig. 6: A miner in deep mud re-supplying the mine with 30kg to 40kg of rice, oil, small river fish and cigarettes. The miner walked barefoot as regular shoes are stripped off by the deep mud.

The helicopter took off from Ambohibe with instructions to return to Amba, but this time carried an unauthorized blind passenger aboard. The pilot logged everyone by first and last name, except the blind passenger identified by his first name "A." We assumed that the pilot was bribed. According to someone, he was the same 'chief' who had previously demanded passage tax. After the entire trip was over, the pilot acknowledged modifying the passenger list and the routing instructions without the financer's permission. The maverick group overflew the mines, taking pictures and tossing business cards from the helicopter. The unfortunate result of this ill-thought-out activity was that GRS lost exclusivity on documenting the scene, and every dealer operating in the mine was now alerted that foreigners could invade their working space. Those business cards signaled that the mine was about to go mainstream, which increased the risk. Was the crew easily influenced into doing something unethical for business gain? Were they coerced by A's influence and nobody wanted to talk about it, or was it an act of favor to "A" to secure a strategic alliance? Most likely the other non-Malagasy nationals had pre-planned this promotional farce to strengthen their buying power.

The helicopter had flown back and forth unnoticed by Peretti and Hahn. So, had the route been carefully chosen to avoid being discovered?

IN THE JUNGLE ON THE TRAIL TO THE MINE Lunch break, noon

During the trip, we ultimately shared two-thirds of the rations with the porters and guide who brought no food along. They had a single bottle of water that they shared and refilled in streams (Fig. 8).

In sharp contrast to the white group, they hardly broke a sweat during the walk. They also carried heavier loads; but a lifetime in this searing climate had prepared them.

The terrain was becoming muddier, more overgrown and elevations became steeper; the speed was reduced to 2km per hour airline distance. A couple dozen friendly people crossed our path. We were asked several times if we had been circling with a helicopter. We explained that we were gemologists not journalists, and tourists not buyers. We did not know that they were referring to the helicopter they saw just hours before. Some asked if we wanted to buy stones, but we decided not to buy anything as we thought that showing money should be avoided at all costs. Not buying permission to buy stones anyway, and we did not want to

give the impression to Malagasy dealers that we were going to cut them out from their business. Some fellows who made offers were in reality agents who did not intend to sell us stones, but wanted to test us to see whether we were seeking gemstones. We stressed that we were Swiss and German citizens working for a private company. A rumor circulated that American journalists were coming – noticeably not welcome. Local miners and dealers were showing signs of distress over the repeated helicopter visits.
We crossed two rivers and twice accepted our guide's offer

Fig. 7A: A typical example of a 4-carat rough ruby from Didy. It's not a fragment but a completely preserved rough formed in the rock. Other minerals have formed simultaneously with the ruby and left different types of negative imprints. No signs are found for transportation by a river (no rounded edges and scratches). Blue color zoning in the stone is formed only on the side where it was exposed to interaction with minerals that must have contained titanium. (Hahn Collection).

Fig. 7B: On the left-hand side is an 85-carat rough Padparadscha sapphire that is completely clean and is estimated to exceed US$1 million in value. Another example of a high-value faceted Padparadscha sapphire of 18 carats is shown in face-up and in profile position. This Padparadscha from Didy is loupe-clean, has perfectly mixed orange and pink color, is spared of thermal enhancement and does not show any color-zoning. It is one of the largest faceted magnificent Padparadscha sapphires ever tested.

Fig. 8: The picture shows a resting point in the middle of the forest about 5 miles from the mine, equipped with a small field kitchen and the local river as drinking source and bathroom. Photo shows Peretti (in red shirt) and the porters carrying the equipment.

to carry us across, sparing our trousers and shoes from becoming soaked. We were happy with our porters' offer. They were really on board with our team after we shared provisions with them, and showed their respect by carrying our heavy equipment.

15:30 THE ENTRANCE TO THE MINE IS DISCOVERED IN THE JUNGLE

http://www.gemresearch.ch/video/Didy2.htm

On the next to last elevation to the mine, we saw the first signs of deserted mining spots with unearthed boulders and holes adjacent to little ponds used for washing.

The weak stream was definitely not in its natural formation, but this was not worrisome. Tropical rain would soon restore the stream's natural flow. The receding flora would soon flourish. Little hills of washed rock were piled up everywhere with dark round boulders to the size of sand. Obviously a small alluvial riverbed was mined.

Bordered by steep hills, it rapidly became depleted, so miners moved on to easier pickings. The abandoned improvised huts showed that this was not just an exploration site, but had active mining for some time.

The trail narrowed and split into little trails overgrown with roots from the surrounding trees. They were everywhere in the rainforest but were visible here as thousands of miners passed over the surface.

Fig. 9: The mining scene in the upper part of the valley with tents housing six to eight people each, re-supply shops (middle right side), water reservoirs for washing mud, mining sites under the trees and debris dumping places. Damage to nature has been minimal compared to wood-logging activities in the same forest. (S 18 20.31 E 48 33.83, 3486 ft)

16:00 AN IMPORTANT GEMOLOGICAL DISCOVERY

The entry of the mine was a muddle of tents and makeshift huts on the slopes with countless holes and ditches in the valley. Blue improvised tents hosted up to eight people. We carefully collected this information, to later calculate the number of miners in the area when using aerial surveillance data. We were asked repeatedly, "What are you doing here? Who are you? Were you in the helicopter?" The ones that did inquire about this were distinguished in their dress; not muddy, with shoes, sunglasses and holding torches to inspect gemstones. They wanted to know if we were the competition who would threaten their profit margin.

Many organized miners deliver to agents who provide them with small credits either in cash, tools or food. These agents do not want intruders making counter offers to miners. Larger stones are routinely brought to the next centres looking for multiple offers and sold to the highest bidder. Obtaining or observing samples directly from the mine is vital, since it is 100 percent proof of its origin. We were able to inspect some rough in the mine and establish absolute proof of the rough's unique crystal habit.

16:10 Ten minutes into the mine we were still at the entry. The valley widened farther in, where the stream originated. The mine entry had an internal river joining the main stream. The farther we walked, the more miners and housing we saw. We estimated that about 30 percent of those around the mine were actually digging, the rest idling by. Some were women in charge of food and necessities, others were dealers socializing.

Fig. 11: The filming platform from where high-resolution shots were taken for a documentary that was shown at a GRS seminar during the September Hong Kong Jewellery & Gem Fair.

THE FILMING PLATFORM AT THE MINE

We reached a platform with clusters of mining and washing pits adjacent (Fig. 9, 10, 11 and 12). Each cluster contained three to four people displacing mud from small holes with one person disposing the soil by basket right next to their washing place. We were moving on the slope, as the valley was now impenetrable without disturbing the claims and getting knee-high in mud. We planned to make this expedition more downstream but a security breach required a change. At this point, we were consumed by the mining activity having reached a critical stage in our adventure.

It was like the California gold rush that prospectors encountered a century ago. This time, it was for the largest sapphires and rubies ever unearthed (Fig. 14 and 16).

THE ACTOR AT THE MINE

We found 'actors' here who demanded that their pictures be taken. One such show-off swung a thick wooden stick, shouting in Malagasy at miners on the other side, as if he were the King of the Mines. Some people, probably neighbors from Didy, approached. Suddenly, everyone was looking in one direction as shouting escalated. We saw no carbonate rocks on this visit. It was too risky getting closer to pick up samples. We did this later at an abandoned mining spot.

THE AGITATOR AND THE ATTACK AT THE FILMING STATION A highly intoxicated miner approached Hahn, chattering nonsensically in French. He was trying to explain that Malagasy people were poor, expecting a handout and calling us American journalists. The drunk persisted, he was dissatisfied with the attention received. He slapped away Peretti's video camera. Eugene intervened. This drunk had converted his small liquor bottle into a weapon with Eugene and the miner facing off in Malagasy. A crowd gathered round, and we did not expect them to take our side. Our own porters were frozen in fear, watching helplessly. Eugene commanded the drunken miner to back away, warning him about consequences. He was stunned by the harsh presence of our bodyguard, but resumed his threats. The drunk began shouting across the mining site to the other slope saying, "Americans," and agitating them to incite riot by falsifying our intentions and mobilizing them to his side. We had to leave the site now. People were still not fully convinced that we were not the American journalists threatening their mining efforts. Our original plan to camp close to the mine was no longer realistic. Getting as far away as possible from the site became our objective. Eugene looked at us with his typical smile; we smiled too, simulating confidence. The three porters followed silently as they had the entire trip. They did their job well, but our real safety line proved to be Eugene's bravado. Fortunately, Eugene's head-cam captured some of the most interesting footage.

THE SAPPHIRE ROUGH AT THE MINE, A REVELATION While exiting, our "King of the Mine" reappeared proudly showing a sapphire rough weighing approximately 10 carats (see cover photo). It lacked fine color and was worth no more than US$200. What was very interesting was that the crystal exhibited no growth phases nor showed habit. He had broken his posturing to the others and his air of dominance may mean that a US$200-stone actually was a big deal. We could not imagine the outcome had we shown him money and made an offer on the stone. Hahn had kept him on our side by letting him feel admired for his low-value sapphire.

On return, we noticed the pervasive blue tents, with some sitting atop deep pits. An entire village of over 50 tents.

Fig. 12: Miners are digging under the trees to reach a secondary alluvial mining deposit with boulders of gneiss, amphibolite, gabbro and quartzite.

Fig. 13: A 40-carat GRS-type "Royal Blue" rough sapphire from Didy (Madagascar) that can be cut to a 10- to 20-carat gemstone. Estimated wholesale value exceeds US$100,000. Note that this is not a crystal fragment but the sapphire's original shape without crystal terminations as grown in the mother rock.

Fig. 15: Miners digging deeper into the alluvial bed to reach the gem-bearing layers. These layers are carried away with baskets to the washing place.

camped under the trees with improvised shops and gambling platforms with six to eight people inside a single tent. Some huts were double-layered with a professional tent inside covered by a larger one, as a shield against the heavy rain. Some tents covered a mining pit protecting a deep cylindrical hole into the ground.

GEOLOGICAL FIELD WORK AT THE ABANDONED MINE 17:00

http://www.gemresearch.ch/video/Didy3.htm

We were determined to walk until dark by using flashlights for another hour and perhaps throughout the entire night. Possibly some miners might be organizing an ambush to rob us along the way back, so moving fast was our best option.

17:20 We reached the deserted mining place; our last chance to examine and collect rock samples. The porters and Eugene exchanged views on what had just transpired. Finally, Peretti could commence his fieldwork (Fig. 20). With a small hammer he began examining rock samples from the alluvial riverbed. Soon, different types of rocks were identified, like a mica-gneiss, amphibolites, gabbros and quartz boulders. He knew that sapphire often forms in geological systems that produce radioactive minerals, like thorianite-uraninite, zircon or ekanite, which can also be radioactive. So a Geiger counter was brought along. A very slow and systematic scan of smaller pebbles in the waste pile of the mine revealed very highly radioactive minerals after an area of only 40cm^2 by 40cm^2 was searched. The scale measured out-of-limit and its beeping sound attracted the rest of the crew. A large crystal was retrieved for later lab analysis. Hahn and Eugene joined the search attentive to the Geiger counter beeps becoming more intense the closer they got to a specimen. The measurable radioactivity radius with our device was only of 15cm diameter distance (B- and minor Y-rays). It took only 2 minutes to find another sample. 5kg of rock samples were packed and brought back to the laboratory. (Fig. 19)

Fig. 14: At the washing place, we encounter a woman washing, probably from Didy. Her child should be at school. He is most probably searching for platinum and not gold but may not be aware of it (Platinum occurrence See Fig. 17).

Fig. 16: Two strong Malagasy men washing a heavy load of soil that exposes large pebbles from the alluvial bed mostly composed of gneiss, amphibolites and gabbros, but no carbonates.

19:00 Hahn assisted by Eugene quickly set up camp with a professional 2-layer mountain tent and high-tech mosquito nets, and cleared rocks and sticks to level the ground. The torches attracted mosquitoes and flying insects. Humidity emanating from trees creates its own ecosystem in rainforests. The cold nights make rain inevitable. The porters took out their equipment and built a camp with a small sheet of plastic connected between trees offering some protection against the rain. That night, they placed sheets above the mosquito nets but it covered only about 60 percent of the area.

Friday, May 18, 2012

EARLY RISER Around midnight, a downpour started and the schedule needed to change. We decided to be up by 4am. The rain would have made the muddy trail hazardous. Peretti contracted some radiation exposure due to mistakenly using his backpack as a pillow containing the radioactive sample. Thankfully, no contamination occurred since the samples were sealed.

6am Like the flick of a switch, the darkness was replaced by light. It was an amazing event. The misty fog from last night's rain hovered over the hills. Majestic trees of stunning beauty dominated the scenery in this natural wonderland in Madagascar. It was an amazing sight. The area overlooked the place where the largest rubies and sapphires in the world were found – a paradise of exotic fauna and flora accompanied by calls of lemurs and rare birds.

GEOLOGICAL FIELD STUDY OF THE ROCK FORMATIONS

http://www.gemresearch.ch/video/Didy3.htm

Stunned by the wildly diverse and colorful rock formations (Fig. 18A/B) Peretti took dip and angles of gneiss formations and gathered rock samples. Several places on the trail bore signs of small mining activities, signaling that the miners identified this as mother-rock bearing sapphire or ruby. The rock formations were complex layered rocks with different chemistry; with some layers containing amphibole of pyroxene pockets but they were deeply weathered with no fresh specimens available. Interesting boudinage was seen in the rocks' layers. These lenses showed an increase of grain size, and promising to the formation of larger sapphires. The exact position of these rocks was recorded on the integrated handheld GPS, and the integrated GPS in the video camera producing valuable footage.

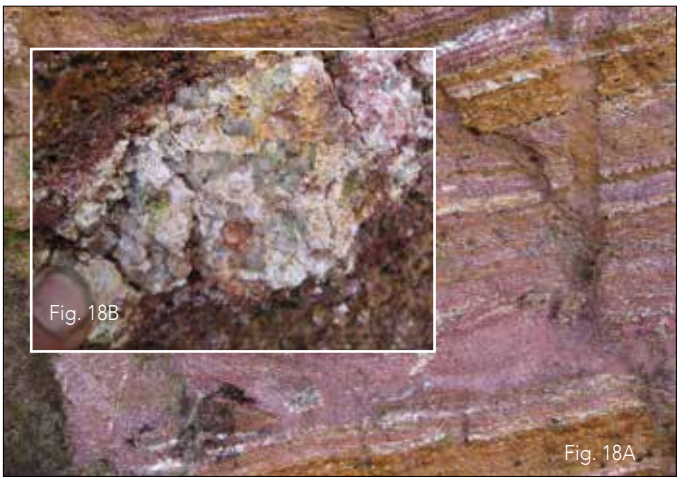

Fig. 18A: An outcrop several miles away from the mine on the hillside (marked in Fig. 5) exposes an extremely tectonized and stretched rock suite with a very inhomogeneous chemical composition shown by its weathered colors. Apart from a few minerals such as probably pyroxene or amphibole (see finger pointing), only quartz layers have survived the deep weathering.
Fig. 18B: The inserted picture shows a strong boudinage of the rocks during tectonics in certain areas with an increase in grain size. Such local occurrence in the rocks would be beneficial and necessary if the rubies and sapphires are formed by metamorphism. Miners did attempt mining at this spot and it seems their experience made them conclude it was not worth the effort.

Fig. 19: Amphibolites and gneiss rocks that were found in the riverbeds of the mines are shown. The rock-type was predicted by the geological mapping (Fig.17) and is a potential good culprit in the general scenario of sapphire and ruby formation. It is only part of the alluvial layer; a primary rock formation containing the gems was not exposed. (GRS Rock Collection.)

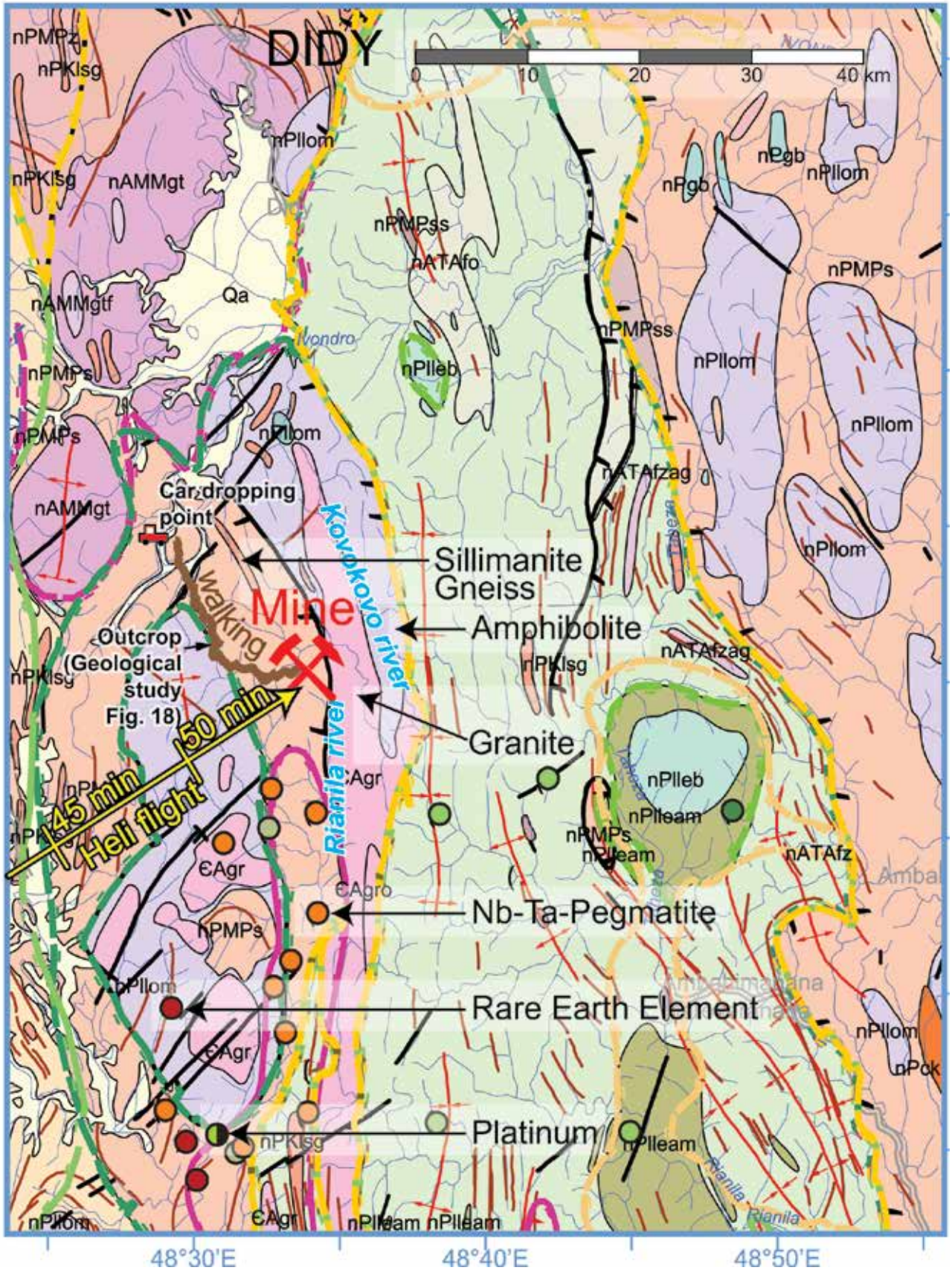
DIDY
0
10
20
30
40 km
nPMPz
nPKlsg
nPllom
nAMMgt
nPMPgs
nATAfo
nPgb
nPMPs
nAMMgtf
Qa
Ivondro
nPMPss
nPlleb
nATAfzag
Car dropping point
Kovokovo river
Sillimanite Gneiss
Mine
walking
Amphibolite
Outcrop (Geological study Fig. 18)
Granite
50 min
45 min
Heli flight
Rianila river
nPlleam
nRMPs
nATAfz
Nb-Ta-Pegmatite
Rare Earth Element
Platinum
nPck
Rianila
48°30'E
48°40'E
48°50'E

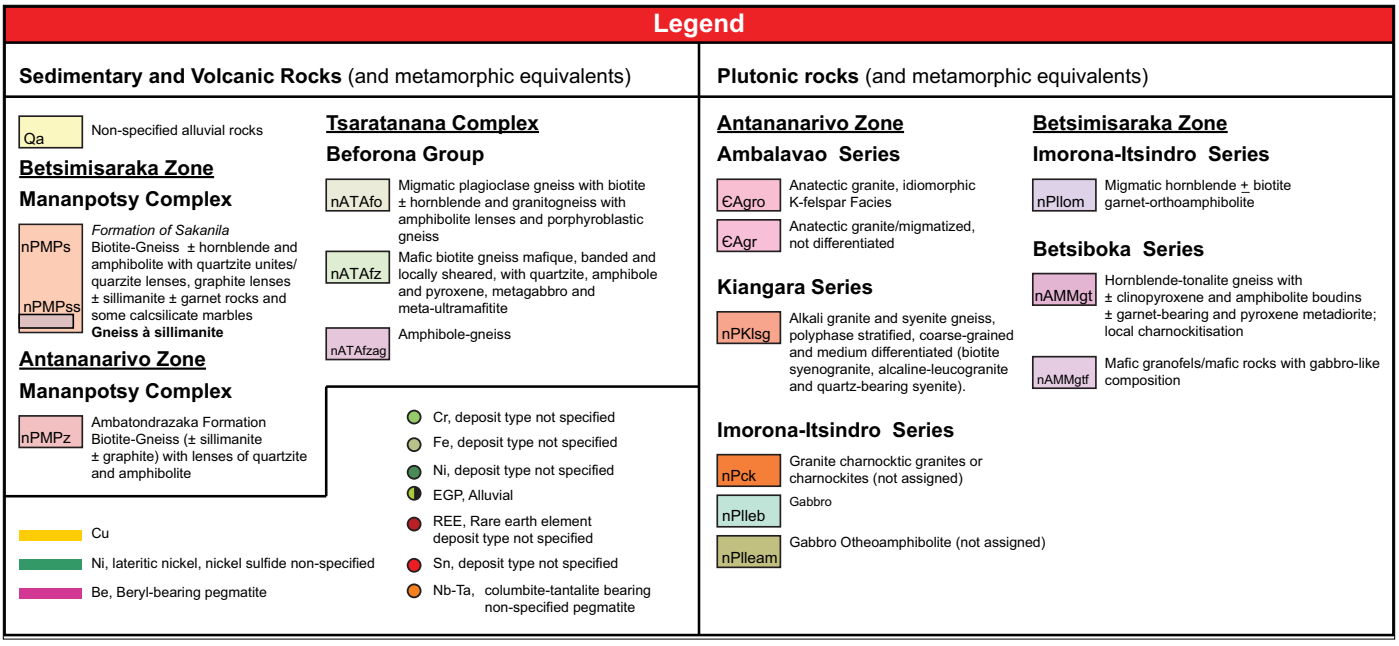

Fig. 17: A map showing the "Geology Dreamland" for the Didy (Madagascar) mine. The mine is situated in the metamorphic rock suite of gneiss, amphibolite, quartzite, intercalated sillimanite-gneiss (complex of Mananpotsy), migmatites garnet and biotite-bearing ortho-amphibolite. The gem-bearing zone is mirrored in the West (approx. 48.50E) with a large intermediate zone of gneiss and amphibolite of the Beforona group and even large bodies of gabbro are found (48.45E and 18.37S). The main difference in the rocks at the mine itself is the presence of Nb-Ta mineralization. As the map shows, this indicates the presence of pegmatite. The Ambalavao rock suite surrounds the mining area and contains quite different rock types including anatectic granites and migmatites. They are partially melted rocks typical for a lower high-metamorphic continental crust. The sillimanite gneisses of Manatopsy corroborate the high grade of metamorphism of this area (high-temperature). The rock types that were predicted by the map (amphibolite, gneiss and quartz) were indeed found in the mining area (Fig.19). Signs for hydrothermal activity were also discovered (most probably in connection with an intrusion) by abundant Fe-Th-Pb-Bi-Zr-Ta-U-Y-Nb-oxide mineral occurrences (Fig. 20) and inclusions (Fig. 26A). Note: the expedition trail in the map and the location of studied outcrop (Fig. 18). The possible scenario of sapphire and ruby formation is different to that in Adranondambo (Madagascar) and Winza (Tanzania) (See Lit.1, 4) and may be related to fluids and/or melts deriving from plutonites and the metamorphism of Si-under saturated and Al-rich rocks at high metamorphic degrees. Because of the large-scale mapping (1 to 500,000), further small-scale geological studies are necessary for further clarification. The Mine location was added from our GPS data collected, and river systems potentially containing gems are indicated with names. Legend selectively edited and translated into English from French. Map cropped from Carte Métallogénique et de Prédiction des Gisments, Métaux de Base et Métaux Précieux, Feuille No 6-Toamasina (See Lit. 3).

RE-STOCKING THE MINES

8am Increasingly, miners and villagers passed us on their way to the mine (Fig. 6). While we were walking out, they were going in with new supplies. They used sticks and metal poles to suspend rice sacks filled with rice, cooking oil, medicine and cigarettes. We could also estimate the population at the mine by calculating the food supplies being brought in. We interviewed the porters on the contents of their load. Then we created a formula based on 5,000 calories of daily consumption per person. By counting the number of porters and inquiring about their cargo, we estimated that approximately 450 people transported 2 tons of consumables including a live cow to the mine daily. There were likely 5,000 to 10,000 miners at the mine.

The average load was between 20kg to 40kg per porter. We were later informed that a pack of rice sells for US$30 at the mine, three times the regular price. People at the mine were not only chasing their dreams, they were making substantial personal investments. Thinking back, we estimated only about 30 people leaving the mine the day before. Only dealers questioned us when we left. A group of 20 to 30 influx miners told our porters they heard the day before that the mine is going to be closed by foreigners, a disturbing forecast. We assured them that we were not interested in shutting them down. Hahn explained in French that like them, our business depends on mining activity.

AT THE CAPITAL ANTANANARIVO

10:20 Arriving in Antananarivo after a one-hour helicopter flight (Fig. 3), Hahn asked the pilot to hold up the flight log "la fiche de vol" so he could take a picture, otherwise we would have never discovered the rogue helicopter trip. Peretti paid US$2,000 surcharge for the extra kilometers flown, most of which were non-authorized.

AVOIDING AN AMBUSH A driver drove us out of the heliport compound and stopped after the window suddenly exploded from the middle out. The right rear window had burst into tiny glass bits just 20cm from Peretti's head. Hahn ordered the driver to leave immediately, thinking they were being ambushed with some type of projectile. The heliport was alerted and the police apprehended a disturbed woman within 30 minutes caught throwing stones. We thought this incident was resolved way too fast and was most likely a fabrication. The person or the object should have been noticed, so it had to be fired from far outside our line of vision, and was never recovered. Peretti could not move for the rest of the ride to the hotel because of the glass shards covering his neck and arms.

Our phones kept on ringing. Someone wanted us to test a large stone while another wanted money. With no stones to be

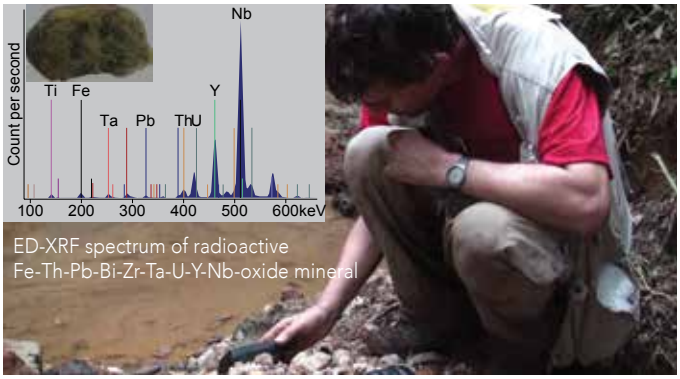

Fig. 20: Peretti examines the leftover gravel of a mining site with a Geiger counter and discovers highly radioactive minerals (Fe-Th-Pb-Bi-Zr-Ta-U-Y-Nb-oxide mineral).

Fig. 21: A set of eight highly valuable faceted rubies ranging from 7 to more than 14 carats in size in the hand of one of the authors (AP) exceeding an estimated market value of US$10 million. Two of the stones over 10 carats were classified as reminiscent to GRS-type "Pigeon's Blood" color category. The Didy (Madagascar) rubies made an overnight appearance to become some of the world's largest rubies unearthed so far, competing in beauty and rarity with the finest Burmese rubies.

Fig. 22: A closer look of an over 7-carat ruby from Didy (Madagascar) demonstrating complete absence of eye-visible inclusions. These rubies from Didy lack silk nests that would potentially disturb the clarity of a stone by producing eye visible whitish reflections. The rubies are so clean that synthetics are easily smuggled into the lots at the mines. (Photo: W. Bieri. © GRS.)

exported except reference specimens (Fig. 26A-D), we boarded our flight to Bangkok. Passing the boarding checkpoint, Hahn was singled out by customs for a random bag search along with four individuals who appeared to be from mainland China. Hahn told the customs officers that it was not necessary to search and make a mess out of his stuff. Miraculously, it worked.

THE AFTERMATH Two days later, mining police moved into Ambatondrazaka and the non Malagasy dealers closed their buying operations, temporarily retreating to the capital for a few days. With the mining area also raided, the miners cleared out. The miners and dealers have gone back by now or relocated to slightly different areas in the forest.

Some passengers traveling with our helicopter were investigated for an unauthorized helicopter trip, and petitioned Peretti for a copy of his authorization. Peretti sent the documents to resolve the matter, but he was not aware that an investigation was ongoing regarding the dissemination of business cards and illegal solicitation in an unauthorized mining site. The man whose name was on the card was imprisoned and had to put up considerable bail. The matter as to how GRS would be compensated for the air hijacking during the expedition is still unresolved.

WORLD RECORD RUBY PRICE At the June Hong Kong Jewellery & Gem Fair, news reached us that a dealer sold a 7-carat vivid red ruby (Didy) for US$1million (Fig. 14). These rubies were true record-breaking treasures of nature. GRS was the only company in the trade that witnessed the activities in this mine firsthand.

GRS RELEASES THE NEWS

http://www.gemresearch.ch/video/Didy6.htm

October 22 GRS hosted a seminar, "New World Record Pigeon's Blood Rubies Discovered," during the September Hong Kong Jewellery & Gem Fair. The new findings were presented at the said event.
see www.jewellerynewsasia.com - keyword: GRS

INVESTORS TAKE MINING RIGHTS

October 30 The following information was received from the gemstone market: A major investor (GF) has taken the mining rights in the upper part of the valley and a private investment group involving non-Malagasy nationals has secured the mining rights in the lower part of the valley. Both are hiring locals from Didy for the work at the mine.

The investment group currently has at least two agents in the forest supervising the operation. Additional wild mining must be taking place since a 128-carat rough sapphire had been submitted to GRS from outside these two mining operations. Submissions of stones originating from Didy to the lab have also resumed.

Fig. 23: A set of sapphires from Didy (Madagascar) ranging from 5 to over 10 carats with the typical GRS-type "Royal Blue" colors normally found solely in sapphires from Sri Lanka, Burma and Ilakaka. (Madagascar). (Photo: W. Bieri. © GRS.)

Fig. 24: Peretti works with a portable microscope to search through lots of rubies and sapphires of dealers in Ambatondrazaka. The presence of illmenite, zircon clusters, blue color zones and absence of silk make these rubies very easily distinguishable through microscopical examination from all other ruby localities, even from the counterparts found in Winza (Tanzania). The same is true for the sapphires that contain large negative crystals accompanied by secondary fluid feathers, isolated zircon crystals, black illmenite inclusions, oriented pargasite needles and the general absence of silk (Lit. 2).

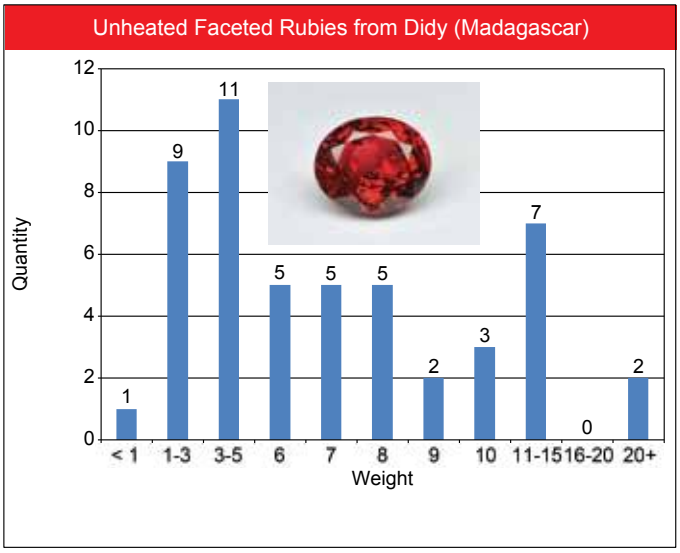

Fig. 25: Statistics of 25 rubies from Didy (Madagascar) tested by GRS just three months after the rubies were discovered. It shows that after only a short period of time two magnificent rubies over 20 carats appeared. Such large rubies are usually the positive by-products from decades of mining in large areas such as Mogok (Burma, Myanmar). Statistics by GRS.

Lit. 1 Adolf Peretti, Francesca Peretti, Anong Kanpraphai, Willy Bieri, Kathrin Hametner and Detlef Günther. Winza Rubies Identified. Contributions to Gemology (2008), 7-97 pp.

Lit. 2 Adolf Peretti, Willy Bieri, Kathrin Hametner, Lawrence Hahn and Detlef Günther (2013). World-record rubies and sapphires from Didy (Madagascar) and the new sapphire mines from Kataragama (Sri Lanka). Expedition Report, Geology and Gemology. Contributions to Gemology, No. 12, in print.

Lit. 3 Carte Métallogénique et de Prédiction des Gisments, Métaux de Base et Métaux Précieux, Feuille No 6-Toamasina (2008) (J. Ramarolahy, D. Rakotomanana, B. Moine, E. Ortega, L. Chevallier, F. Hartzer, G. S. de Kock, S. W. Strauss et, A. F. Randriamanantenasoa, J. Naden, L. Noakes, Editée par: British Geological Survey Keyworth, Nottingham, UK) MINISTÈRE DE L'ÉNERGIE ET DES MINES Projet de Gouvernance des Ressources Minérales (PGRM).

Lit. 4 Edward Gübelin and Adolf Peretti (1997): Sapphires from Adranondambo mine in SE Madagascar: evidence for metasomatic skarn formation. Journal of Gemmology, Vol. 25, No. 7., pp. 453 - 470.

Lit .5 Jewellery News Asia – Show Daily, 24th Sept. 2012, page 10.

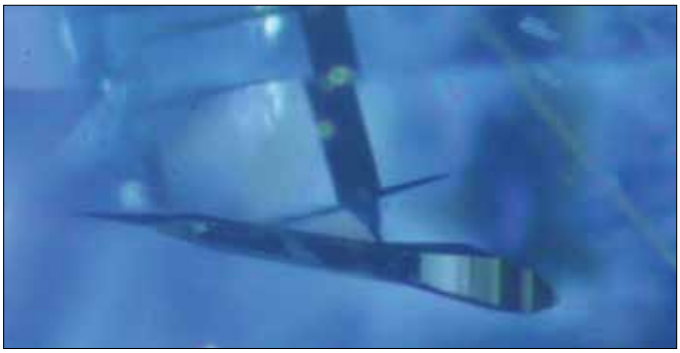

Fig. 26A: Large Mn-Y-Nb-minerals were found as inclusions in Didy sapphires in the shape of ice-picks. This corroborates the theory that the sapphires are formed in connection with Nb-Ta-pegmatites (see Fig. 17)

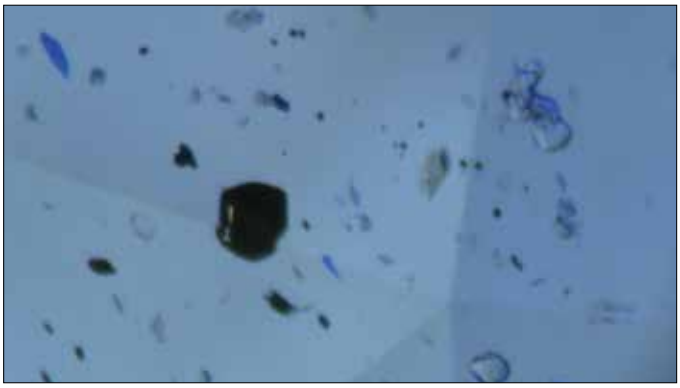

Fig. 26B: Mica, ilmenite and zircon inclusions are found in a Didy sapphire of over 5 carats. (GRS Collection.) These minerals are common in amphibolite-gneiss rock suites found at the mine. Ilmenite was confirmed by GRS using SEM-EDS analysis in July 2012. (M. Meier, SEM-laboratory, Geoscience, University Fribourg, Switzerland)

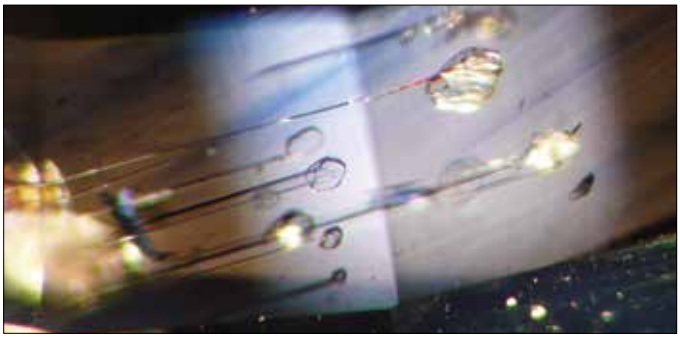

Fig. 26C: Pargasite needles are grown from fluid inclusion voids and have penetrated the entire sapphire in orientation. This is the first time one of the authors (AP) has seen such a phenomena in a sapphire and it shows that the sapphire was grown in a dramatic hydrothermal event. Color zoning is also present in this sapphire and the zoning discontinues irregularly. No whitish milky zones are present such as in other sapphires from Madagascar.

GRS would like to thank the Y. Group for making us discover Didy while providing infrastructure and hospitality on the ground; Tom Cushman for the strategic planning of governmental and local passage permissions, and organizing transportation and data; the Government of Madagascar and the Mayor of Didy for passage permission and providing local support; Gem Paradise and friends for sourcing opportunities; all local miners; Assist Aviation; Ghambi; Diana Jarrett; and most of all, our porters who did an amazing job together with Eugene who might just have saved our lives. And last but not least, the amazing GRS team for holding the fortress at the peak of the laboratory workload.

Fig. 26D: A folded feather within a faceted ruby from Didy (Madagascar). Such features are normally expected in sapphires and not in rubies. (Inclusion Photos: W.Bieri & A.Peretti. © GRS.)

Adolf Peretti

Part A: Identification of CVD-grown Blue Diamonds

Part B: Identification of treated CVD-grown Pink Diamonds from Orion (PDC)

Part C: Origin of Color in Treated CVD-grown Yellow Diamonds and Multistep Treatment Experiments

Part D: Record-breaking Discovery of Ruby and Sapphire at Didy, Madagascar

Adolf Peretti graduated from the Institute of Mineralogy and Petrography at the ETH in Zurich (Switzerland) with a PhD on "Occurrence and Stabilities of Minerals". He also holds an award from the University of Zurich (Switzerland) and is FGA and FGG. He is founder and CEO of GRS laboratories in Switzerland, Hong Kong and Thailand and Partner of CGL-GRS Swiss Canadian Gemlab Inc in Vancouver (Canada). The professional activities of Dr. A. Peretti have been certified by the European Federation of Geologists. He is one of the worlds' diminishing few still practicing gemologists with over 25 years of experience. Dr. A. Peretti is renowned for his adventurous field-gemology films, books, and numerous scientific publications. // www.gemresearch.ch

Branko Deljanin

Part A: Identification of CVD-grown Blue Diamonds

Part B: Identification of treated CVD-grown Pink Diamonds from Orion (PDC)

Part C: Origin of Color in Treated CVD-grown Yellow Diamonds and Multistep Treatment Experiments

Branko Deljanin, B.Sc., GG, FGA, DUG is head gemmologist and director of CGL-GRS Swiss Canadian Gemlab Inc in Vancouver (www.cglworld.ca). A graduate of the University of Belgrade in Geology, Deljanin earned his Advanced Gemology Diploma (DUG) in 2001 on subject "Identification of HPHT treated diamonds" from University of Nantes, France. He is considered an international expert on ID of new diamond treatments and synthetic diamonds (HPHT-grown and CVD-grown). He co-authored book "Laboratory Grown Diamonds" (2007) and has been a regular contributor to trade, gemmological and scientific magazines. Deljanin presented reports on diamonds and colored stones at a number of prestigious research conferences (European Diamond, De Beers, Material Research, Canadian Gemmological, Asian Gemmological and GIA Gemological Conferences). // www.cglworld.ca

Willy Bieri

Part A: Identification of CVD-grown Blue Diamonds

Part B: Identification of treated CVD-grown Pink Diamonds from Orion (PDC)

Part C: Origin of Color in Treated CVD-grown Yellow Diamonds and Multistep Treatment Experiments

Willy Bieri serves as managing director and research scientist at GRS Gemresearch Swisslab AG in Lucerne, Switzerland. Bieri is a graduate of the University of Fribourg, Switzerland earning a Masters Degree in Earth Sciences. He is also a Fellow of the Gemmological Association of Great Britain (FGA diploma), a member of the Swiss Gemmological Association (SGG).

Bieri has been working for GRS since 2005, and co-author of four issues of Contributions to Gemology and co-editor of the GRS documentary films.

Matthias Alessandri

Part A: Identification of CVD-grown Blue Diamonds

Part B: Identification of treated CVD-grown Pink Diamonds from Orion (PDC)

Part C: Origin of Color in Treated CVD-grown Yellow Diamonds and Multistep Treatment Experiments

Matthias Alessandri is a gemologist at GRS Lab (HK) Limited. He is operator of the Photoluminescence analysis system as well as the UV-VIS-NIR instrumentation. Alessandri is Fellow of the Gemmological Association of Great Britain (FGA). He is also a co-author and technical co-editor of Contributions to Gemology.

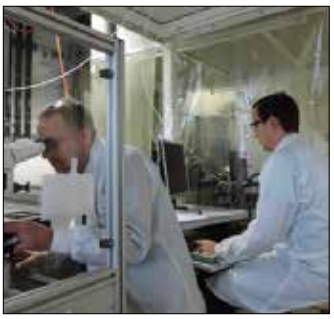

Detlef Guenther & Daniel A. Frick

Part A: Identification of CVD-grown Blue Diamonds

Part B: Identification of treated CVD-grown Pink Diamonds from Orion (PDC)

Detlef Günther is full Professor for Trace element and micro analysis at the Laboratory of Inorganic Chemistry, ETH Zurich, graduated from the Martin-Luther-University of Halle-Wittenberg (Germany) in 1987. His PhD thesis focused on "The Interpretation and Optimization of Sampling and Transport" as well as "Calibration for Quantitative LM-ICP-OES". After post-doc periods at Duisburg University (Germany), the Institute of Plant Biochemistry in Halle (Germany), and the Memorial University of Newfoundland (Canada), he introduced a new homogenized excimer laser ablation system (ArF, 193 nm) that has contributed significantly to improving the applicability of laser ablation technique. One of his major contributions to gemology is his published pioneer work on "Quasi-nondestructive Fingerprinting of Sapphires Using LA-ICP-MS", which led to an extensive study of various gemstones. Since than he published over 320 papers including many articles in Contributions to Gemology, and received awards such as: "Thousand Talents Program, Wuhan – University, China", the "Einstein Visiting Fellow, Einstein-Fundation Berlin", the " Fresenius-Preis", the "European Award for Plasma Spectrochemistry" and the "Ruzicka-Preis". GRS is very proud to have him on board of Directors in Switzerland. // www.analytica.ethz.ch

Daniel A. Frick (right in picture above) studied chemistry at ETH Zürich from 2005 till 2009. After a scientific internship at Macquarie University in Sydney he joined the group of Professor Dr. Detlef Günther in March 2010. He investigates the partitioning of carbon during laser ablation and in the inductively coupled plasma mass spectrometry with a focus on analysis of biological tissues.

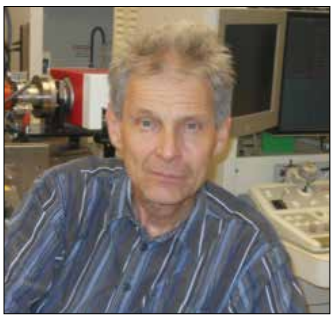

Alexandre M. Zaitsev

Part A: Identification of CVD-grown Blue Diamonds

Part B: Identification of treated CVD-grown Pink Diamonds from Orion (PDC)

Part C: Origin of Color in Treated CVD-grown Yellow Diamonds and Multistep Treatment Experiments

Alexandre M. Zaitsev, MS, PhD, DSc is Professor Engineering Science and Physics College of Staten Island.Alexandre Zaitsev is a professor of physics at the College of Staten Island and the Graduate Centre of the City University of New York. He is an expert in spectroscopy and electronics of diamond materials. His current research interests are focused on nanostructured carbon materials, diamond-based deterministic photon sources, development of novel methods of treatment and characterization of gem diamonds. A recent achievement of Alexandre and his collaborators in Germany is the development of the first diamond-based single photon light emitting diode capable of emission of single photons at room temperature. Alexandre Zaitsev is author of numerous scientific publications, of the monograph "Optical properties of diamond", Springer Verlag, Berlin, 2001, and co-author of the book "HPHT-Treated Diamonds", Springer Verlag, Berlin, 2013.

Lawrence Hahn

Part D: Record-breaking Discovery of Ruby and Sapphire at Didy, Madagascar

Lawrence Hahn is General Manager & Gemologist at GRS Lab (HK) Ltd. in Hong Kong. He graduated from Oxford Brookes University with an upper Honours Degree in Business Administration and Accounting & German Studies. He is a GIA Alumni (Graduate Gemologist), IGI Rough Diamond Grader and lifetime member of the Gemmological Association of Hong Kong (GAHK). He is co-author and co-editor of Contribution to Gemology Volume No.13 & 14 and has co-headed and documented GRS field expeditions. Lawrence Hahn has gained extensive insight into the gemstone and pearling industry through 8 years of direct trade sourcing exposure before joining GRS in early 2011. He has now gained 3 years of direct lab experience.

Franz Herzog

Part A: Identification of CVD-grown Blue Diamonds

Part B: Identification of treated CVD-grown Pink Diamonds from Orion (PDC)

Franz Herzog, PhD, FGA, is educated as a Physicist (Studies, Master and Ph.D. (Dr. Phil. Nat) in Theoretical Elementary Particle Physics at the Institute of Theoretical Physics of the University of Basel, Switzerland; Post-Doctoral fellowship at the University of Wisconsin in Madison, USA; research assistant at the Institute of Theoretical Physics in Berne. Dr. Herzog obtained his FGA diploma in 2011.

Ed Cleveland

Part A: Identification of CVD-grown Blue Diamonds

Part B: Identification of treated CVD-grown Pink Diamonds from Orion (PDC)

Ed Cleveland is an independent gemstone wholesaler and cutter and provides field-research consulting services to GRS.

Worldwide GRS Locations

www.gemresearch.ch

GRS in Switzerland
GRS Gemresearch Swisslab AG
Sempacherstrasse 1
CH-6002 Lucerne
Switzerland

T: +41 41 210 31 31
F: +41 41 210 31 34

Shipping Address Laboratory
GRS Gemresearch Swisslab AG
Baldismoosstrasse 14
6043 Adligenswil/LU

GRS in Thailand
DR Peretti Co. LTD
Unit 501, Silom 19 Building, Soi 19, Silom, Bangrak, Bangkok 10500, Thailand

T: +66 2237 5898 / +66 2630 0112
F: +66 2237 5899 / +66 2630 0114

GRS in Hong Kong
GRS Lab (Hong Kong) Ltd.
Unit B 6/F
9 Queens Road, Central
Hong Kong

T: +852 2376 3888
F: +852 2568 3888

The diamond industry is undergoing one of the most dynamic changes of all time. Challenges confronting it today are in large part due to the massive influx of newer generations of synthetic diamonds and diamond treatments permeating every level of the market. As a contribution to safeguarding the fancy diamond industry, we have made considerable research efforts in the identification of CVD-grown diamonds, presented on a scientific level and requiring expert knowledge. In Part A, we analysed a new generation of CVD-grown blue diamonds and in Part B, multi-step treatment applied to CVD-grown diamonds to produce pink colors. The final part of our diamond-trilogy is an 'experiment-report' on how to produce yellow color in CVD-grown diamond.

Our jungle expedition into Madagascar to the source of world-record setting rubies is for all reading levels. Unlike previous gemological publications, we include QR codes that link to corresponding YouTube videos. Besides text and images, the reader can watch video sequences to gain better insight into our research trips. GRS is the first to introduce this new type of interactive publishing in the world of gemology.

ISBN
9 783952 386750